INSTITUTO SUPERIOR DE ENGENHARIA DO PORTO
MESTRADO EM ENGENHARIA MECÂNICA




ESTUDO EXPERIMENTAL DA INFLUÊNCIA DO COMPRIMENTO DE CORTE NO COMPORTAMENTO DE DESGASTE DE FERRAMENTAS COM REVESTIMENTO DE TiN/TiAlN DURANTE O FRESAMEN

NAIARA POLI VENEZIANI SEBBE
junho de 2023

POLITÉCNICO
DO PORTO

Instituto Superior de Engenharia do Porto

EXPERIMENTAL STUDY OF THE CUTTING LENGHT INFLUENCE ON THE WEAR BEHAVIOUR OF TiN/TiAlN COATED TOOLS DURING MILLING OF INCONEL 718

Naiara Poli Veneziani Sebbe

2023

Instituto Superior de Engenharia do Porto

Departamento de Engenharia Mecânica

P.PORTO


P.PORTO

Instituto Superior de Engenharia do Porto

EXPERIMENTAL STUDY OF THE CUTTING LENGHT INFLUENCE ON THE WEAR BEHAVIOUR OF TiN/TiAlN COATED TOOLS DURING MILLING OF INCONEL 718

Naiara Poli Veneziani Sebbe

1210206

Dissertation presented to School of Engineering, Polytechnic of Porto to fulfill the requirements necessary to obtain a Master's degree in Mechanical Engineering, carried out under the guidance of Prof. Dr. Francisco José Gomes da Silva, Associate Professor with Habilitation of the Department of Mechanical Engineering, and Co-supervised by Prof. Dr. Filipe Daniel Fernandes, Assistant Professor at the Department of Mechanical Engineering.

2023

Instituto Superior de Engenharia do Porto

Departamento de Engenharia Mecânica

P.PORTO


P.PORTO

JURY

President
Prof. Dra. Rafaela Carla Barros Casais
Assistant Professor, Instituto Superior de Engenharia do Porto
Supervisor
Prof. Dr. Francisco José Gomes da Silva
Associate Professor with Habilitation, Instituto Superior de Engenharia do Porto
Cosupervisor
Prof. Dr. Filipe Daniel Fernandes
Assistant Professor, Instituto Superior de Engenharia do Porto
Arguer
Prof. Dr. Abílio Manuel Pinho de Jesus
Associate Professor with Habilitation, Departamento de Engenharia Mecânica, Faculdade de Engenharia da Universidade do Porto

ACKNOWLEDGEMENTS

First, to God, for giving me life and for guiding my path.

I would like to thank Prof. Dr. Francisco José Gomes da Silva for the teachings transmitted, patience and guidance throughout this work, fundamental for its completion.

To the co-supervisor, Prof. Dr. Filipe Daniel Fernandes for the clarifications provided, and for always being available and helping with whatever was necessary.

The research initiation scholarship from the MCTool21 - ref. "POCI-01-0247- FEDER-045940" project is also acknowledge.

To Dr. Rui Rocha, Scanning Electron Microscopy technician at the Materials Center of the University of Porto (CEMUP), for obtaining the images and helping with their interpretation.

To Eng. Fátima Andrade, technician from the laboratory of Metallography at Instituto Superior de Engenharia do Porto (ISEP), for assistance in the preparation of all analyzed samples.

To the company INOVATOOLS, S.A. (Leiria, Portugal), on behalf of Mr. Nuno André for providing the tool substrates studied, and the company TEandM – Tecnologia, Engenharia e Materiais, S. A. (Coimbra, Portugal), on behalf of Eng. Ricardo Alexandre for the coatings applied to these tools.

To my colleague Vitor Sousa, for all his help and availability in carrying out the tests.

To my family, especially my parents, brother, grandmother and nephews for their unconditional support, friendship, and constant encouragement, necessary for this stage to be completed.

To my friends for their friendship, companionship, support, and encouragement throughout this course.

Finally, to everyone who, even though not mentioned, contributed to the realization of this work, thus making this dream come true.

ABSTRACT

The Inconel 718 alloy displays high mechanical strength at high temperatures, high hardness, tendency to undergo work hardening and low thermal conductivity, which makes it widely used in the aeronautical, aerospace, biomedical and petrochemical industries. However, due to these characteristics, this alloy is considered a difficult-to-machine material, which can cause great damage or breakage in the cutting tools, excessive wear, and short tool lifetime. Milling process is the most used in the machining of this alloy, since it is a flexible process in the production of dissimilar shapes and high surface quality finishing parts. The use of coatings applyed over the surface of the machining tools has been observed to improve their performance and the surface quality of the machining parts. Based on this, the objective of this project was to evaluate the wear behavior of endmill coated tools during the machining of Inconel 718 alloy, using multi-layered TiN/TiAlN coating, deposited by sputtering HiPIMS process. For this, different machining parameters such as cutting speed, cutting length and feed per tooth were varied. After the machining tests, the surface quality of the machined material was assessed, the wear of the tool was evaluated, the wear mechanisms characterized, and the tool lifespan analyzed. It was found that the cutting length has a great influence on the machined surface and the resulting wear. The greater this parameter, the worse the surface quality and the higher the resulting wear. As for the predominant wear mechanisms, abrasion and material adhesion were identified, both on the coating and on the substrate of the tool, in all tested conditions. In addition, in some cases, built-up edges were developed. It was also observed that the TiN undercoat improved resistance to crack propagation, as this phenomenon was not identified in tools after milling operations. As for tool lifespan, it was found that the higher the cutting speed, the higher the flank wear, and consequently, the shorter the tool lifespan. Thus, the parameter that had the greatest influence on tool lifespan, in addition to cutting length, was the cutting speed.

KEYWORDS

Machining; Milling; Tool wear mechanisms; TiN/TiAlN films; Inconel 718; PVD coatings; HiPIMS; Machined surface quality.

RESUMO

A liga Inconel 718 apresenta alta resistência mecânica mesmo em altas temperaturas, alta dureza, tendência a endurecimento por trabalho a frio, e baixa condutividade térmica, o que a torna amplamente utilizada nas indústrias aeronáutica, aeroespacial, biomédica e petroquímica. No entanto, devido a essas características, essa liga é considerada um material de difícil maquinar, podendo causar grandes danos ou fraturas nas ferramentas de corte, desgaste excessivo e curta vida útil da ferramenta. O processo de fresagem é o mais utilizado na maquinagem desta liga, por ser um processo flexível na produção de formas dissimilares e peças com acabamento de alta qualidade superficial. Verificou-se que o uso de revestimentos sobre a superfície das ferramentas de maquinagem permitem melhorar o seu desempenho e a qualidade superficial das peças maquinadas. Com base nisso, o objetivo deste projeto foi avaliar o comportamento ao desgaste de ferramentas revestidas, nomeadamente fresas de topo, protegidas com um revestimento multicamada do sistema TiN/TiAlN, depositadas pelo processo de *sputtering* HiPIMS, durante a maquinagem da liga Inconel 718. Para isso, foram variados diferentes parâmetros de maquinagem como velocidade de corte, o comprimento de corte e o avanço por dente. Após os ensaios de maquinagem, foi avaliada a rugosidade da superfície maquinada, o desgaste da ferramenta, caracterizados os mecanismos de desgaste e determinado o tempo de vida útil da ferramenta. Verificou-se que o comprimento de corte tem grande influência na superfície maquinada e no desgaste resultante, sendo que quanto mais elevado for esse parâmetro, pior é a qualidade superficial e maior o desgaste resultante. Quanto aos mecanismos de desgaste predominantes, foram identificados abrasão e adesão de material, tanto relativo ao revestimento, quanto ao substrato da ferramenta não revestida, em todas as condições ensaiadas. Além disso, em alguns casos, pode ser observado a formação de aresta postiça. Observou-se ainda que a subcamada de TiN melhorou a resistência à propagação de fissuras, visto que nenhuma fissura foi identificada nas ferramentas após as operações de fresagem. Quanto à vida útil da ferramenta, verificou-se que quanto maior a velocidade de corte, maior o desgaste de flanco e, consequentemente, menor a sua vida útil. Assim, o parâmetro que teve maior influência na vida da ferramenta, além do comprimento de corte, foi a velocidade de corte.

PALAVRAS-CHAVE

Maquinagem; Fresagem; Mecanismos de desgaste das ferramentas; Revestimento multicamada de TiN/TiAlN; Inconel 718; Deposição PVD; HiPIMS; Qualidade da superfície maquinada.

INDEX

FIGURES INDEX

TABLES INDEX

LIST OF ABBREVIATIONS AND SYMBOLS

List of abbreviations

BUE	Built-up Edge
CAD	Computer-aided design
CAM	Computer-aided manufacturing
CBN	Cubic boron nitride
CF	Clearance Face
C-HPMS	Continuous high-power magnetron sputtering
CNC	Computer numerical control
CVD	Chemical vapor deposition
DC	Direct-current
DCMS	Direct-current magnetron sputtering
DLC	Diamond-like carbon
DMS	Dual magnetron sputtering
EDS	Energy-dispersive X-ray spectroscopy
FCC	Face-centered cubic lattice
GLAD	Angle-of-view deposition
HFCVD	Hot filament chemical vapor deposition
HiPIMS	High-power impulse magnetron sputtering
HPMS	high power magnetron sputtering
HPPMS	High-power pulsed magnetron sputtering
ISEP	Instituto Superior de Engenharia do Porto
LAMM	Laser-assisted micro-milling
MDC	Microcrystalline diamond coating
MEP	Magnetically enhanced plasma
MRR	Material removal rate
MT-CVD	Medium temperature chemical vapor deposition
MQL	Minimum quantity lubrication
NDC	Nanocrystalline diamond coating
P.Porto	Instituto Politécnico do Porto
PCD	Polycrystalline diamond
PEEK	Polyetheretherketone
PVD	Physical vapor deposition
RF	Rake face
RD	Radio frequency
SEM	Scanning electron microscopy
TiN-NRs	Titanium nitride nanorods plasmon
UBMS	Unbalanced magnetron sputtering

UVAM	Ultrasonic vibration assisted milling

List of symbols

%	Percentage	%
Ø	Diameter	µm
µ	Micron	µ
a_e	Radial cutting depth	mm
Ag	Silver	Ag
Al	Aluminum	Al
AlCrN	Aluminum chromium nitride	AlCrN
Al_2O_3	Aluminium oxide	Al_2O_3
AlTiN	Titanium aluminum nitride	AlTiN
$AlSi_9Cu_1$	Aluminum Silicon Copper	$AlSi_9Cu_1$
a_p	Axial cutting depth	mm
Be	Beryllium	Be
Bi	Bismuth	Bi
C	Carbon	C
Ca	Calcium	Ca
Co	Cobalt	Co
Cr	Chromium	Cr
CrAlN	Chromium aluminum nitride	CrAlN
CrAlSiN	Chromium aluminum silicon nitride	CrAlSiN
CrC	Chromium carbide	CrC
CrN	Chromium nitride	CrN
Cu	Copper	Cu
E	Elastic Modulus	GPa
F	Adhesive strength	N
Fe	Iron	Fe
f_n	Feed per revolution	mm/rev
f_z	Feed per tooth	mm/tooth
GPa	Gigapascal	GPa
HBW	Brinell hardness	HBW
HK	Knoop hardness	HK
h_m	Average chip thickness	mm
L	Length	mm
K_{Ic}	Fracture toughness	MPa
Mg	Magnesium	Mg
$Mg_1Al_2O_4$	Magnesium aluminum oxide	$Mg_1Al_2O_4$
MgO	Magnesium oxide	MgO

Mn	Manganese	Mn
Mo	Molybdenum	Mo
MoN	Molybdenum nitride	MoN
MoS_2	Molybdenum disulfide	MoS_2
MPa	Megapascal	MPa
Mz	Torque	N.m
n	Rotational speed	rpm
N_2	Nitrogen	N_2
NbC	Niobium carbide	NbC
NbN	Niobium nitride	NbN
Ni	Nickel	Ni
O	Oxygen	O
Pb	Lead	Pb
Ra	Surface roughness	nm
Ru	Ruthenium	Ru
S	Sulfur	S
Si	Silicon	Si
SiC	Silicon carbide	SiC
Si_3N_4	Silicon Nitride	Si_3N_4
t	Thickness	µm
T	Temperature	°C; K
Ta	Tantalum	Ta
TaN	Tantalum nitride	TaN
Ti	Titanium	Ti
TiAlN	Titanium aluminum nitride	TiAlN
Ti6Al4V	Titanium aluminum vanadium	Ti6Al4V
TiAlCN	Titanium aluminum carbon nitride	TiAlCN
TiAlCrN	Titanium aluminum chromium nitride	TiAlCrN
TiAlCrSiN	Titanium aluminum chromium silicon nitride	TiAlCrSiN
TiAlCrYN	Titanium aluminum chromium yttrium nitride	TiAlCrYN
TiAlN	Titanium aluminum nitride	TiAlN
TiAlTaN	Titanium aluminum tantalum nitride	TiAlTaN
TiAlTaYN	Titanium aluminum tantalum yttrium nitride	TiAlTaYN
TiAlSiN	Titanium aluminum silicon nitride	TiAlSiN
(TiAlSiY)N	Titanium aluminum silicon yttrium nitride	(TiAlSiY)N
TiAlVN	Titanium aluminum vanadium nitride	TiAlVN
TiAlYN	Titanium aluminum yttrium nitride	TiAlYN
TiB_2	Titanium di-boride	TiB_2
TiBCN	Titanium boron carbon nitride	TiBCN

TiBN	Titanium boron nitride	TiBN
TiC	Titanium carbide	TiC
TiCN	Titanium carbon nitride	TiCN
TiN	Titanium nitride	TiN
TiN-NRs	Titanium nitride nanorods plasmon	TiN-NRs
TiSiN	Titanium silicon nitride	TiSiN
V_c	Cutting speed	m/min
V_f	Feed speed	mm/min
V	Vanadium	V
VN	Vanadium nitride	VN
Y	Yttrium	Y
W	Tungsten	W
WC	Tungsten carbide	WC
ZrN	Zirconium nitride	ZrN

1. INTRODUTION

In this introductory chapter, a contextualization of the subject of this dissertation, as well as their objectives are presented. The methodology to be followed in the development of the project is also indicated and, finally, its structure is described.

1.1. Contextualization

With the increase in industrial competition and energy costs, it is very important for companies to reduce the production cycles and the price of products, at the same time that the good quality parts are ensured during fabrication. Machining is one of the most used processes by companies to transform raw materials in finals parts. Therefore, this is a process of great industrial and scientific importance, continuously, subject to improvements.

Ni alloys are considered difficult-to-cut materials, since they display very high mechanical properties, tendency to hardening under room temperature work and low thermal conductivity, which consequently leads to the premature failure of the cutting tools. In the literature there is a large gap regarding milling and surface finishing of these alloys after machining. One of the most used Ni alloys in the aeronautical and aerospace industries is the Inconel 718. Since aeronautical and aerospace parts are of extremely high responsibility and this Ni alloys is of great difficulty to machine, it is extremely important that the machining process of this alloy is optimized to improve the lifetime of the machining tools for reducing costs and ensure the good surface finishing of the machined parts.

1.2. Objectives

The objective of this work was to evaluate the wear behavior of endmills coated with a multilayer TiN/TiAlN film, the machining of an Inconel 718 alloy. Multilayer films are known to be more performing than monolayer films during machining, and the performance of TiN/TiAlN multilayered film in the machining performance of Inconel alloy is a subject that is still few explored. Thus, the specific objectives of this thesis were:

- Perform the analysis of the machined surface roughness and correlate it with the wear of the coated tool;
- Analyze the cutting forces resulting from the milling process;
- Analyze and compare the results with the different selected parameters;
- Evaluate and study the wear mechanisms taking place in the tools after machining, using scanning electron microscopy technique;
- Evaluate the tool lifespan until the tool reaches the established end of operation criterion.

1.3. Scientific methodology

The investigation methodology used for the development of the present work was the experimental research methodology. Therefore, an object of study was defined, the variables that can influence it were selected, and the method of analysis and observation defined, so that it was possible to reach the desired conclusions. For this, the methodology was divided into four main sections: State-of-the-Art; Materials and Methods; Results; and Discussion.

In the State-of-the-Art section, a bibliographic review was carried out using recent scientific articles, books and works on the proposed subject. First, an approach to machining was presented, emphasizing the milling process and the various parameters affecting it; coatings for cutting tools, highlighting the PVD and CVD processes as techniques for enhancing the surface performance of cutting tools; recent advances in coatings for cutting tools; and a description of possible wear mechanisms associated with cutting tools, as well as tool lifespan. So that in the Results and Discussion sections it is possible to identify the wear mechanisms associated with this work.

In the Materials and Methods section, a brief description of the Inconel 718 alloy is made, with an analysis of scientific articles on the machining of this alloy, emphasizing the parameters used, so that it was possible to establish and select the machining parameters to use in this work, such as cutting speed, cutting length and feed per tooth; and analyze how these influence the process, both in terms of associated wear, tool lifespan, cutting forces, and quality of the machined surface. This section also describes the methods that were used for these objectives.

Finally, in the Results and Discussions sections, the tools lifetime were presented and discussed based on the machining conditions, wear mechanisms, compare the influence of the various parameters surface roughness of the machined parts, cutting forces.

1.4. Dissertation structure

This dissertation is divided into seven chapters: 1. Introduction, 2. State-of-the-art, 3. Materials and Methods, 4. Results, 5. Discussion of the Results, 6. Conclusions, and the Bibliographic References used. The first chapter, the introductory part, briefly presents the topic addressed in the report, with its respective context, objectives, and methodology.

The second chapter is focused on an extensive literature review, divided into four subchapters/sub-subjects. Subchapter 2.1. presents an approach regarding the machining process; subchapter 2.2. concerns the main deposition technologies used to produce coatings on cutting tools, highlighting the PVD and CVD processes and the characterization of the coatings formed by these methods; subchapter 2.3. reviews recent advances in coatings for cutting tools; and, finally, subchapter 2.4. mentions the wear mechanisms that occur in cutting tools, and makes an approach regarding tool life.

The third chapter presents the materials used and methods applied. Thus, subchapter 3.1. emphasizes the materials, being divided into three more subchapters: 3.1.1. Machined Material, which features Inconel 718 alloy; 3.1.2. Substrate and tool geometry, which references the tool used and its respective geometry; and 3.1.3. Coating, which concerns the coating deposited on the cutting tool. In turn, subchapter 3.2. presents all the methods and equipment necessary for its execution, thus describing the procedures used for each analysis used in this work. Thus, this

subchapter is divided into eleven more subchapters: 3.2.1. PVD Coating; 3.2.2. Milling equipment and conditions; 3.2.3. Characterization of the thickness and morphology of the coatings; 3.2.4. Characterization of the roughness of machined surfaces; 3.2.5. Characterization of wear mechanisms; 3.2.6. Characterization of cutting force measuring equipment and 3.2.7. Tool Lifespan evaluation.

The fourth chapter concerns the results obtained. For this, it is subdivided into six subchapters. The subchapter 4.1. Analysis of coatings; presents the results obtained regarding the thickness of the coating and its characterization. Subchapter 4.2. Machined surface analysis; performs an analysis of the roughness of the machined surface. Subchapter 4.3. Analysis of cutting forces; presents the cutting forces developed in the process, subchapter 4.4. Wear measurements and characterization; presents measurements of flank wear, subchapter 4.5. Analysis of wear mechanisms; shows and identifies the wear mechanisms resulting from the process, and finally, subchapter 4.6. Tool Lifespan analysis; presents the analysis and results regarding tool lifespan. For this, sub-chapters 4.2., 4.4. and 4.5. were divided into four subchapters referring to the test condition based on cutting speed and cutting length of 25 meters.

The fifth chapter reports the discussions regarding the results obtained, substantiating the comments with scientific articles already published. Thus, the chapter was subdivided into four subchapters: 5.1. Comparison of the surface state obtained on the machined part; 5.2. Comparison of wear generated on tools; 5.3. Tool lifespan comparison; and 5.4. Comparison with other coatings used in machining. And, the sixth chapter presents the relevant conclusions of the study, as well as proposals for future work. And finally, the last part, corresponds to the references used to prepare this dissertation.

2. STATE-OF-THE-ART

In this chapter, a bibliographic review will be presented on topics that are of extreme importance for the development of this work, and which will be applied in the various phases of the same, namely, machining, coating for cutting tools, recent advances in coatings for cutting tools and wear mechanisms associated with cutting tools.

2.1. Machining principle

The machining operation is a technological process responsible for changing the shape of bulk blocks until a desired shape is reached, through the removal of material [1]. This process, is even today, very important and the most used by the industry to produce high precision and quality parts [2]. Therefore, research involving machining is still a hot topic today and the efforts are oriented to the improvement of the machining process [3]. As the aeronautical and aerospace industries need parts with high dimensional accuracy, the machining process has great prominence in these sectors, being the turning and milling processes the two most used ones [4,5].

The CNC (Computer Numerical Control) machining industry has seen significant growth in recent years, and it is expected that by 2025 it will reach a $100 billion industry [6]. However, as in every process, there are advantages and disadvantages, since while the parts produced have good surface quality and dimensional accuracy, the acquisition cost of the equipment increases exponentially. Additionally, specialized operators are needed to handle the equipment [7]. Therefore, it can be said that machining is defined as a manufacturing process carried out through a computer with CAD (computer-aided design) and CAM (computer-aided manufacturing) systems that control the process and the operations performed on the machine [8]. Figure 1 illustrates this process.

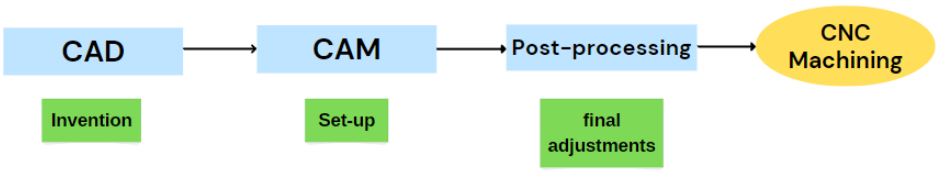

Figure 1 - Representation of the CAD-CAM process. Reproduced from [9]

Within the machining processes, the most used processes are milling and turning [3]. Turning can be understood as the process by which the material to be machined rotates using a stationary tool [2]. With the evolution of turning machines, the necessary tools also had a great evolution. Nowadays, 80 % of the tools are coated to improve machining performance and good finishing of the machining parts [2, 10].

In turn, milling is a process with great dimensional accuracy, in which a rotating tool with multiple cutting edges runs through the material, thus generating a planar surface. This process can be carried out in two ways known as peripheral or end milling, as seen in Figure 2 [11]. As the name suggests, in the peripheral milling the axis of the tool is parallel to the face of the workpiece, and in the top milling, the axis of rotation of the tool is perpendicular to the direction of feed direction [12]. In end milling there are different operations that can be performed, such as: i) facing, to obtain

a flat face, which is the process used in this work; ii) channel milling, for opening a channel in the material; iii) box milling, to dig a "box" inside the part; iv) contour milling, in which 90° angles can be formed together with peripheral milling; and v) surface contour, which produces three-dimensional shapes from a curved path, using a spherical milling cutter [2].

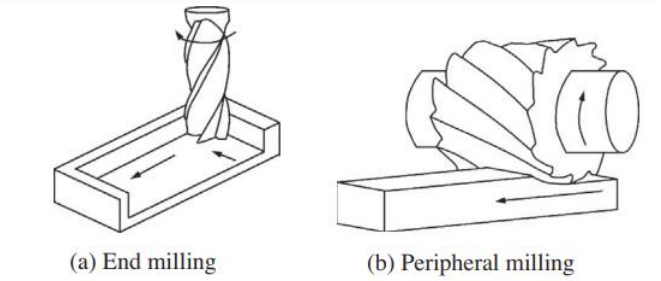

Figure 2 - Milling operations: a) end milling and b) peripheral milling. Reproduced from [11]

Regarding the machining parameters, it is known that they are very important, as they influence the quality and stability of the process, as well as the lifetime of the cutting tools [2]. Thus, the parameters to be used must be properly chosen. Table 1 summarizes the main machining parameters, their symbology, unit, and description [13].

Table 1 – Milling parameters [13]

Parameter	Symbol	Unit	Description
Cutting Speed	V_c	m/min	Tool peripheral speed
Rotational Speed	n	rpm	Number of revolutions per minute of the tool
Feed Speed	V_f	mm/min	Distance traveled by the tool per unit of time
Feed per Tooth	f_z	mm/tooth	Chip thickness that each tooth of the tool removes from the material as it passes through it
Feed per Revolution	f_n	mm/rev	Linear distance traveled by the tool during one complete rotation
Cutting Length	L	mm	Total distance traveled by the tool
Depth of cut	a_p	mm	Required depth of material to be removed in the process
Width of cut	a_e	mm	Is the total thickness of the cut
Average chip thickness	h_m	mm	Required parameter for calculating the cutting force
Material Removal Rate	MRR	mm^3/min	Amount of material removed per unit of time

In addition, the number of rotary axes must also be taken into account in a machining operation. 3-axis machining is the simplest processing method within machining, where the part is fixed in a single position, and the tool movement is in the X, Y and Z axes. 3-axis machines are normally used for 2D drawings, and with that it is possible to machine up to six sides of the part with the help of a clamping configuration for each side, which makes the process more costly [7]. Based on this, Gray et al. [14], in their work, compared a 3-axis machining with a 5-axis machining on hydroforming die inserts, in order to adequately demonstrate the capabilities of 5-axis machining. They concluded that 3-axis toolpaths are longer than 5-axis toolpaths by at least 247 %.

By adding an axis, called the A axis, there is one more rotation for the X axis, thus forming the 4-axis machining. In this configuration the material can be machined on five sides, making the process more profitable and economical [15]. Using a 4-axis milling machine, Souza et al. [16], developed a method capable of estimating the time required to machine a component, with a maximum error of less than 6%. Such methodology is very important for an adequate production planning, since based on that investigation, the machining time estimated by the commercial CAM was 716% to 1456% shorter than the real 4-axis milling.

In turn, 5-axis machining is the most important equipment related to cutting in industries and has one more rotary axis, which makes it a process widely used in the manufacture of blades, rotors, dies, molds, propellers, and others [17, 18]. When the material to be machined is a material of high hardness and fracture toughness, this process becomes even more important and the vibrations generated and the simultaneous movement of the tool must be taken into account, since there is a great possibility of imperfections on the surface of the machined part and thus lower surface quality [19]. Figure 3 exemplifies a 5-axis machining equipment with table tilt A-C and X, Y, Z axes [20].

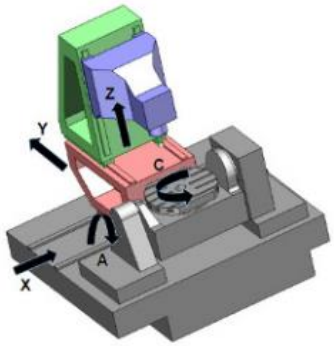

Figure 3 - 5-axis machining equipment with table tilt A-C and X, Y, Z axis. Reproduced from [20]

Lasemi et al [21], made an extensive review regarding freeform surfaces, also called sculptured surfaces, especially those manufactured through 5-axis machining, taking into account three main aspects: tool path generation, identification of tool orientation and tool geometry selection. They concluded that the programming and machining time are two main variables that still need to be developed so that the efficiency of the process increases. In addition, the quality of the part must also be considered because sometimes it was neglected so that the time of the process would be reduced. Therefore, 5-axis machining has an advantage in terms of its flexibility and efficiency [22], and its precision is the determining factor for the success of the manufacturing [23].

6-axis machining is also available in the market. The 6 axes increase both the variety of movements and transitions and reduces cutting time. With that, extremely complex shapes can be obtained such as turbines or engine blocks [24]. Thus, since machining processes are heavily used in the industry and improvements are still needed, this is still a hot topic of research specially in the machining of the so called hard-to-cut materials.

2.2. Coating technologies for protecting the surface of cutting tools (PVD/CVD)

Even with the great advancements and developments of new technologies, modern industries are still facing problems to improve the productivity and quality of their products. For example, the main problem faced during machining operations such as turning and milling is the fast tool wear, which is accelerated when difficult-to-cut materials such as nickel-based alloys are regarding. In these materials higher shear forces and temperature are generated during the process, leading to the premature failure of the tool [25].

As the tool directly influences the machining process, a lot of research has been done based on the development of coatings and the creation of new geometries for these tools [3]. For example, Ji et al. [26], studied tools for high-speed machining of difficult-to-cut materials, such as the gradient cermet composite cutting tool, which is composed of surface layer, subsurface layer and substrate. This means that layers with different hardness values were overlapped, giving to the tool greater wear resistance, increased tool life and better machining quality.

In addition, hard coatings offer many advantages in improving the wear resistance of various surfaces. Many studies have been carried out in this context on difficult-to-machine materials, as is the case of the work by Chowdhury et al. [27], in which titanium alloy Ti6Al4V was tested against tool coated with AlTiN and CrN. Significant improvements on the machining performance were observed as compared to the uncoated tools. In turn, Hovsepian et al. [28], studied the machinability performance of Al alloys, such as Al7010-T7651 and $AlSi_9Cu_1$ in high-speed dry milling, using several types of coatings, TiAlN/VN, DLC (diamond-like carbon), and TiAlCrYN. The results were then compared with uncoated tools. In the case of Al7010-T7651 alloy, TiAlN/VN and DLC coated tools showed comparable performance, and in case of $AlSi_9Cu_1$ alloy, TiAlN/VN coated tools performed much better. In addition, the TiAlN/VN coating contributed to reducing cutting forces, improving surface finishing, and reducing built-up edges formation.

These coatings can be applied to various surfaces of parts for different industries, such as: automotive, aeronautics, aerospace, etc. Examples of coatings include DLC, monolayer coatings such as TiB_2, TiAlCrSiN and TiAlSiN, multilayer coatings such as TiAlN/TiN and TiAlVN/TiAlN. Multilayered coatings are widely used for machining operations as compared to monolithic coatings, since they allow an improvement in the performance of the tools [2]. The coatings are normally produced by two different processes called Chemical Vapor Deposition (CVD) and Physical Vapor Deposition (PVD) [29]. Within these two processes, there are specific techniques, as shown in Table 2 [30].

Table 2 - Deposition techniques used in the production of coatings.

Deposition method	PVD	CVD
Deposition techniques	- Cathodic arc (sputtering); - Vacuum evaporation; - Ionic deposition.	- CVD performed in vacuum; - CVD with no vacuum.

Deposition techniques have experienced strong growth and development, with several variants of the process. Depending on the material to be coated and the application to which it will be

subjected, the deposition process needs to be properly selected to obtain the necessary properties [31]. In the next subchapters, a description of those deposition processes is summarized.

2.2.1. Physical Vapor Deposition

The term Physical Vapor Deposition emerged in 1960s with the need to develop vacuum coating processes. Basically, there are two ways in which particles can be extracted from the target, i.e. sputtering and evaporation, with the latter having lower atomic energy, less adhesion to the substrate and higher deposition rate [31]. Thus, sputtering is more used in applications that require good surface quality and adequate surface morphology [32, 33].

In the PVD process, the material to be deposited is transformed into atomic particles through a physical thermal collision process. The atoms of the material to be deposited are ejected out from the target by ions bombardment of the inserted inert gas (usually argon) [34]. The advantages of the PVD process are: it allows deposition on substrates presenting a lower melting point; greater energy efficiency; allows variation of coating characteristics; and the possibility of deposition of alloy compounds and/or multilayer composition [35]. Due to these advantages, several techniques were developed within the sputtering and evaporation techniques, as shown in Table 3 [31].

Table 3 – Sputtering and Evaporation Techniques. Reproduced from [31]

Sputtering		**Evaporation**	
- Ions Beam		- E-Beam	
- Diode		- Inductive	
- Triode		- Resistive	
- Reactive Sputter			- Stirred
- Deposition		- Arc	- Random
	- Radio Frequency (RD)		- Cathodic Arc Deposition
	- Direct Current (DC)		
	- Magnetically Enhanced Plasma (MEP)		
	- UBMS - Unbalanced Magnetron Sputtering		
- Magnetron	- DMS - Dual Magnetron Sputtering		
	- HiPIMS /HPPMS - High-Power Impulse / Pulse Magnetron		
	- Sputtering		

In the sputtering processes, densification of the films is possible by playing with the deposition pressure and voltage applied to the subtract [32]. In this process, cleaning the substrate surface to remove contamination is also possible by applying a very high bias at the substrate. In an e-beam evaporation process, the target acts as a cathode and with the heating through the electron beam, the atomic-sized particles undergo evaporation and collide with the gas molecules that are

introduced into the reactor to accelerate these particles, and thus, are deposited onto the substrate, forming successively compressed layers with excellent adhesion. This process has the disadvantage of contaminating the film. Moreover, due to the higher temperature, some materials cannot undergo the process [31]. Figure 4 illustrates these two processes, emphasizing the difference between them [36].

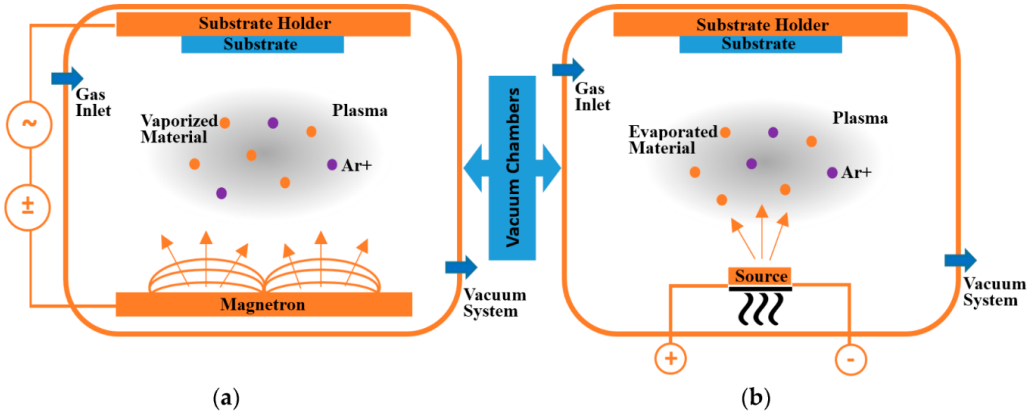

Figure 4 - PVD methods: (a) sputtering (b) evaporation. Reproduced from [36]

In the PVD process, good adhesion is always reached in steel substrates however such adhesion depends on the level of contaminants on the surface, use of interlayers and gradient layer and on the deposition conditions in general. The PVD coatings deposition on complex geometries are considerably more difficult to conduct when compared to the CVD process [2].

As seen earlier, there are many techniques within the PVD method. The most used method to produce PVD coatings is the magnetron sputtering technique, however, the HiPIMS (High Power Impulse Magnetron Sputtering) technique has shown to be very promising. This technique allows to tune the direction and ionization fraction of the sputtered species, producing films with differentiated properties [37].

As it is a technique under development, many studies have been carried out in the last 10 years. Wang et al. [38], deposited TiN coatings by HiPIMS with different N_2 flow rates. They showed that the nitrogen flow rate is of great importance because it influences the surface microstructure of the coatings. Promjantuk et al. [39], using the high-power reactive magnetron sputtering technique with the angle-of-view deposition (GLAD) technique at room temperature, analyzed the structural and optical properties of alternative films of titanium nitride nanorods plasmon (TiN-NRs). Furthermore, Azim et al. [40], using CrAlN and TiAlN coatings deposited by high power magnetron sputtering (HiPIMS), analyzed the wear of coated microdrills in Incoloy 825 microdrilling. They demonstrated that the TiAlN coating allowed superior performance than the CrAlN coating due their higher hardness, better coating adhesion and better tribological properties.

Therefore, this technique shows a strong potential in the production of coatings with good properties, and much of this is attributed to the high ionization rate allowed by this technique, making the technique very promising to protect the surface of tools used in machining. In the literature it has been reported that the mechanical properties of HiPIMS coatings are in the most of the cases much higher than the ones possible to get by conventional sputtering techniques [41].

Choosing the ideal technique is essential to succeed in the desired application, and with that, there have been some studies comparing the properties of films deposited by different techniques.

Tillmann et al. [42], analyzed the DCMS (Direct Current Magnetron Sputtering) and HiPIMS techniques, in the deposition of TiAlN and TiAlN/TiAlCN coatings, in AISI H11 quenched and tempered tool steel. The samples were evaluated regarding wear resistance and residual stresses, and the results were interesting, showing that the adhesion of the coatings obtained by DCMS was higher, and the wear coefficients of all the evaluated HiPIMS systems were lower than DCMS. In addition, the coatings obtained by HiPIMS had higher residual stresses than the DCMS coatings. Table 4 presents several recent articles, carried out on deposition through the PVD process.

Table 4- Summary table of studies carried out on PVD process.

Authors	Summary
Zauner et al. [43]	In this work, the R-HiPIMS technique was used for the deposition of TiAlN coatings using different composite targets ($Ti_{0.6}Al_{0.4}$, $Ti_{0.5}Al_{0.5}$ and $Ti_{0.4}Al_{0.6}$). Several deposition parameters were studied, such as pulse frequency and duration, N_2 flux rate and substrate polarization potential, in order to evaluate different growth mechanisms by surface diffusion, with several possibilities of final coating properties.
Alami et al. [44]	In this review paper focused on the HiPIMS process, addressing the advantages and limitations of the method, the mechanisms that occur in the discharge and on the surface of the coating during its deposition, resulting properties, control and improvement were studied. Finally, TiAlN coatings were deposited using an industrial coater, thus producing a coating with a high density nanocrystalline structure, and a smoother surface compared to coatings applied by DCMS. Furthermore, the authors found that the deposition rate compared to the DCMS process was equal on the flank face of the substrate and 60 % higher on the rake face.
Chang et al. [45]	In this work, thin films of Ti1-xAlxN were deposited on silicon Si (100), tungsten carbide (WC-Co) and SUS304 substrates using the high power magnetron reactive sputtering technique, and showed that the atomic ratio Al/(Al + Ti) of the alloy target determines the final structure of the coating, so they used the ratios 0.19; 0.36 and 0.57 for comparative purposes. The highest hardness and elastic modulus values were obtained using the ratio of 0.19, and the friction coefficients observed were between 0.68 and 0.77, both in relation to the Ti1−xAlxN thin films.
Romero et al. [46]	In this study nanoscale TiAlN/TaN multilayer coatings were deposited by DC magnetron sputtering on AISI M2 steel, and their tribological microstructure evaluated. The deposition was performed with the first layer of TiAlN/TaN followed by the second layer of TiAlTaN and adding four more possible combinations. The multilayer architecture was done by controlling the rotation speed of the substrate to obtain different period thicknesses. Regarding the compressive residual stresses, a reduction from -8 GPa to -1 GPa was observed for multilayer coatings compared to the monolayer constituent. In addition, it was identified that the best combination in layer percentage is 48% TiAlTaN and 52% of TiAlN/TaN, given the best balance between mechanical properties, such as high adhesion, hardness (29 GPa) and friction coefficient (0.68).
Liu et al. [47]	In this work, the morphology, adhesion strength, tribological properties, corrosion resistance and oxidation resistance of Al-rich TiAlN coatings produced using the HPMS technique were evaluated. The hardness obtained was 34.4 GPa with a deposition rate of 0.45 µm/min, and an adhesive strength (F) of 75 N. In addition, one of the most important aspects of this work was the surface roughness of 17.8 nm, with few particles produced on the surface, a priority factor desired in that work.

2.2.2. Chemical Vapor Deposition

The CVD deposition process was the first process used in the production of TiN and TiC to extend the surfaces' lifetime. The process consists of producing the coatings with a precursor pumped into a reactor, and with that, the precursor molecules pass through the substrate which is inside this reactor, being then deposited on the surface of this substrate by the reaction with other gas stimulated by the temperature [29]. The process can reach 900 °C, much higher than the temperature of a PVD process. The generated film has good hardness and small thickness, which is uniform across the substrate surface [3]. In addition, the CVD process involves the production of toxic gases, unlike the PVD process [31]. Another aspect worth mentioning is energy efficiency, which in the PVD process is considerably lower, as shown in Figure 5 [36].

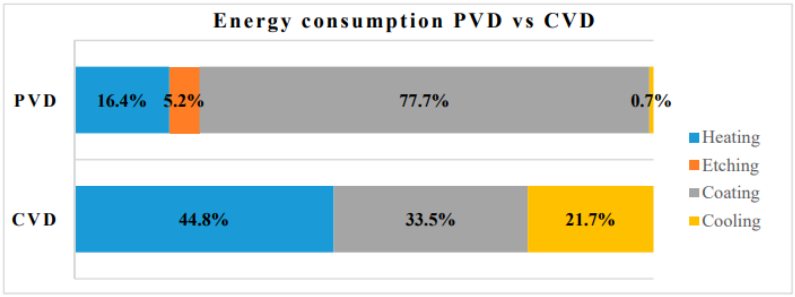

Figure 5 - Energy consumption of PVD and CVD methods. Reproduced from [36].

However, the process also has some advantages, such as the ability to deposit coatings on refractory materials; the possibility of controlling the grain size of the coating just by changing the process parameters; and furthermore, it is a method carried out at atmospheric pressure [29]. An important characteristic of the CVD technique is that it allows to produce coatings with uniform thickness and low porosity even on substrates with complex geometry [48].

A wide range of materials can be deposited by the CVD technique as thin films, including semiconductors, insulators, barrier layers, metals, silicates, superconductors, and organics. The applications are diverse as in the manufacture of microelectronic and optoelectronic devices, optical devices, protective and decorative coatings [49]. However, among the applications the most important use is in the deposition of functional materials for use in the electronics areas [50].

As stated earlier, the gaseous reactants are placed into the reactor. Thus, five reaction zones involving gas flows and temperature occur during the process and influence the final properties of the formed film. Figure 6 illustrates the principle of the process [48].

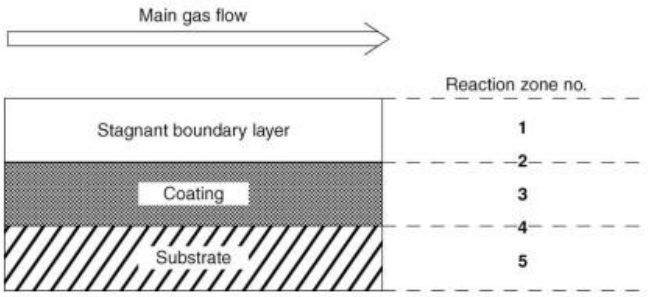

Figure 6 - Main reaction zones in a CVD process. Reproduced from [48]

In reaction zone 1, homogeneous reactions can occur characterized by a flaky and non-adherent coating, however, in some cases, these reactions are favorable, for example in the formation of Al_2O_3 coating, since the reaction occurs but no homogeneous nucleation takes place. In zone 2, heterogeneous reactions occur, which determine the reaction rate and final properties of the coating, because this zone is where the boundary phase between the vapor and the coating takes place. In zones 3 to 5, solid-state reactions such as precipitation, recrystallization, grain growth and even phase transformation occur. In turn, in zone 4, diffusion occurs and is where intermediate phases responsible for adhesion to the substrate are developed [48].

Another important feature of the process is its temperature dependence, which follows the scheme shown in Figure 7. Based on this scheme, it is possible to see that at low temperatures (region I), the growth rate of the film follows the Arrhenius Law. By increasing the temperature (region II) a plateau is reached in which the process of diffusion from the material to the substrate controls the deposition rate. At elevated temperatures, deposition rates decrease, as desorption processes begin to compete with the deposition process (region III) [50].

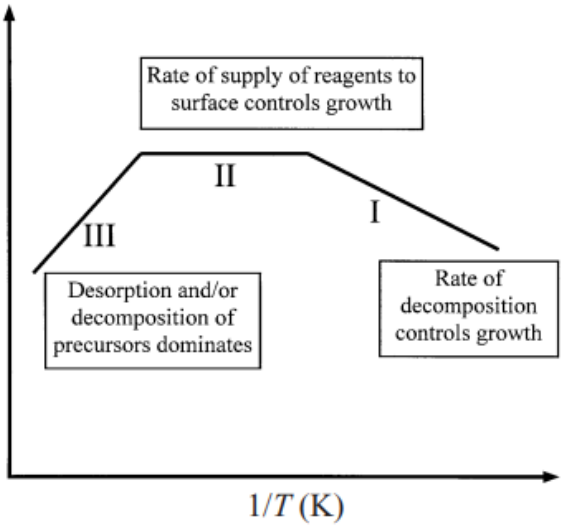

Figure 7 - CVD process temperature variations. Reproduced from [50]

Based on this, it seems that the different techniques give different properties to the coatings. Therefore, choosing the ideal technique is crucial to determine the correct properties for a given application [51]. Both the CVD technique and the PVD technique have advantages and limitations,

and those should be taken into account depending on the application for which the part need to work [52]. Table 5 presents several recent articles, carried out on deposition using the CVD process.

Table 5 - Summary table of studies carried out on CVD process.

Authors	Article abstract
Davim et al. [53]	In this work, the performance of CVD-coated tools with diamond in the turning machining of PEEK (polyetheretherketone) and PEEK CF30 was analyzed, and the cutting forces and surface roughness were measured. The results showed superior performance of these tools when compared to polycrystalline diamond (PCD) and carbide (K10) tools.
Schalk et al. [54]	In this work TiB_2 coatings were deposited over carbide substrate using CVD process, with and without TiN-based layers focused on analyzing the residual stresses. Thus, it was verified that the TiN base layer presented tensile stresses, and in the TiB_2 layer compressive stresses were observed, which increased as the layer thickness increased. Furthermore, the origin of the compressive stresses was determined to be due to the nanocrystalline nature of the coatings.
Kainz et al. [55]	In this work, TiN, TiBN, TiCN and TiBCN coatings were deposited via CVD, since according to the authors, adding elements in the TiN coating improves their performance. Based on this, it was found that TiBCN has the highest hardness (32.2 ± 1 GPa), Young's modulus (587 ± 29 GPa) and level of residual stresses (8.5 ± 0.4 GPa). The TiBN coating showed higher fracture toughness (5.0 ± 0.3 MPa).
Shen et al. [56]	In the present work, a new method was developed to manufacture single layer diamond tools by the CVD technique. The layer was formed from diamond powders in the range of 7–180 µm, randomly distributed on SiC substrates. In these substrates, CVD diamond growth occurred both in the substrates and in the seeds simultaneously. Thus, it was found that CVD diamond tools had the highest wear resistance, due to the epitaxial grain structure.
Jetpurwala et al. [57]	In the study, the authors produced MDC (microcrystalline diamond coating) and NDC (nanocrystalline diamond coating) coating on tungsten carbide drills, using the HFCVD (Hot Filament Chemical Vapor Deposition) technique, with the objective of evaluate the adhesion of the films to the substrate. These drills were evaluated at 250,000 rpm after cavity preparations in the teeth, and the NCD coating adhered better compared to the MDC.
Silva et al. [58]	In this work, the authors investigated the machining of GX2CrNiMoN26-7-4 Duplex Stainless-Steel, using PVD- and CVD-coated tungsten carbide inserts with different coatings: PVD-coated with AlTiN, and CVD-coated inserts with $TiN/TiCN/Al_2O_3$. It was verified that the substrate on which the CVD coating was deposited suffered more severe degradation. Furthermore, the longer the coating was in operation, the less wear on the substrate was observed, and the better the roughness of the machined surface. In addition, the wear suffered by the AlTiN coating deposited by PVD was lower and, therefore, it is more suitable for machining the DSS alloy.

2.2.3. Characterization of coatings for machining tools

Coatings are produced in such a way that they are functional for a specific application. This can be done by controlling their thickness, geometry and composition, which are interrelated with the resulting microstructure and mechanical properties. For this to be possible, there must be several types of coating which can be produced: monolayer (single layer) coating; bilayer (double layer) coating; gradient coating; multilayer coating; nanolayer coating; and nanocomposite coating [59]. These types of coatings are illustrated in Figure 8 [60]. Among these coatings, multilayer coatings are the most used in the machining area, due to their excellent combination of mechanical and thermal properties, such as greater resistance to crack propagation, hardness, adhesion, and consequently, wear resistance [29]. Based on this, Kainz et al. [61] compared the performance of multilayer TiN/TiBN coatings produced by CVD process, with the coatings of these individual compounds. They noticed through micromechanical bending tests an increase in strength and fracture toughness with the addition of Boron, and with the increase in the number of layers. Moreover, multilayered TiN/TiBN has shown greater hardness as compared to individual layers.

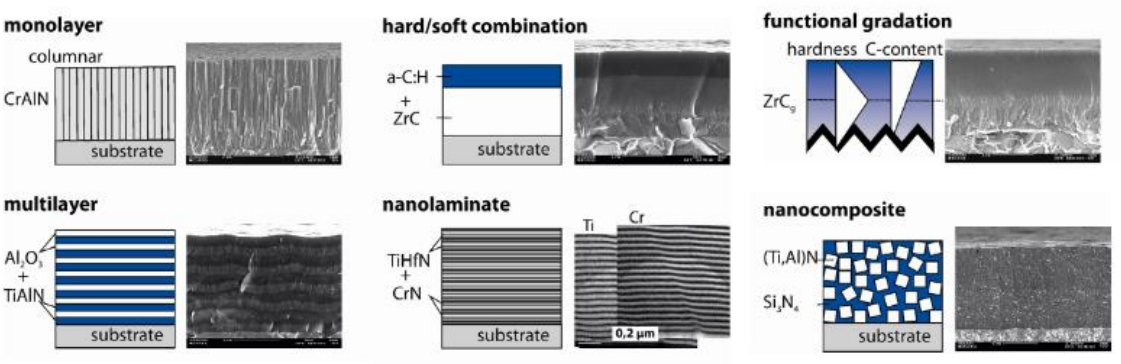

Figure 8 – Possible configuration/architecture of coatings. Adapted from [60].

Coatings can also be characterized regarding their chemical composition: nitrides, oxides, borides, carbides, carbo-nitrides, etc. Coatings chemical composition must be thus selected according to the application to which they will be subjected [29].

In single-layer coatings, increasing hardness usually results in brittleness, which can cause cracks formation and propagation [62]. To prevent this propagation, multilayer coatings can be used which can act as a crack propagation inhibitor [63]. Another aspect related to multilayer coatings, depending on the characteristics of the layers and materials involved, is that it prevents the propagation of frictional heat to the cutting tool, significantly reducing the interaction between the part and the tool, and contributing to a lower residual stress [64]. In addition, since the multilayer configuration is composed of several layers, different combinations of materials and properties are possible, and that by combining the advantage of each component, it can result in the optimization of mechanical processes, tribological properties and ensure the chemical stability of the coating [62].

2.3. Recent advances in coatings for cutting tools

It is known that the coatings commonly applied to tools are nitrides, carbides, borides and transition metal oxides [2]. Table 6 exemplifies some of these coatings.

Table 6 - Examples of compounds used for cutting tool coating [29]

Chemical Compost	Coatings for Cutting Tools
Nitrides	TiN, TiAlN, CrN, ZrN, TiSiN, TiAlSiN, CrAlN, TiAlCrN, CBN;
Carbides	TiC, CrC and WC
Borides	TiB_2
Transition metal oxides	Al_2O_3
Others	Diamond-Like Carbon (DLC), MoS_2 and WC-C

Many recent works made their analysis based on the comparison between coated and uncoated cutting tools, and with that, it was verified that the coating makes the machining process more efficient. This have shown also to depend on the type of coatings and the type of material to be machined. Table 7 summarizes some recent studies on the coatings that have been applied to cutting tools.

Table 7 - Summary table of studies carried out on coatings applied to cutting tools

Authors	Article abstract
Ucun et al. [65]	In this work, the machinability of the Inconel 718 superalloy was analyzed, through a tool coated with DLC in dry cutting conditions and changing the feeds and cutting depths. It was observed that the use of the coating improved the surface roughness, reduced the formation of burrs, and the Built-up Edge (BUE), which was significantly higher in the uncoated tool. With these coatings, there was thus a great improvement in the performance of the machining operation of the Inconel 718 alloy.
Durmaz et al. [66]	Durmaz et al., in their work, used carbide tools coated with TiAlSiN, AlCrN and TiAlN films in end mills to evaluate the machining of Impax steel. The TiAlN coating had better adhesion and lower surface roughness. The TiAlSiN coating had the highest wear, and the lowest wear rate was obtained for the uncoated tool. Furthermore, among the coated tools, the tool with TiAlN presented the highest wear resistance.
Bohleya et al. [67]	In this study, micro end mills with a diameter smaller than 50 µm and coated with Titanium di-boride (TiB_2) were investigated, since B_2 in the coating is known by reducing the friction in the contact. It was possible to determine the minimum diameter that the tool must have, so that, the process is still possible, i.e., tools with a diameter (Ø) of less than 6 µm with a TiB_2 layer of 200 nm.
Bjerke et al. [68]	In this study, the chemical degradation mechanisms of Al_2O_3-coated tools were analyzed as a wear mechanism, showing that alumina is resistant to chemical degradation by steel in the absence of oxygen, during the machining operation, however, it degrades into mixed oxides of the spinel type $(Al,Fe)_3O_4$. Beyond that, the presence of Ca, Si, Mn, Mg and Fe oxides in contact with the coating was observed, with MgO being the most aggressive, due to the formation of $Mg_1Al_2O_4$ spinel and complete dissolution of the coating. With this study, it will be possible to predict the possible wear and tear that may occur and take precautions against this phenomenon.

Table 7 - Summary table of studies carried out on coatings applied to cutting tools (continuation).

Authors	Article abstract
Gobivel et al. [69]	Gobivel et al., analyzed chip formation, cutting force, thrust force, temperature and wear of tools coated with TiN and Al_2O_3 in machining Ti-6Al-4V alloy. It was observed that the Al_2O_3 coating had lower shear forces as compared to the TiN coating. In Al_2O_3 the predominant wear was abrasion and in TiN flanking at higher cutting condition. In addition, the Al_2O_3 coated tool had higher interface temperatures than TiN.
Grigoriev et al. [70]	In this work, the tribological properties, wear resistance, and fracture behavior of multicomponent nanostructured coatings of Zr-ZrN-(Zr,Cr,Al)N and Zr-ZrN-(Zr,Mo,Al)N, using Ti-TiN-(Ti,Cr,Al)N as a reference coating, during the turning of Inconel 718 alloy was studied. As a result, it was verified that the tool coated with Zr-ZrN-(Zr,Mo,Al)N had a wear resistance of 2.4 times larger than the reference tool. In addition, the formation of oxides was verified in both test coatings, which brought a positive aspect to the process.

2.3.1. TiAlN-Based Coating

As the coating to be analyzed in this work is the multilayer TiN/TiAlN coating, this section will be dedicated to the summary of the main properties of the TiAlN-based coatings. The first coating system applied to cutting tools was the TiN (Titanium Nitride), which has excellent corrosion and erosion resistance, high hardness, and can be applied in various ways, such as “magnetron sputtering”, ion beam depositions, plasma, and CVD [71]. Aluminum was added to these coatings forming TiAlN (Titanium Aluminum Nitride), which shows better performance in high speed machining and holds a good oxidation resistance because of the type of oxide layer formed on its surface [72].

Thus, these coatings are widely used nowadays, and analyzed as object of study of several researches in different applications [3]. As stated in section 2.2.3, the coatings can be deposited and formed by different layers, as in the case of TiAl-based coatings, which can be commonly observed as TiAlN-based monolayers, multilayers or nanolayered coatings. Regarding the first one, this coating has been deeply analyzed nowadays mainly doped with other elements, aiming to improve the performance of the tool in the machining process. Table 8 summarizes some studies regarding the monolayer TiAlN coating.

Table 8 - Summary table of studies carried out on monolayer TiAlN-based coating

Authors	Article abstract
Aninat et al. [73]	Aninat et al., carried out a comparative study between Ti-Al-N, Ti-Al-Y-N, Ti-Al-Ta-N and Ti-Al-Ta-Y-N coatings, observing that Y (Yttrium) element increases the hardness value; the element Ta increases the compressive stress and makes oxidation possible. Thus, in the case of the Ti-Al-Ta-Y-N coating, in which these two elements were added to the TiAlN base coating, it is verified that the hardness is related to the element Y, and the rate of oxidation is due to the element Ta.

Table 8 - Summary table of studies carried out on monolayer TiAlN-based coating (continuation).

Authors	Article abstract
Yang et al. [74]	This work evaluated the influence of Mo additions on the properties of TiAlN coatings. Five different Mo contents were added by magnetron sputtering. In all cases good adhesion was observed in the WC-Co tool, better wear resistance was observed for Mo content of 8.3 at.%, due to the formation of molybdenum trioxide and increase in hardness and Young's modulus as the element content increased.
Yi et al. [75]	In this work, the behavior of AlTiN-Ni coatings with different concentrations of Ni (Nickel) and AlTiN were compared. It was observed that increasing Ni content, the hardness decreased, and with a Ni content of 1.5at%, the coating presented high fracture toughness and adhesion strength, which dropped significantly when increasing the Ni content to 3at%. Still, Ni content of 1.5at% has provided the coating with the longest useful life, increasing by 160%.
Liu et al. [76]	In this work, the influence of Ru (Ruthenium) addition at various levels on the thermal decomposition and oxidation behavior of TiAlN coatings was evaluated. The coatings produced were: $Ti_{0.46}Al_{0.54}N$; $Ti_{0.43}Al_{0.50}Ru_{0.07}N$ and $Ti_{0.34}Al_{0.51}Ru_{0.15}N$. In the latter case, precipitation of AlN and a drop in hardness are observed, which had a significant improvement in the second case. Regarding the tool life with the coatings, an improvement by ~32% through 5 at.% Ru addition was verified, under certain machining condition.

Regarding multilayered coatings, this is the type of coating most used, given its flexibility and the possibility of combining properties for different applications [77]. Due to these possibilities, many studies are focused on this purpose, and TiAlN-based coatings are not excluded from this trend. In addition, nanolayer coatings, which are also considered multilayer, have, among the coatings mentioned in this section, the highest resistance to crack propagation, as the crack can be deflected through the interface of the surface layers.

In relation to recent studies, what is observed is the search for the improvement of the coating mechanical properties, and with that, many authors make their work based on the addition of elements, such as Mo, Ta (Tantalum) and Cr (Chromium), which are characterized by improving the mechanical properties of the coating, such as hardness, resistance to crack propagation and adhesion. Thereby, Table 9 summarizes some studies regarding the multilayered TiAlN-based coating.

Table 9 - Summary table of studies carried out on multilayered TiAlN-based coating

Authors	Article abstract
Li et al. [78]	In this study, TiAlSiN coatings with five different multi-layer configurations were deposited through HiPIMs to evaluate the machining of Inconel 718. The layers were: single-layer TiAlSiN-A (with higher adhesion strength), single-layer TiAlSiN-B (with higher hardness), bilayer, four layers and eight layers. Among the five coatings, the 8-layer coating had the highest toughness and longer service life. In general, an increase in toughness and compressive stress was observed, which brought a positive aspect as it alleviates the damage caused by the impact of the tool with Inconel 718, which is a high hardness alloy.

Table 9 - Summary table of studies carried out on multilayered TiAlN-based coating (continuation)

Authors	Article abstract
Çomaklı [79]	In the present study, ceramic films TiN, TiAlN monolayer and TiAlN/TiN multilayer deposited by cathodic arc PVD were compared and the resulting properties of the films were evaluated. The grain sizes of the multilayer film are thinner, more stable, and harder, and the surface has shown hydrophobic behavior. With this, the author concluded that the multilayer coating has superior properties.
Li et al. [80]	In this study, multilayer TiN/TiAlN coatings with various numbers of bilayers were analyzed, to identify the influence of the number of bilayers on mechanical properties and corrosion behavior. It was found that by increasing the number of bilayers, the resulting hardness also increased, reaching 3800 $HK_{0.025}$ in the coating with twelve bilayers. This same coating showed a tendency to corrode.
Varghese et al. [81]	In this work, Varghese et al., analyzed the wear performance of the multilayer TiAlN/NbN coated tool in dry end milling of AISI 304 austenitic stainless steel. Microchipping and coating peeling were observed during the machining operation, which may have occurred due to the lack of lubricant in the process.
Zheng et al. [82]	In this study, the antifriction characteristics, and the wear mechanisms of the TiAlN/TiN coated tool in high strength steel (300 M steel) were evaluated. As a wear mechanism, the authors observed adhesion, abrasion, chipping, and coating delamination. This wear may have been caused due to the high operating temperature. An important aspect in this work was the formation of oxide films on the worn surface, which was responsible for the lubrication of the process, as it prevented the direct contact of the tool with the part.
Wang et al. [83]	In this study, TiN/TiAlN coating was characterized based on its mechanical properties, after cathodic arc deposition. The authors identified that the ideal thickness of the layers, i.e., the one in which the best mechanical properties were obtained, was 13 nm. The main highlight in this study is the resistance to crack propagation, which was improved due to the thin layer thickness, and also improved the coating wear behavior.
Pshyk et al. [84]	Pshyk et al., in their study, evaluated (TiAlSiY)N nanocomposite and (TiAlSiY)N/MoN nano-scale multilayer coatings. The (TiAlSiY)N/MoN nano-scale multilayer coating had 10 nm layers thickness. The authors observed that the multilayered coating had the preferred orientation, and better wear performance. On the other hand, the mechanical properties of the multilayered coating were better.
Geng et al. [85]	In this work, TiSiN/AlTiN multilayer film was deposited by cathodic arc evaporation technique and the microstructure, mechanical properties, high temperature wear rate and milling performance of the multilayer film were analyzed. The tool was tested on dry milling of SKD 11 tool steel. The hardness and elastic modulus obtained are 41.7 ± 1.6 GPa and 340 ± 17 GPa, respectively. The authors noticed an increase in the wear rate with increasing temperature, however, the presence of the film decreased the adhesion of the tool material to the machined material, increasing the cutting tool lifespan.

2.4. Wear mechanisms associated with cutting tools

Firstly, it is known that tool wear is related to its performance, being the main indicator of tool lifespan. The more the tool wear the shorter the lifespan is [29]. In machining, it can be said that wear is caused through interactions between the tool, the part to be machined and the chip generated during machining [2]. As the part to be machined can be composed of different materials, as well as the tool, and the parameters can vary from process to process, the wear mechanism can be observed in different ways and differs from case to case, being an important aspect that touches on the optimization and improvement of machining processes [3].

The tools, therefore, can experience abrasive wear, mechanical wear, adhesive, chemical and thermal wear. Within these mechanisms, there are types of wear, for example flank wear is abrasive wear, built-up edge is adhesive, among others. Table 10 summarizes the mechanisms and the respective types of wear, and its corresponding description [13]. Figure 9 illustrates the aspect of some types of wear whose can be found in cutting tools [86].

Table 10 - Mechanisms, types, and description of wears [84]

Type of wear	Description
Flank wear	Wear caused by abrasion between material and tool. Very common wear that generally does not affect the life of the tool, which remains functional.
Chipping	Chipping occurs when the machining parameters have not been correctly selected, or due to chip yielding, which causes a compressive stress load above the supported limit.
Notch wear	It occurs due to the formation and propagation of microcracks in the flank and face of the tools, resulting in fractures in the cutting edge.
Built-up edge	As the machining process is carried out at high pressures, the material may weld on the tool, and this generates problems in the final quality of the machined part.
Crater	Wear due to chemical reaction that takes place between the material and the leading edge of the tool.
Deformation	As temperatures increase during the machining process, the tool undergoes plastic deformation.
Fracture	Fractures perpendicular to the cutting edge due to sudden temperature changes can occur in the tool during the machining process.

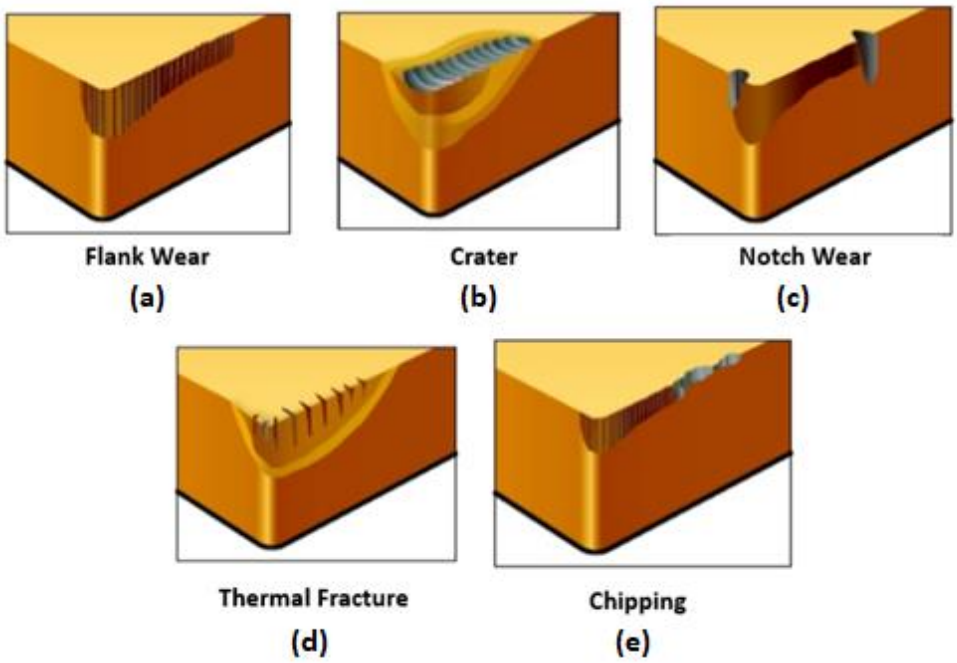

Figure 9 - Wear types occurring in cutting tools during machining operations: (a) flank wear; (b) crater; (c) notch wear; (d) thermal fracture; and (e) chipping. Adapted from [86]

Thus, the tool wear mechanisms can be an indicator that the process parameters are not well fitted and must be improved and optimized, or even, changing the type of coating, and adjusting the parameters for this new coating [29]. Thus, analyzing the wear of the coated tool is also a great way to optimize the process, and even further increase the tool life. When tools are coated, they can suffer the same wear mechanisms as described above, and in addition, they present coating wear mechanisms, such as delamination, cracking and chipping of the coating itself [2]. Figure 10 illustrates an adhesive wear on a coated tool [87], and Figure 11 illustrates a flank wear and crater wear of CVD TiN/TiCN/Al_2O_3 [58].

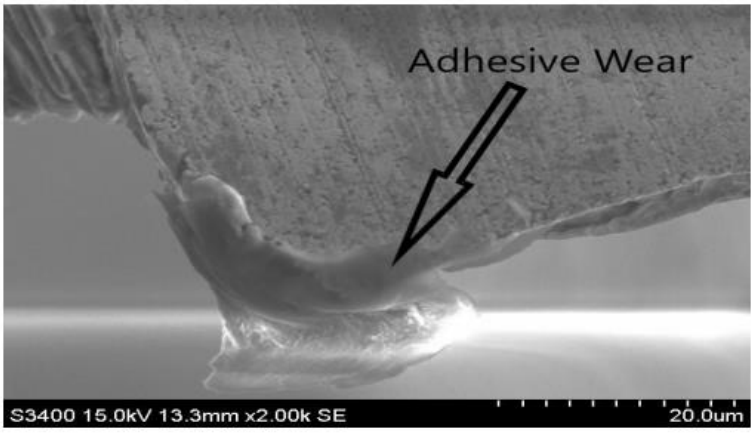

Figure 10 - Adhesive wear on a coated tool. Reproduced from [87].

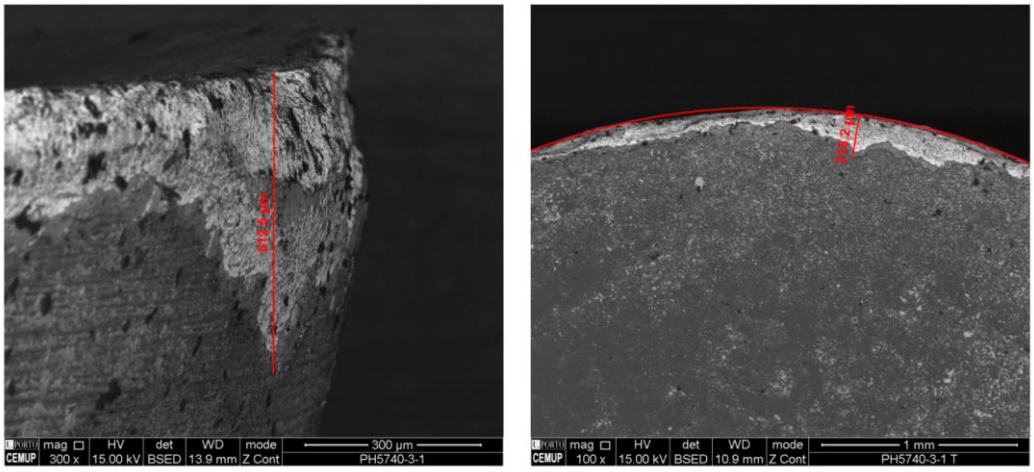

(a) (b)

Figure 11 - Wear of CVD TiN/TiCN/Al_2O_3: (a) Flank wear (b) Crater wear. Reproduced from [58].

Therefore, studies have been carried out on the wear mechanisms of different coatings to be used in machining operations. Table 11 shows some studies related to the milling process, which is the operation analyzed in this work. It is important to note the different wear patterns that the coatings in these studies suffered. The machining parameters used are related to the tool life, and as wear increases, the performance of the coating decreases until failure of the cutting tool is observed.

Table 11 - Summary table of studies carried out on wear mechanisms in milling tools

Authors	Article abstract
Martinho et al. [88]	In this work, the wear present in tools with diamond coated Si_3N_4, and without coating was analyzed, showing that the wear mechanisms present in all cutting conditions were of mechanical, adhesive, and chemical origin, i.e., abrasion, adhesion, and diffusion. However, the authors found that the useful life of diamond inserts was longer.
Liu et al. [89]	Liu et al., based on previous results of their work, analyzed the effects of cutting speed on tool life, wear mechanism and surface quality of parts in uncoated and CrAlN and TiAlN PVD coated Si_3N_4 tools at high-speed face milling of gray iron at various cutting speeds ranging from 600 m/min to 1500 m/min. The results showed that at lower speed the life of the coated cutting inserts decreased with increasing cutting speed, and on the other hand, when reaching a certain value of cutting speed, the tool life increased with the increase of this cutting speed. Abrasive wear was observed, and at the end of the tool life, adhesive wear was observed along with the abrasive wear. Furthermore, an important aspect was that the adhesive wear suffered by the TiAlN coating was more significant than that of CrAlN.
Bandapalli et al. [87]	In this study, PVD AlTiN and TiAlN coatings in high-speed micro milling of Titanium-Grade 12 were analyzed and the results compared with uncoated tungsten carbide tools. It was verified that the uncoated tools had a better performance than the AlTiN and TiAlN coated tools, being verified mechanisms of diffusion, oxidation, adhesive and abrasive wear, and delamination of the coating.

Table 11 - Summary table of studies carried out on wear mechanisms in milling tools (continuation)

Authors	Article abstract
Zuo et al. [90]	In the work by Zuo et al., a comparison of the wear mechanism was made among different cutting speeds (200 m/min, 400 m/min, 600 m/min, 800 m/min and 1000 m/min) in machining Be/Cu alloy with cemented tungsten carbide tools coated with PVD TiAlN. At 400 m/min, notch wear in the cutting edge and built-up edge was observed; at 600 m/min, built-up edge, notch wear and adhesive damage were observed, at 800 m/min Built-up layer and adhesive damage, and at 1000 m/min, built-up edge, notch wear and adhesive damage were reported, which shows that wear is influenced by cutting speed. For example, at higher speeds, the process temperature increases, and with that, above 600 m/min, adhesive wear appears, which according to the authors, wear and adhesive effects come from the thermomechanical effect.
Sousa et al. [91]	In the following work, a comparative analysis was carried out and the influence of cutting length and feed rate on the wear and performance of the tools in milling operations of AMPCO (Cu-Be) Alloy was evaluated. The analysis was performed with end-mill tools coated by multilayer DLC/CrN and uncoated solid-carbide. It was observed that both tools showed abrasion wear and material adhesion, and the coated tools presented more material adhered to their surface. Delamination and cracking of the coating were observed, with increasing cutting length.
Ni et al. [92]	In this work, the wear mechanism of PVD TiAlN coated cemented carbide was evaluated when milling Ti-6Al-4V, by three processes: conventional milling, UVAM (ultrasonic vibration assisted milling) and this process aided by MQL (minimum quantity lubrication). It was verified that this last method conferred to the machined material the best quality surface finish and even with wear (adhesive and chipping) had better performance. In conventional milling, a large amount of adhesive wear was observed, including small amounts of Ti (titanium) adhered to the tool. In the second process, the greatest damage observed was chipping.
Kumar et al. [93]	Kumar et al., in their work, compared different coated cutting tools (TiSiN, Al_2O_3, Al_2O_3+ZrN) with commercially available tools (TiCN, TiAlN), for LAMM (laser-assisted micro-milling). Delamination was the main wear mechanism for tools coated with TiCN, TiSiN and Al_2O_3, showing that the wear performance of tools coated with TiAlN and Al_2O_3+ZrN was superior.
Çalışkan et al. [94]	In this study, the wear behavior and cutting performance of carbide cutting tools coated with AlTiN/TiN and TiAlSiN/TiSiN/TiAlN in face milling without lubrication of AISI 02 tool steel was investigated, and it was verified that the main wear mechanism was abrasive and oxidative wear, being the better adhesion to the substrate provided by the AlTiN/TiN coating, as well as a greater wear resistance in the milling process.
Chang et al. [95]	In this work, the performance of TiAlN, CrAlSiN and TiAlSiN coatings on the wear behavior and cutting performance of the carbide cutting tools in the machining of Ti6Al4V alloy was analyzed. Adhesive and abrasive wear were found for the TiAlSiN and, TiAlN coated- and uncoated tools, however, the TiAlSiN nanocrystalline coatings caused the wear to be slower compared to the TiAlN coated tools. In turn, CrAlSiN coatings showed high wear resistance in this case, being therefore superior to other coatings and having better cutting performance and tool life.

Table 11 - Summary table of studies carried out on wear mechanisms in milling tools (continuation)

Authors	Article abstract
Kursuncu et al. [96]	In this study, the magnetron sputtering method was used to deposit a multilayer coating of TiAlSiN/TiSiN/TiAlN, and then to analyze the wear mechanism that the tools presented during the face milling process of the Inconel 718 under dry conditions. Abrasive and adhesive wear were verified as the main wear mechanisms, and when comparing the coated tools with those without coatings, it was noticed that the coated tools had better wear resistance, 1.7 times longer tool life and a smoother surface on the material.

2.4.1. Tool Lifespan

Based on the possible main types of wear mechanisms and the failure methods of the tool, Table 12, correlates the potential cause of the wear mechanism to occur, and how the tool would eventually fail [29].

Table 12 - Main types of wear mechanisms, with the potential cause to occur, and failures modes. Adapted from [29]

Main types of Wear Mechanisms	Potential Cause	Failure Mode
Abrasive Wear	High material hardness, dry conditions	Fracture, Crater formation, Coating delamination
Adhesive Wear	High temperatures during the machining process, Metallurgical affinity, soft material	Delamination, Edge build-up, Notch wear
Chipping	Conditions of the process, including dry condition, material with high hardness, crack propagation	Crater formation
Delamination	Crack propagation	Fracture, spalling

As seen in Table 12, the wear caused by machining on the tool and its coatings causes the tool life to decrease, which can, for example, cause high replacement or maintenance costs. Based on this, and with a view to reducing operating costs, many works have emerged as a way to improve the useful life of machining tools, through process optimization and product quality improvement [97]. Furthermore, it is known that the main parameters able of influencing the wear mechanisms in the milling operation are cutting speed, feed rate, machining temperature, vibrations, cutting forces and cooling/lubrication conditions [98]. Another important aspect when considering tool life is the design of the coatings applied, such as monolayer coatings, multilayer coatings, nanostructured coatings or diamond coatings, since the mechanical properties and chemical composition of these coatings will impact the tool's performance, and each design has their own properties and characteristics [29].

Thus, when comparing the different types of design among themselves, different wear mechanisms and tool life are observed. For example, multilayered coatings have a higher resistance to crack propagation compared to monolayer coatings, thus providing them with a better wear resistance, and, consequently, longer life [29]. In turn, nanostructured coatings compared to multilayer coatings have a longer life due to their excellent mechanical properties [99]. Diamond coatings have shown promising properties, with the highest wear resistance due to their high hardness value, and they can have monolayer or multilayer designs [100]. At this point, it is important to note that there are some exceptions, emphasizing the importance of knowing the right coating for the certain application, as is the case, for example, of having a monolayered coatings with a higher tool-life compared to a multilayered coating [101]. There are many recent studies on improving the life of machining tools, as shown in Table 13.

Table 13 - Summary table of studies carried out on tool lifespan.

Authors	Article abstract
Sortino et al. [101]	In this work, AlCrN, TiSi-based, ZrN monolayered coatings; AlCrN-based and TiCN multilayered coatings; TiAlN nano-based coating and a PCD were studied, in order to analyze tool lifespan, since in Nickel-coated Nickel-Silver machining, the nickel coating improves wear resistance and gloss of the product (winder keys). However, the same coating makes the milling operation difficult, and the life of the cutting tool is reduced. The PCD tool presented the best result, and the AlCrN coating, with a maximum lifetime of 200 minutes, showed the lowest result.
Vereschaka et al. [102]	In the work carried out by Vereschaka et al., the microhardness, substrate adhesion strength and tool lifespan of a multilayer cutting tool coated with nanostructured Ti-TiN-(Ti,Al,Cr)N were analyzed. For comparative purposes, the layers had different thicknesses (t): 2.0, 3.0, 5.0, 6.0 and 13.0 µm. Machining (longitudinal turning) was performed on AISI 321 steel, at various cutting speeds (85, 100, 120 and 150 m/min), showing that 6 µm is the ideal thickness for the coating. Furthermore, the authors showed that at a higher thickness (13 µm) and with increasing cutting speed, tool life has a marked decrease, and in coating thicknesses between 2.0-6.0 µm there was a decrease in wear resistance with increasing cutting speed.
Oganyan et al. [103]	In this study, the Ti-TiN-(Ti,Cr,Al)N and Zr-ZrN-(Zr,Cr,Al)N coatings in VT20 titanium alloy milling with end mills were analyzed and compared with tools without coating. As for wear resistance, it was found better resistance of the Zr-ZrN-(Zr,Cr,Al)N coating to crack formation and brittle fracture compared to the Ti-TiN-(Ti,Cr,Al)N coating. In addition, when comparing the tool life, it was found that the tools provided with coating had a tool lifespan 2.5 to 3 times longer compared to the uncoated tool lifespan, and the Zr-ZrN -(Zr,Cr,Al)N coating had a longer tool lifespan than the Ti-TiN-(Ti,Cr,Al)N coating.
Aurich et al. [104]	Aurich et al., evaluated the relationship between the diameter of cutting tools (50 µm, 25 µm, 12.5 µm and 6 µm) and tool life in tools coated with a 200 nm thick layer of TiB_2 in micro-milling of pure titanium. Longer tool lifespan has been found when coating the tools, especially for the smallest diameters, 12.5 µm and 6 µm. Under these two conditions, the positive impact of coatings hence compensates the negatives. The authors suggested that this positive influence of coatings on small diameters is related to the increase in the proportion of the coating volume compared to the carbide volume.

Table 13 - Summary table of studies carried out on tool lifespan (continuation)

Authors	Article abstract
Zhang et al. [105]	In this work, two types of coatings were compared and evaluated in face milling of 316L stainless steel: TiN/MT-$TiC_{0.7}N_{0.3}$/TiCNO/α-Al_2O_3 (cm-Al_2O_3 based) and PVD nano-multilayered $Al_{0.55}Ti_{0.45}N$/TiN (pn-AlTiN based). The result showed that the coating based on pn-AlTiN has greater wear and delamination resistance, and the tool life is 2.1 times longer than that of the coating based on cm-Al_2O_3. In addition, the coatings showed edge chipping as predominant wear, which is the fatigue failure mechanism.
Beake et al. [106]	In the following work, the wear resistance of end mill tools coated with AlCrN-TiAlN and AlTiN, both deposited via PVD, in H13 tool steel machining, was analyzed. The study showed that the tool life, when compared to the AlTiN coating, improved by 100% when the AlCrN-TiAlN bilayer coating was used. In addition, the wear mechanisms observed were chipping from thermal fatigue and crater wear accompanied by build-up edge. Furthermore, the authors verified that the performance of the tool is related to the micromechanical properties of the coatings, since in the microscratch test the AlCrN-TiAlN coating had a superior integrity in relation to the AlTiN coating. With this, it was verified how the use of bilayer coatings are beneficial, resulting in better process stability, and generating superior performance with regard to wear resistance in H13 machining.

3. MATERIALS AND METHODS

In this chapter, the materials used will be presented as well as the methods that were approached for the execution of this work. For this, the chapter is divided into two subchapters, 3.1. Materials and 3.2. Methods.

3.1. Materials

In this subsection, all the materials used to carry out this work are presented. Those materials are: the base material that was machined, its shape, mechanical properties and chemical composition, and the cutting tools, emphasizing the material of the substrate and coating, and its geometry.

3.1.1. Machined Material

The material that was machined was the Inconel 718 alloy, which have a wide variety of applications, especially in areas such as chemical industries, marine, nuclear engineering [107], automotive, aeronautical and aerospace industries, due to its high mechanical strength, resistance to creep, and resistance to corrosion and oxidation [108]. This alloy displays high mechanical strength at elevated temperatures, of up to 650 °C [109], high hardness, low thermal conductivity, and tendency to work hardening at room temperature. However, these properties together make it an alloy that is difficult to machine, a process for which it is extremely important to produce engine parts and aircraft components [110].

Furthermore, this alloy tends to adhere to the surface of cutting tools, generates high cutting forces and raises the process temperature, which can reach around 1100 °C [111]. In addition, a significant number of hard carbides are observed in its final metallurgical structure, mainly Titanium Carbide (TiC) and Niobium Carbide (NbC). These carbides are responsible for the high abrasive behavior during the machining process, which increases the wear suffered by the tool, and the tendency to occur premature cutting failure [112]. Elements such as nickel, chromium, iron and traces of niobium, molybdenum, titanium, and aluminum can be found on the chemical composition of the Ni alloy. The composition of the Inconel 718 alloy in wt% is shown in Table 14.

Table 14 - Inconel 718 chemical composition (wt%).

Element	Percentage (wt%)
Nickel	53.89
Chromium	18.05
Iron	17.78
Niobium	5.35
Molybdenum	2.90
Titanium	0.96
Aluminum	0.51

Other elements in smaller percentage (wt%) are also observed such as cobalt (0.20), copper (0.10), silicon (0.08), manganese (0.078), boron (0.039), carbon (0.023), phosphorus (0.010), nitrogen (0.0070) and magnesium (0.0017). Furthermore, the presence of residual elements such as Ag, Ca, Pb, Bi, S and O can be observed. It is observed that in the alloy structure, the elements are dispersed through the nickel γ matrix in a face-centered cubic lattice (FCC) [108].

The workpiece was supplied in the form of a round bar with a diameter of 158 mm and underwent the following heat treatment: (1) solution annealing at 970 °C, followed by quenching in water; (2) precipitation hardening at 718 °C for 8 hours, oven cooling at 621 °C for 8 hours, and air cooling. As the initial bar supplied was 1 meter high, it was necessary to cut it with a band saw into 32 mm height sections. The material's mechanical properties are presented in Table 15.

Table 15 - Inconel 718 mechanical properties.

Material property	**Value**
Yield strength [MPa]	1188
Tensile strength [MPa]	1412
Elongation [%]	15
Hardness [HBW]	441

3.1.2. Substrate and tool geometry

The cutting tools used in the tests were end mills, composed of Tungsten Carbide (WC-Co) grade 6110, which has an average grain size of 0.3 µm. In addition, Cobalt (~6 wt%) was used as a binder. The tools were provided by the company INOVATOOLS, S.A. (Leiria, Portugal). The tool geometry is shown in Table 16.

Table 16 - Machining tool geometry

Tool geometry	**Value**
Cutting diameter	6 mm
Maximum cutting depth	13 mm
Total length	57 mm
Chamfer	45°; 0.20 mm
Helix angle	35°/38°
Rake angle	12°
Clearance angle	10°
Number of flutes	4

3.1.3. Coating

The coating used was the multilayer TiN/TiAlN, deposited by HiPIMS process using a CemeCom CC800/HiPIMS equipment. The deposition parameters, as well as the methodology used will be explained in section 3.2. This coating is known to be promising in the machining of Inconel 718, due to the formation of Al_2O_3 protective films between the coating and the material to be machined, which can help reduce wear and prevent premature failure of the cutting tool [113].

In addition, this coating has good wear and oxidation resistance. Because it is a multi-layer coating, the surface properties of the coating tend to be superior and beneficial for milling difficult-to-machine materials [114]. For example, in the work by Chen et al. [115], the performance of TiAlN single-layer and TiN/TiAlN multilayer coating was compared, showing that TiN/TiAlN multilayer coating gives high hardness value, that is, it had a superior performance to the single-layer coating.

In turn, Adesina [116] compared the tribological properties of TiN/TiAlN, CrN/TiAlN and CrAlN/TiAlN bilayer coatings deposited by cathodic arc PVD with thin and thick TiAlN monolayer coatings at 500 °C. As a result, it was observed that the hardness, modulus of elasticity and wear resistance of the bilayer coatings were higher, which may be associated with the formation of the oxide layer and improved adhesion of these coatings. In addition, Hsieh et al. [117], developed TiN/TiAlN multilayer coatings in three different modes varying shutter control, power supply control and rotational stage control using unbalanced magnetron sputtering. These multilayer TiN/TiAlN coatings were found to have lower wear rate than single-layer TiAlN, and in some cases, lower wear rate than single-layer TiN, with varying sliding speeds.

Thus, the tools were coated with a TiN/TiAlN multilayer coating after the substrate machining process. At this point it is important to highlight that before the coating process, the tools were subjected to a cleaning operation. Figure 12 illustrates a cutting tool coated with TiAlN/TiN multilayer coating.

Figure 12 - Cutting tool coated with TiN/TiAlN multilayer coating.

3.2. Methods

In this subsection, all the methods applied to carry out this work will be presented, that is, the PVD process of deposition of the multilayer coating, the machining parameters, characterization of the

thickness and morphology of the coating, hardness, adhesion, state of stress, roughness, wear mechanisms, cutting forces and tool lifespan analysis.

3.2.1. PVD Coating

As previously mentioned, the deposition of the TiN/TiAlN multilayer coating was performed by the PVD HiPIMS process using an CemeCom CC800/HiPIMS equipment, with four target holders. The adopted deposition parameters can be observed in Table 17. These parameters were selected from successful experiments performed before on similar substrates.

Table 17 - Parameters for deposition of TiN/TiAlN tool coatings.

Deposition parameters	**TiN layer**	**TiAlN layer**
Deposition time [min]	40	260
Reactor gases	$Ar^+ + Kr + N_2$	$Ar^+ + Kr + N_2$
Target amount/composition	2/Ti	2/TiAl
Pressure [MPa]	580	580
Temperature [°C]	450	450
Bias voltage [V]	-110	-110
Target current density [A/cm^2]	20	20
Holder rotational speed [rpm]	1	1

The deposition of the coating by HiPIMS process was carried out through the following procedure: (1) opening the obturators of the two pure titanium targets, resulting in the deposition of the first thin layer of TiN; (2) closing of these obturators and opening of the TiAl targets, resulting in the deposition of the outer layer of TiAlN. This layer was thicker than the TiN layer. After deposition of the coating, the tools were packed, and the cutting area was no longer handled. Other deposition conditions can´t be here disclosed since they were produced in coater enterprise.

3.2.2. Milling equipment and conditions

Machining tests were performed using a milling center of three axes to machine, CNC machining center HAAS VF-2 (HAAS Automation, Oxnard, CA, USA), with a maximum speed of 10.000 rpm and a maximum power of 20 kW. The equipment has a table with 914 mm long and 356 mm wide. The machine is located in the Mechanical Technology Laboratory of the Mechanical Engineering department of Instituto Superior de Engenharia do Porto (ISEP). Figure 13 illustrates the equipment. A spiral milling strategy was chosen, as the workpiece was supplied in circular geometry. With that, the milling was done from the center towards the periphery. Based on this strategy, the radial depth of cut was kept constant, in order to mitigate phenomena related to wear that could appear as a result of changing this parameter throughout the test. In addition, tests were performed using cutting fluid with 5 % oil in water, Alusol SL 61 XBB, which is a semi-synthetic metalworking fluid, that has 35 wt% of mineral oil content, with boron, formaldehyde releasing agent and surface finishing additives.

Figure 13 - CNC machining center HAAS VF-2 (HAAS Automation, Oxnard, CA, USA).

To fix the Inconel 718 workpiece, a self-centering bushing with three jaws, Bison 3575 (BISON-BIAL, Bliesk Podiaski, Poland), was used, as shown in Figure 14. In addition, the tools were fixed to the equipment using an ISO40 DIN69871 cone, an ER32 H70 collet holder, an ISO 7388-2 tie rod and an ER DIN 6499 collet. Tool clamping when measuring cutting forces will be explained in section 3.2.9. Characterization of cutting force measuring equipment.

Figure 14 - Assembly of the Inconel 718 part to be machined.

To determine the zero of the machining tool in relation to the surface of the workpiece in the machining center, a contact probe with optical transmission, from Renishaw (United Kingdom, England), model OMP40, was used (Figure 15). The probe was placed in the machining center, as close as possible to the center of the part, the approximate values of X and Y being assigned in the program, and the height of the probe tip to the workpiece surface, making it possible to determine the initial position of the axes X, Y and Z.

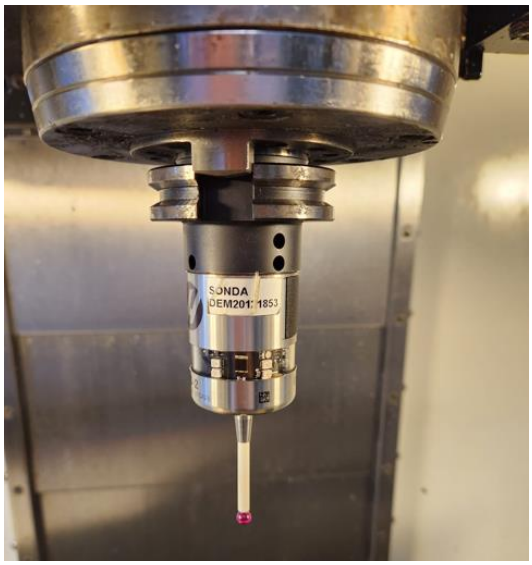

Figure 15 - Contact probe with optical transmission, from Renishaw (United Kingdom, England), model OMP40

Regarding the milling parameters, these were initially chosen from the tool's substrate provided, however, with the performance of some preliminary tests to confirm these parameters, some changes had to be made for the success of the process. For example, for the axial cutting depth (ap) values of 0.2 mm and 0.1 mm were selected. However, these values caused the tool to fail and break shortly after the initial plunge. Based on this, axial cutting depth had to be gradually reduced until reaching the value of 0.08 mm, in which it was verified that the tools were able to reach the end of the tests even at higher cutting lengths.

The parameters that varied in the tests were feed per tooth, cutting length, and cutting speed. Regarding the feed per tooth, the center value (100%) was 0.0700 mm/tooth, and varied 25 % for less, and 50 % for more. For the cutting length, the values of 5 and 15 m were selected, in order to verify the progression of wear in different cutting lengths, as well as the resulting surface roughness. The same happened with the cutting speed, in which three values of this parameter were fixed, 75 m/min, 100 m/min and 125 m/min, making it possible to verify the influence of the parameters in the milling of Inconel 718. Furthermore, as the tool diameter was 6 mm, the value of the radial depth of cut (ae) was 75% of this value, i.e., 4.5 mm, and kept constant in all conditions. All parameters and test conditions are shown in Table 18.

Table 18 - Parameters selected for the tests.

Reference	Vc [m/min]	fz [mm/tooth]	Cut. Length [m]	ap [mm]	ae [mm]
S75F75L5	75	0.0525	5	0.08	4.5
S75F75L15	75	0.0525	15	0.08	4.5
S75F100L5	75	0.07	5	0.08	4.5
S75F100L15	75	0.07	15	0.08	4.5
S75F150L5	75	0.105	5	0.08	4.5
S75F150L15	75	0.105	15	0.08	4.5
S100F75L5	100	0.0525	5	0.08	4.5

Table 18 - Parameters selected for the tests (continuation).

Reference	Vc [m/min]	fz [mm/tooth]	Cut. Length [m]	ap [mm]	ae [mm]
S100F75L15	100	0.0525	15	0.08	4.5
S100F100L5	100	0.07	5	0.08	4.5
S100F100L15	100	0.07	15	0.08	4.5
S100F150L5	100	0.105	5	0.08	4.5
S100F150L15	100	0.105	15	0.08	4.5
S125F75L5	125	0.0525	5	0.08	4.5
S125F75L15	125	0.0525	15	0.08	4.5
S125F100L5	125	0.07	5	0.08	4.5
S125F100L15	125	0.07	15	0.08	4.5
S125F150L5	125	0.105	5	0.08	4.5
S125F150L15	125	0.105	15	0.08	4.5
S75F75L25	75	0.0525	25	0.08	4.5
S125F150L25	125	0.105	25	0.08	4.5

As can be seen, the last two conditions were performed at 25 meters of cutting length. These two conditions were selected based on minimum and maximum conditions, i.e., 75 m/min cutting speed and 0.0525 mm/tooth; and 125 m/min cutting speed and 0.105 mm/tooth, respectively.

3.2.3. Characterization of the thickness and morphology of the coatings

In order to characterize the thickness and morphology of the coating, it was necessary to proceed with the preparation of three samples through the techniques of cutting, embedding, grinding and polishing. For this, a tool was cut to analyze its cross-section. This cut was made using a Struers Minitom diamond blade saw (Struers, Inc., Cleveland, OH, USA). Then, the sample was embedded in thermosetting resin to aid in the grinding and polishing steps. The inlay was made with Struers Pedopress hot pressing equipment (Struers, Inc., Cleveland, OH, USA). As the substrate material is a high hardness material, the wear of the resin may be greater than the sample. To avoid this problem, the samples were embedded with two sections of tungsten carbide from an uncoated area of the tool, which would make the wear more uniform in the next step. Figure 16 illustrates a sample embedded in thermosetting resin with two sections of tungsten carbide.

Figure 16 - Sample embedded in thermosetting resin.

With that it was possible to start the grinding process. The samples were polished to obtain a flat, mirrored surface with low average roughness. In this step, silicon carbide (SiC) sandpaper was used. It started with 220 grit, followed by 550, 800 and 1200 grit sandpaper. The change to the next sandpaper was performed only when all the scratches in the sample were unidirectional, and cross-cutting risks were eliminated. Continuing the preparation of the samples, they were submitted to the polishing stage. The samples were polished for approximately 15 minutes, when it was not possible to observe any scratches on the samples, with two types of diamond paste with different average particle sizes, 3 µm and 1 µm.

The scanning electron microscopy (SEM) technique was used to characterize the thickness and morphology of the coating. For this, an FEI QUANTA 400 FEG scanning electron microscope was used (FEI, Hillsboro, OR, USA), equipped with an EDAX Genesys Energy Dispersive X-Ray Spectroscopy microanalysis system, which allowed the chemical characterization of the samples. EDS analyzes were performed using a beam potential of 15 kV, being sporadically reduced to 10 kV. It is important to point out that the increases used were the same for all samples, thus allowing a comparative analysis between them. The thickness of the coating was measured in several regions of the cross section, and an average of the values were used.

3.2.4. Characterization of the roughness of machined surfaces

Regarding the roughness of the machined surface, this was measured using a Mahr Perthometer M2 profilometer (Mahr, Gottingen, Germany), Figure 17, and following the DIN EN ISO 4288:1996 [118]. A cut-off of 0.8 mm and measuring length of 5.6 mm was used, and measurements were taken in the radial and tangential direction (relative to the machining direction).

Figure 17 - Mahr Perthometer M2 profilometer

In addition, variation was observed in the values obtained in the center of the workpiece and on the periphery, taking a minimum of five measurements in different areas. With this, it was determined the arithmetic average roughness value (Ra). Thus, it was possible to evaluate the stability of the milling process, the performance of the tool and its correlation with the resulting wear in each tested condition.

3.2.5. Characterization of wear mechanisms

The wear suffered by the machining tools was evaluated through the SEM analysis. Beforehand, however, the tools underwent ultrasonic cleaning with acetone as a cleaning agent, to remove all impurities present in the substrate. This cleaning was done in two stages: (1) 10 minutes and (2) acetone change and cleaning for 5 minutes. These two steps were carried out using the J.P Selecta ultrasonic cleaning equipment, as shown in the Figure 18.

Figure 18 - Equipment used for ultrasonic cleaning of tools.

Then, all tools were subjected to SEM analysis. With this, it was possible to verify the wear mechanisms, and thus, perform the measurement of this wear, according to the ISO 8688-2:1986 [119]. This standard recommends analyzing the presence of all wear phenomena and adopting as a life criterion the one that has the greatest influence, that is, it is necessary to analyze the influence

of the milling parameters on the type of wear generated. Figure 19 details the types of flank wear (VB1, VB2 and VB3) on a tool's cutting edge, according to the ISO 8688-2:1986 [119].

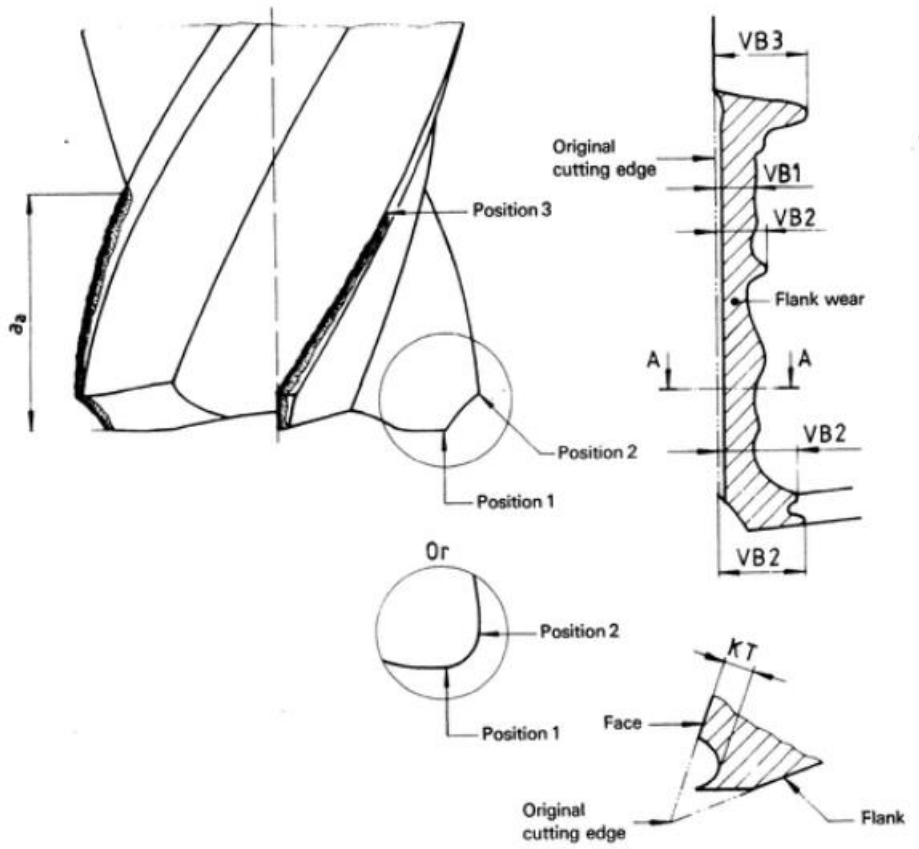

Figure 19 - Types of flank wear on end-milling cutters. Reproduced from *[119]*

Thus, it can be seen in Figure 19:

- VB1 (uniform flank wear): constant and uniform wear present on a large part of the tool flank;
- VB2 (non-uniform flank wear): is wear with an irregular width and that undergoes dimensional variations in each measured position in relation to the original edge;
- VB3 (localized flank wear): localized wear that occurs in a specific region of the tool flank, is the maximum wear.

Thereby, the VB3 was selected because the wear present in the tools and observed in the analysis was the flank wear located close to the chamfer of the tools. Wear measurements were performed in “Position 1”, shown in Figure 19.

In addition, EDS analysis was used to verify and confirm the possible substrate adhesion phenomena on the tool. Furthermore, a new tool was used to compare the loss of material and change in the geometry of the tools in all tested conditions. Rake face (RF) and clearance face (CF) of all tools were analyzed, making a comparison between them based on the test condition to which they were submitted. In addition, a reference was created for the four cutting teeth of the tool, indicating them with the numbers 1 to 4, as shown in Figure 20.

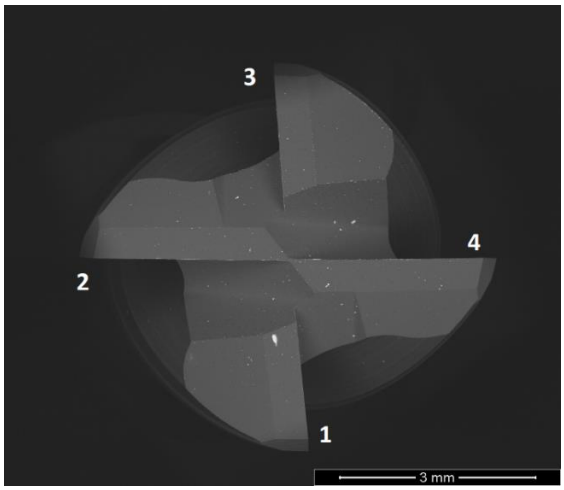

Figure 20 - Reference used for the tool wear evaluation.

3.2.6. Cutting force analysis

The cutting forces developed during the machining process bring relevant information about the stability of the process (vibrations and existence of overload) [120], and machinability of the material [121], being their knowledge essential for making the process optimization [122]. In addition, the cutting forces correlate with the lifespan of the cutting tool, and the state of the tool can be monitored during the process [123]. For example, Martinho et al. [124], in their work, verified the wear behavior of Si_3N_4 tools coated with a thin diamond film during high-speed machining. For this, cutting forces were analyzed, and the authors observed that the cutting speed does not influence this force, but the feed per tooth has great influence, because when increasing the feed per tooth, the cutting force also increased.

Thus, for the analysis of cutting forces, a KISTLER 9171A four-component rotary dynamometer was used, coupled to a KISTLER 5697A1 data acquisition system. This equipment has an ISO 40 DIN 69871 taper, an ER32 H70 collet holder and an ISO 7388-2 tie rod. Figure 21 illustrates the equipment.

Figure 21 - Equipment used to measure cutting forces: KISTLER 9171A dynamometer.

The dynamometer allowed the recording of the cutting forces developed in the X, Y and Z axes, and the torque developed (Mz), through the appropriate software supplied with the equipment. The cutting force values were obtained for all conditions of feed per tooth analyzed in this work, and for cutting speeds of 100 and 125 m/min. Thus, the rotary dynamometer was coupled to the spindle of the CNC machining center, and the cutting tool was fixed to the equipment. The data acquisition of the cutting forces was selected from the selected spindle rotation speed, allowing to record the cutting forces generated on the cutting edges of the tools in each rotation performed.

3.2.7. Tool lifespan evaluation

To determine tool lifespan, six conditions were selected, as shown in Table 19. These conditions were selected according to the cutting speed analyzed in this work, and two feed values (100 % of fz, and 150 % of fz). The other parameters remained constant: axial depth of cut of 0.08 mm; and radial depth of cut of 4.5 mm. In addition, the machining tests were performed using cutting fluid (5 % oil in water).

Table 19 - Conditions selected for tool lifespan analysis.

Reference	Vc [m/min]	fz [mm/tooth]
S75F100	75	0.07
S75F150	75	0.105
S100F100	100	0.07
S100F150	100	0.105
S125F100	125	0.07
S125F150	125	0.105

The tests were carried out every 5 meters of cutting length, that is, when reaching this value, the test was stopped, and the wear suffered by the tool was measured. The measured wear was VB3, and its end-of-life criterion was stipulated according to ISO 8688-2:1989 [119]. Thus, the end of useful life was considered to be a maximum VB3 of 0.5 mm in any individual tooth. The analysis of the flank wear and its subsequent measurement was carried out with the aid of the Dino-Lite Edge digital microscope, as shown in Figure 22.

Figure 22 - Dino-Lite Edge digital microscope.

4. RESULTS

In this chapter the results obtained in the tests carried out will be presented. Therefore, the chapter was subdivided into the following subsections: 4.1. Coating's analysis 4.2. Machined surface analysis; 4.3. Analysis of cutting forces; 4.4. Wear measurements and characterization; 4.5. Analysis of wear mechanisms and 4.6. Tool lifespan analysis. It should be noted that sections 4.2.; 4.4; and 4.5. were subdivided according to the cutting speed used, that is, 75 m/min, 100 m/min and 125 m/min, and a section of the analyzed conditions at 25 meters of cutting length.

4.1. Coating's analysis

The coating was analyzed according to the method described in section 3.2.3. With this, it was possible to determine the average value of the coating thickness using the SEM analysis, as well as its chemical composition, by performing EDS analysis. Figure 23 illustrates the measurements performed to evaluate the total coating thickness, and the zone where the EDS analysis was carried out to characterize the chemical composition of the coating.

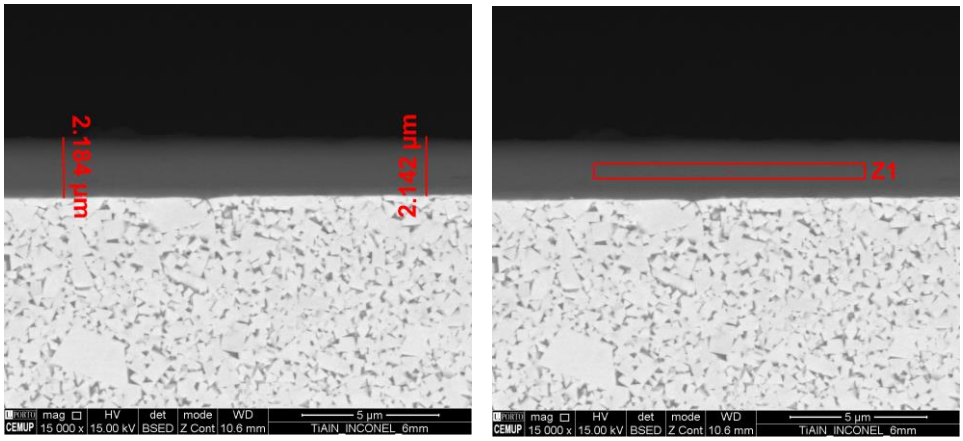

(a) (b)

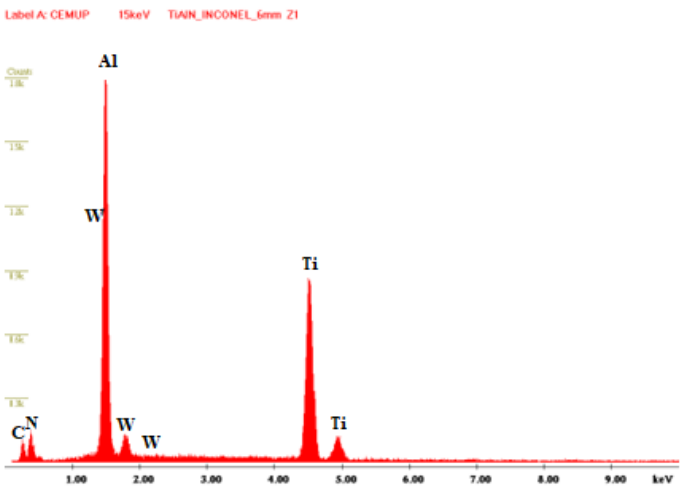

(c)

Figure 23 - Coating characterization: (a) thickness measurement; (b) EDS evaluation zone and (c) EDS spectrum obtained.

In Figure 23, the presence of a lighter tone zone can be seen, close to the substrate material of the tool, referring to the TiN adhesion layer. This layer was deposited before the final multilayer architecture to improve the adhesion of the final coating to the substrate. For this analysis to be more conclusive, since it is not so noticeable in the SEM analysis, and could not be evaluated by direct EDS analysis, as there is interaction of the surrounding elements with those of this thin layer, the elemental mapping of the samples was carried out. With this, it was confirmed that was a TiN layer. The base image used for mapping the elements can be seen in Figure 24, and Figure 25 illustrates the mapping of elements.

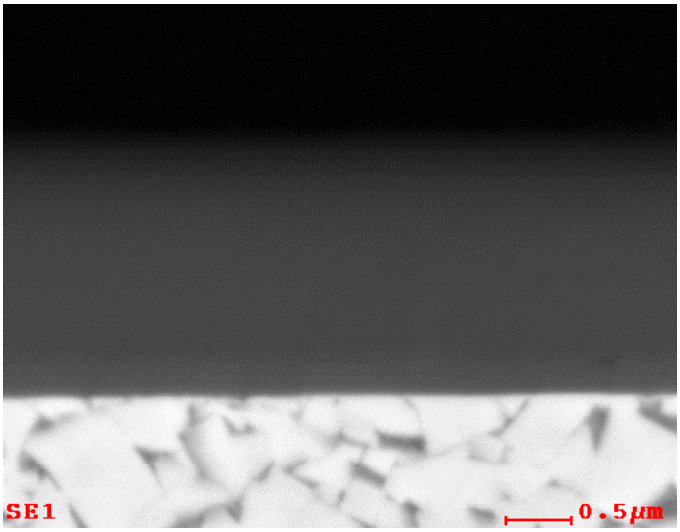

Figure 24 - Image obtained with secondary electrons used for mapping.

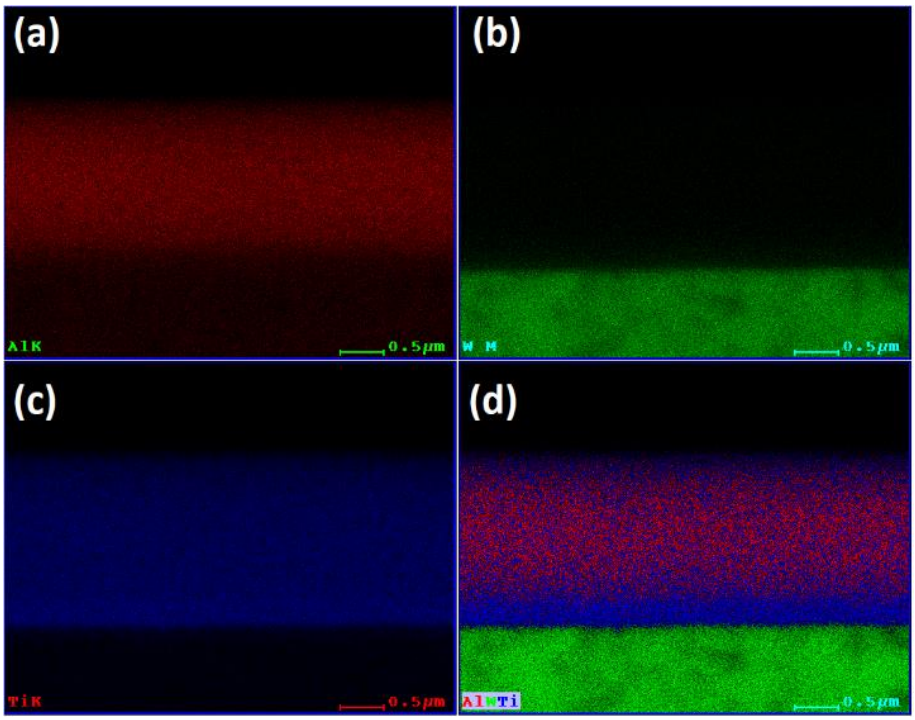

Figure 25 - Element mapping: (a) Al distribution, (b) W distribution, (c) Ti distribution and (d) Al, W and Ti distribution overlapped.

It is noted in Figure 25(d) that Al is present mainly in the upper layer of the coating, and the lower layer has predominantly Ti. Thus, it can be concluded that this layer was the layer of TiN. In addition,

regarding the thickness of the coating, this was measured in several regions, thus resulting in an average value, as shown in the Table 20.

Table 20 – Average thickness values, both TiN/TiAlN coating and of its layers.

Coating	Average thickness value [µm]
TiN layer	0.25 ± 0.023 µm
TiAlN layer	1.80 ± 0.12 µm
TiN/TiAlN (total coating)	2.10 ± 0.16 µm

Based on this, it can be said that this is a multilayer TiN/TiAlN coating, and the TiN layer, deposited close to the substrate, promotes the adhesion of the coating to this substrate, which makes the wear resistance and their behavior in machining with better performances.

4.2. Machined surface analysis

To analyze the machined surface, the surface roughness was measured after each tested condition. This measurement was performed both in the tangential and radial direction, regarding the machining direction, and no notable difference was observed between the values obtained. For a better interpretation of the data, the results will be divided according to the cutting speed used, as well as an analysis with the conditions at 25 meters of cutting length.

4.2.1. Cutting speed of 75 m/min

The results obtained for all conditions tested with a cutting speed of 75 m/min are shown in Table 21.

Table 21 - Average values of surface roughness (Ra) for all conditions tested with a cutting speed of 75 m/min.

Reference	Average Ra value [µm]
S75F75L5	0.355 ± 0.0098
S75F75L15	0.424 ± 0.0364
S75F100L5	0.370 ± 0.0566
S75F100L15	0.589 ± 0.0166
S75F150L5	0.589 ± 0.0484
S75F150L15	0.615 ± 0.0539

Observing Table 21, it is verified that when increasing the cutting length, the surface roughness values also increased. This was already expected for Inconel 718, because even in small cutting lengths, it already induces high levels of tool wear, that is, this directly influences the surface quality obtained. In addition, it was verified that the measurements in the center were a little smaller than in the periphery of the workpiece, which is consistent with the evolution of wear during the test. Figure 26 illustrates the results obtained for a cutting speed of 75 m/min. The graph is divided into

two series, one referring to the parameter cutting length of 5 meters (L5) and the other for a cutting length of 15 meters (L15).

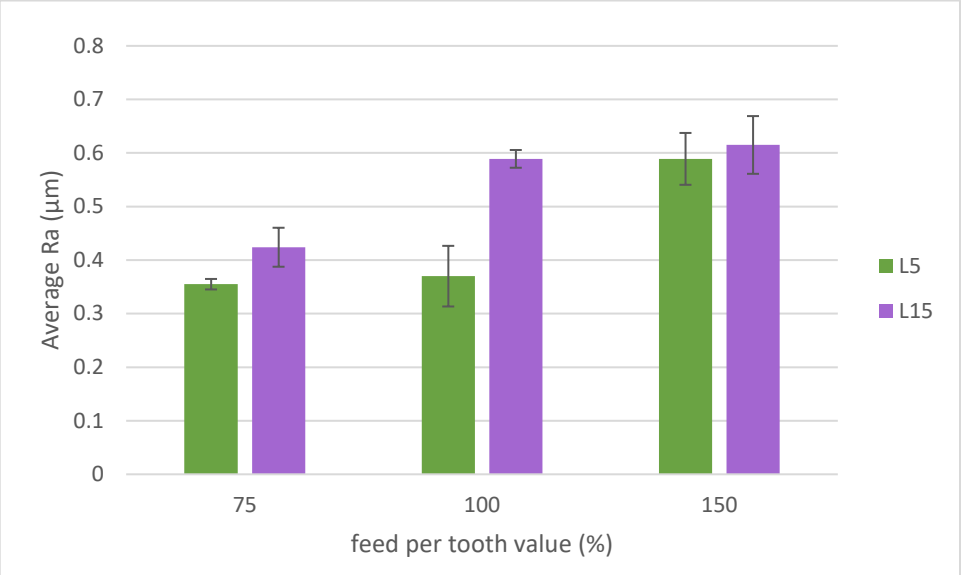

Figure 26 - Machined surface roughness value obtained for all conditions tested with a cutting speed of 75 m/min.

From Figure 26, it can be seen that for cutting lengths of 5 meters, the greatest influence of feed per tooth was when it was increased to 150 %. On the other hand, for cutting lengths of 15 meters, its influence was notable as it was increased from 75 % to 100 %. Therefore, under these conditions, the maximum value of Ra is obtained for the condition that uses 150% of feed per tooth and 15 meters of cutting length, that is, for condition S75F150L15. In turn, the lowest Ra value was obtained for the condition with 75% feed per tooth and 5 meters of cutting length, that is, S75F75L5, but the value obtained for condition S75F100L5 was very close.

4.2.2. Cutting speed of 100 m/min

The results obtained for all conditions tested with a cutting speed of 100 m/min are shown in Table 22 and in Figure 27. It is important to point out that the values obtained in the center of the workpiece were slightly lower than in its periphery (end of path and greater wear).

Table 22 - Average values of surface roughness (Ra) for all conditions tested with a cutting speed of 100 m/min.

Reference	Average Ra value [µm]
S100F75L5	0.409 ± 0.0588
S100F75L15	0.692 ± 0.0538
S100F100L5	0.452 ± 0.0521
S100F100L15	0.737 ± 0.0511
S100F150L5	0.517 ± 0.0713
S100F150L15	0.637 ± 0.0703

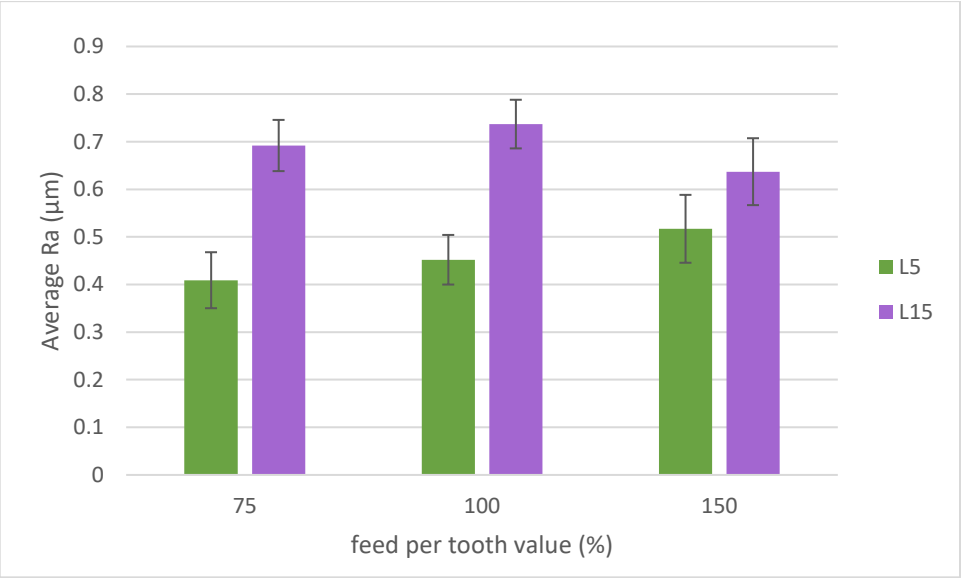

Figure 27 - Machined surface roughness value obtained for all conditions tested with a cutting speed of 100 m/min.

From Table 22 and Figure 27, it can be seen that, similar to the conditions at 75 m/min cutting speed, as the cutting length was increased from 5 meters to 15 meters, there was an increase in surface roughness. In addition, regarding the feed per tooth, this showed a certain difference from the previously analyzed condition. In this case, for the tests carried out in 15 meters of cutting length, there was an increase in the surface roughness when from 75 % to 100 % of the value of this parameter, however, this value had a slight decrease from 100 % to 150 % of feed per tooth value. On the other hand, for conditions at 5 meters of cutting length, for smaller values of feed per tooth, the quality of the machined surface is better than that obtained for larger values of this parameter. Therefore, for the conditions analyzed at a cutting speed of 100 m/min, the condition with the lowest resulting surface roughness was S100F75L5, and the highest S100F100L15. Normally, lower values of feed per tooth result in better quality of the machined surface than that obtained for higher values of this parameter [125]. In general, increasing the feed per tooth will affect the quality of the machined surface. Furthermore, this parameter has a high influence on the roughness of the machined surface [126].

4.2.3. Cutting speed of 125 m/min

The results obtained for all conditions tested with a cutting speed of 125 m/min are shown in Table *23* and Figure 28.

Table 23 - Average values of surface roughness (Ra) for all conditions tested with a cutting speed of 125 m/min.

Reference	Average Ra value [µm]
S125F75L5	0.429 ± 0.0509
S125F75L15	0.674 ± 0.0613
S125F100L5	0.502 ± 0.0415
S125F100L15	0.786 ± 0.0550

Table 23 - Average values of surface roughness (Ra) for all conditions tested with a cutting speed of 125 m/min (continuation).

Reference	Average Ra value [µm]
S125F150L5	0.596 ± 0.0691
S125F150L15	0.824 ± 0.0947

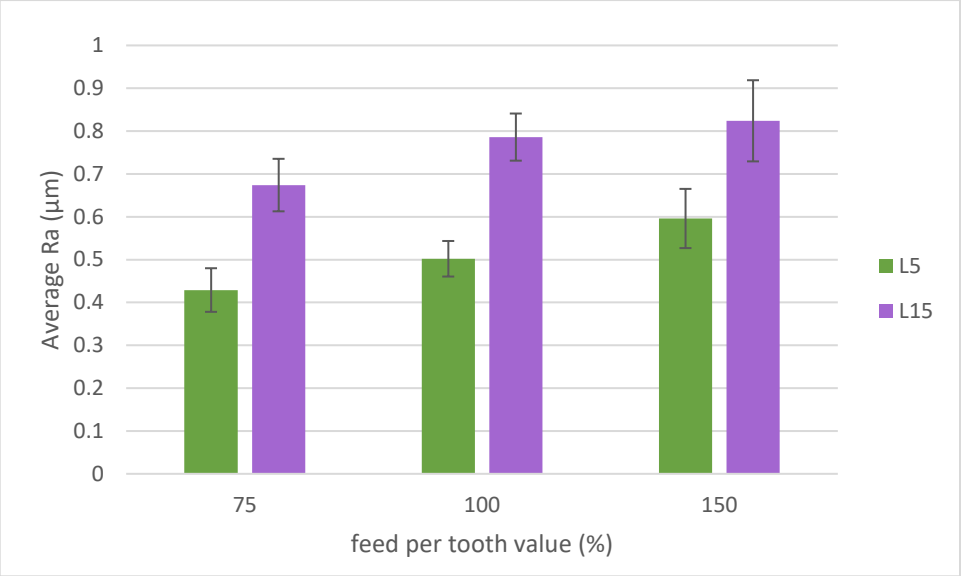

Figure 28 - Machined surface roughness value obtained for all conditions tested with a cutting speed of 125 m/min.

It is observed in Table 23 and Figure 28 that, in the same way as in the conditions at 75 m/min and 100 m/min of cutting speed, when increasing the cutting length from 5 meters to 15 meters, the surface roughness also increases. Regarding the feed per tooth, under these conditions, the trend is the same as that registered for cutting lengths of 5 meters and 15 meters, and the quality of the machined surface deteriorates as the value of the feed per tooth increases, that is, the roughness value obtained is greater when the feed per tooth is greater.

When comparing the cutting speed, the roughness values of the machined surface obtained at 125 m/min of cutting speed tend to be slightly higher than those recorded at 100 m/min of cutting speed, which in turn is higher than the first analyzed condition. This fact is not commonly observed and may be related to the sustained wear of cutting tools [127]. Furthermore, when observing the standard deviation, it seems that it has a higher value for tests performed at 150 % of the fz value, mainly at 125 m/min. This is indicative of greater sustained tool wear, leading to a difference in roughness obtained in the center of the workpiece to its periphery (end of path, greater wear) [128].

4.2.4. 25 meters cutting length

As seen in section 3.2.2., two conditions were analyzed at 25 meters of cutting length. These two conditions were selected based on minimum and maximum conditions, i.e., 75 m/min cutting speed and 0.0525 mm/tooth; and 125 m/min cutting speed and 0.105 mm/tooth, respectively. The results obtained for these conditions are shown in Table 24.

Table 24 - Average values of surface roughness (Ra) for conditions with 25 meters of cutting length.

Reference	Average Ra value [µm]
S75F75L25	0.676 ± 0.1812
S125F150L25	0.917 ± 0.0606

Figure 29 illustrates a comparative graph of surface roughness as a function of cutting length, with two series, one with 75 m/min of cutting speed and the other with 125 m/min of cutting speed, so that it is possible to carry out the analysis of maximum and minimum conditions at 25 meters of cutting length. In this comparative graph, the value of feed per tooth was 75% fz for cases with 75 m/min of cutting speed, and 150% fz for 125 m/min of cutting length.

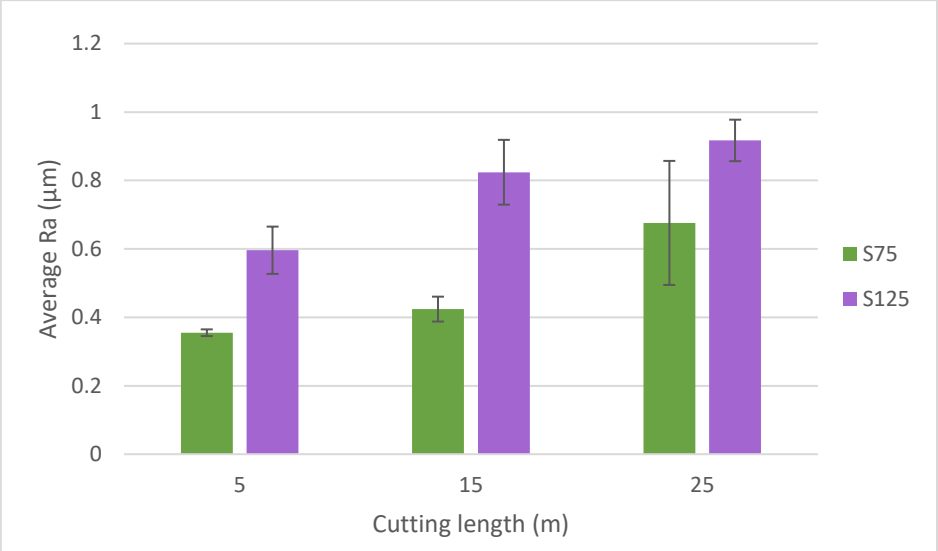

Figure 29 - Machined surface roughness value obtained for all conditions tested with 25 meters of cutting length.

For the conditions at 75 m/min and 125 m/min of cutting speed, as the cutting length increased, the quality of the machined surface decreased. Indeed, an increase in surface roughness of the machined part was observed. This increase in roughness was more pronounced when going from 15 meters of cutting length to 25 meters of cutting length, in the 75 m/min condition, and when going from 5 meters of cutting length to 15 meters of cutting length, in the condition at 125 m/min. Furthermore, at 75 m/min, in 25 meters of cutting length, the standard deviation had a significant value, indicating that the wear on the periphery had different values from the wear on the center of the workpiece. In addition, as already observed in the previous conditions, and confirming the analysis, the roughness increased when the cutting speed increased, which is not commonly observed, but may be related to sustained tool wear [129].

4.3. Analysis of cutting forces

As explained in Section 3.2.6., the cutting forces were recorded for the feed per tooth values analyzed in this work, and for the conditions with 100 and 125 m/min of cutting speed. As a result, it was verified that the recorded values were low due to the value of the axial depth of cut of 0.08 mm, which is a value considered low.

Even with these low values, it was observed that there was a tendency for the cutting force values to be higher for higher values of feed per tooth (fz). This can be justified due to the increase in chip thickness and contact area, given the influence of these parameters on the development of cutting forces [29]. Furthermore, another trend observed in all analyzed conditions was that the values of cutting force were higher at the end of the test than at the beginning of the test, namely Fy and Fx, and thus, Fa, due to the increase in tool wear during the test as its geometry is changed through interaction with the workpiece. In addition, the influence of the cutting speed in these tests in relation to the cutting force was not verified, possibly due to the small increase in the cutting speed between the test conditions.

Thus, the variation of the cutting forces in the tested conditions is, and the parameter that had a greater influence was the feed per tooth, however the variation was very small. The maximum recorded cutting force value for 0.07 mm/tooth was about 56 N for the Fx force component and 51 N for the Fy force component. These forces decreased by about 8% for smaller values of feed per tooth and increased by around 10% for higher values of feed per tooth. Furthermore, the increase in cutting force over the course of the tests was around 4%. Therefore, as said, these variations were very small, not giving a clear indication that tool wear is increasing the cutting force values throughout the test.

Furthermore, it is known that sustained tool wear is commonly associated with an increase in cutting forces for milling processes [130]. Thus, the cutting torque developed was also evaluated. However, the recorded value was very small, and its behavior was constant throughout the tests.

4.4. Wear measurements and characterization

As explained in section 3.2.5., the measurement of tool wear was carried out in accordance with the ISO 8688-2:1986 [119] in the top view of the tools (flank wear, VB3). To facilitate the analysis, the results will be divided and grouped according to the cutting speed used, as well as an analysis with the conditions at 25 meters of cutting length.

4.4.1. Cutting speed of 75 m/min

The results of flank wear for the conditions in which 75 m/min of cutting speed were used are shown in Table *25* and illustrated in Figure 30.

Table 25 - Cutting speed of 75 m/min: average values of flank wear (VB3).

Reference	Average VB3 value [µm]
S75F75L5	91.01 ± 10.89
S75F75L15	247.57 ± 42.55
S75F100L5	115.02 ± 14.99
S75F100L15	235.92 ± 29.19
S75F150L5	88.78 ± 13.85
S75F150L15	352.97 ± 91.87

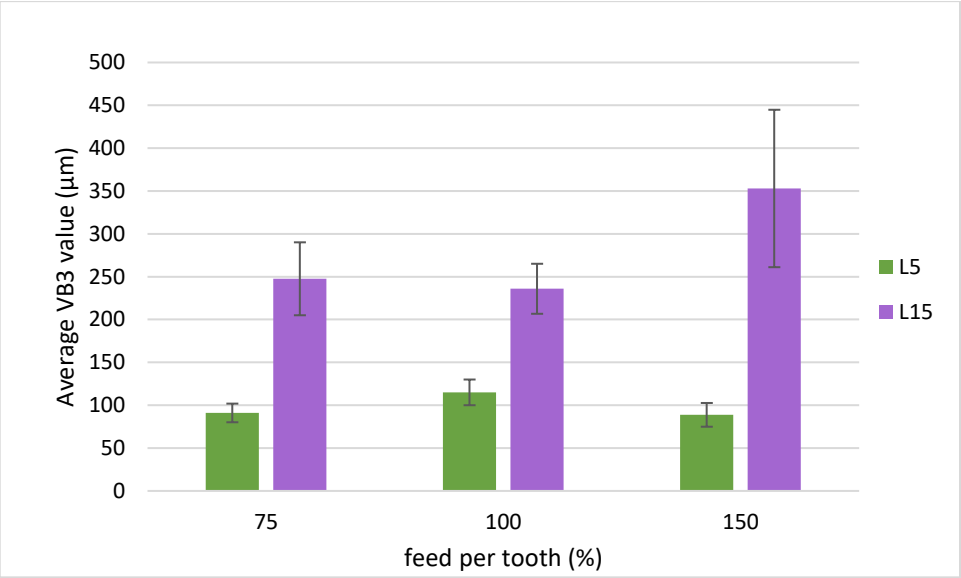

Figure 30 - Average flank wear (VB3) value obtained for all conditions tested with a cutting speed of 75 m/min.

Table *25* and Figure 30 show the clear influence of the cutting length on tool wear, in which when increasing the cutting length from 5 to 15 meters, there was a large increase in flank wear. Regarding the influence of the variation in the feed per tooth on the flank wear of the tools, it can be observed that for tools with 5 meters of cutting length, the lowest value obtained was for condition S75F75L5. The wear increased when the feed per tooth also increased to 100 % of fz, presenting a maximum value in this case, that is, for condition S75F100L5. By varying the feed per tooth at 150 % of fz, the wear decreased, having a value only slightly higher than in the S75F75L5 condition. On the other hand, when considering 15 meters of cutting length, this same tendency is not observed. In this case, the lowest flank wear value was obtained for the S75F100L15 condition and the highest for the S75F150L15 condition, that is, when increasing the feed per tooth from 75% to 100% there was a decrease in wear, and when increasing from 100% to 150% the wear had a significant increase.

4.4.2. Cutting speed of 100 m/min

The results of flank wear for the conditions in which 100 m/min of cutting speed were used are shown in Table 26 and illustrated in Figure 31.

Table 26 - Cutting speed of 100 m/min: average values of flank wear (VB3).

Reference	Average VB3 value [µm]
S100F75L5	92.67 ± 10.06
S100F75L15	488.02 ± 21.80
S100F100L5	89.37 ± 8.53
S100F100L15	536.60 ± 34.61
S100F150L5	75.45 ± 4.91
S100F150L15	471.11 ± 42.13

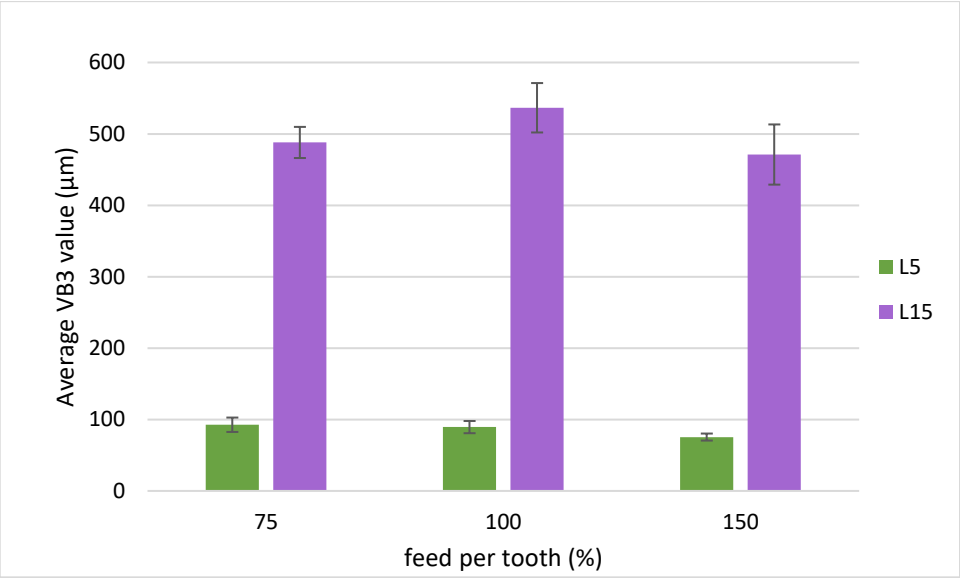

Figure 31 – Average flank wear (VB3) value obtained for all conditions tested with a cutting speed of 100 m/min.

Thus, observing Table 26 and Figure 31, the same situation is verified as in the condition at 75 m/min of cutting speed: the flank wear of the tools was influenced by the cutting length, being greater for the tests carried out for 15 meters of cutting length. That is, when increasing the cutting length from 5 meters to 15 meters, the resulting wear increases significantly, which is in line with expectations, since Inconel 718 is a difficult to machine alloy which can generate severe abrasive wear.

In addition, for the tests carried out with a cutting length of 5 meters, it can be identified that there was a tendency: the values of VB3 are higher for the tests carried out at 75 % of the feed per tooth, decreasing with the increase of this parameter. However, this was not verified for the tests carried out at 15 meters of cutting length, in which the condition that had the most wear was S100F100L15, and the least S100F150L15. This variation is similar to that recorded for the average Ra values of the machined surface under these conditions, where the highest values obtained with 15 meters of cutting length were for 100 % of fz, and the lowest for 150 % of the initial feed per tooth value. This may be related to the amount of wear presented by the tools, as tools that suffer less wear will produce a better quality machined surface [131].

4.4.3. Cutting speed of 125 m/min

The results of flank wear for the conditions in which 125 m/min of cutting speed were used are shown in Table *27* and illustrated in Figure 32.

Table 27 - Cutting speed of 125 m/min: average values of flank wear (VB3)

Reference	Average VB3 value [µm]
S125F75L5	199.16 ± 16.08
S125F75L15	561.93 ± 39.64
S125F100L5	190.05 ± 11.81

Table 27 - Cutting speed of 125 m/min: average values of flank wear (VB3) (continuation)

Reference	Average VB3 value [µm]
S125F100L15	545.34 ± 23.65
S125F150L5	168.03 ± 24.50
S125F150L15	613.55 ± 19.71

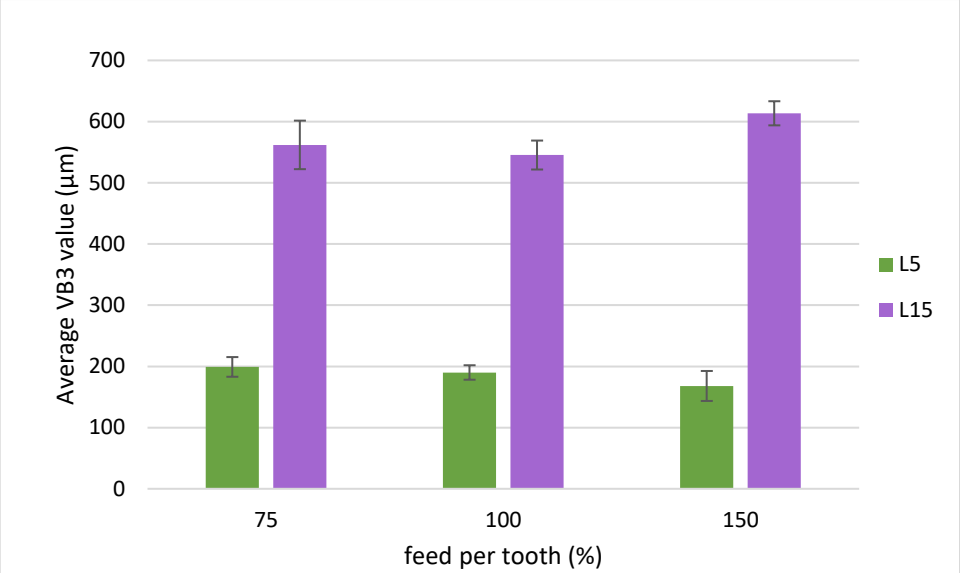

Figure 32 - Average flank wear (VB3) value obtained for all conditions tested with a cutting speed of 125 m/min.

Observing Table 27 and Figure 32, in the same way as for the tests carried out at 75 and 100 m/min of cutting speed, in this case at 125 m/min, it is also noted that when increasing the cutting length to 15 meters, the resulting wear has increased significantly, being a parameter that showed to have a greater influence when it is increased, than the feed per tooth. This is consistent, since even in small cutting lengths, Inconel 718 already generates significant wear.

Furthermore, the same trend observed in the previous cases, was verified for the tests with 5 meters of cutting length. In this case of 125 m/min: the VB3 values are higher for the tests performed at 75 % of the feed per tooth, decreasing with the increase of this parameter. Contrary to what was previously observed, in these cases at 125 m/min and 15 meters of cutting length, the condition with the greatest wear was the one with 150% fz (S125F150L15), and the one with the least wear at 100% fz (S125F100L15).

4.4.4. 25 meters cutting length

As seen in section 3.2.2., two conditions were analyzed at 25 meters cutting length: 75 m/min cutting speed and 0.0525 mm/tooth, and 125 m/min cutting speed and 0.105 mm/tooth. The results obtained for these conditions are shown in Table 28. Figure 33 illustrates a comparative graph of the average of the flank wear as a function of cutting length, with two series, one with 75 m/min of cutting speed and the other with 125 m/min of cutting speed, so that it is possible to carry out the analysis of maximum and minimum conditions at 25 meters of cutting length. In this

comparative graph, the value of feed per tooth was 75% fz for cases with 75 m/min of cutting speed, and 150% fz for 125 m/min of cutting length (minimum and maximum conditions).

Table 28 - 25 meters of cutting length: average values of flank wear (VB3).

Reference	Average VB3 value [µm]
S75F75L25	577.34 ± 20.40
S125F150L25	631.05 ± 73.75

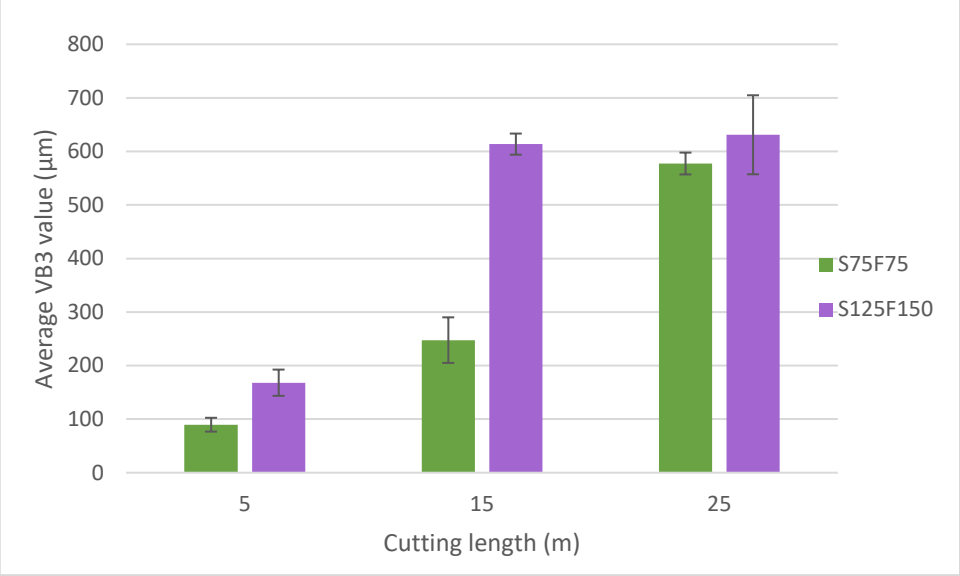

Figure 33 - Comparative graph of the average of the flank wear (VB3) as a function of cutting length.

Observing Table 28 and Figure 33, it is noticed that the two values recorded for 25 meters of cutting length are similar, being a little higher for condition S125F150L25, which was to be expected. In addition, it is noted that when considering 75 m/min of cutting speed, there was a large increase in flank wear at 25 meters of cutting length, and this also increased when the cutting length was increased from 5 meters to 15 meters. Furthermore, the same trend was observed at the cutting speed of 125 m/min, however the increase in wear observed between 15 meters of cutting length and 25 meters of cutting length was not as accentuated, indicating that after a certain range of length of cut, wear tends to be more constant across its length but greater across its width. So, in this comparison, as predicted, the condition with the most wear was S125F150L25. It is important to point out that the average roughness value obtained for the S125F150L15 condition was below the value for the condition at 25 meters of cutting length, indicating better surface roughness in conditions of less resulting wear.

4.5. Analysis of wear mechanisms

As exposed in section 3.2.3., the wear suffered by the machining tools was evaluated through the SEM analysis. As in the previous sections, to facilitate the analysis, the results will be divided and grouped according to the cutting speed used, as well as an analysis with the conditions at 25 meters of cutting length.

4.5.1. Cutting speed of 75 m/min

Figure 34 illustrates the top view of the tools tested at 75 m/min cutting speed, making it possible to clearly observe the influence of the cutting length on the resulting wear, that is, for longer cutting lengths, the wear that the tools experience is more severe. This is evidenced by the mean values of VB3 recorded and previously presented.

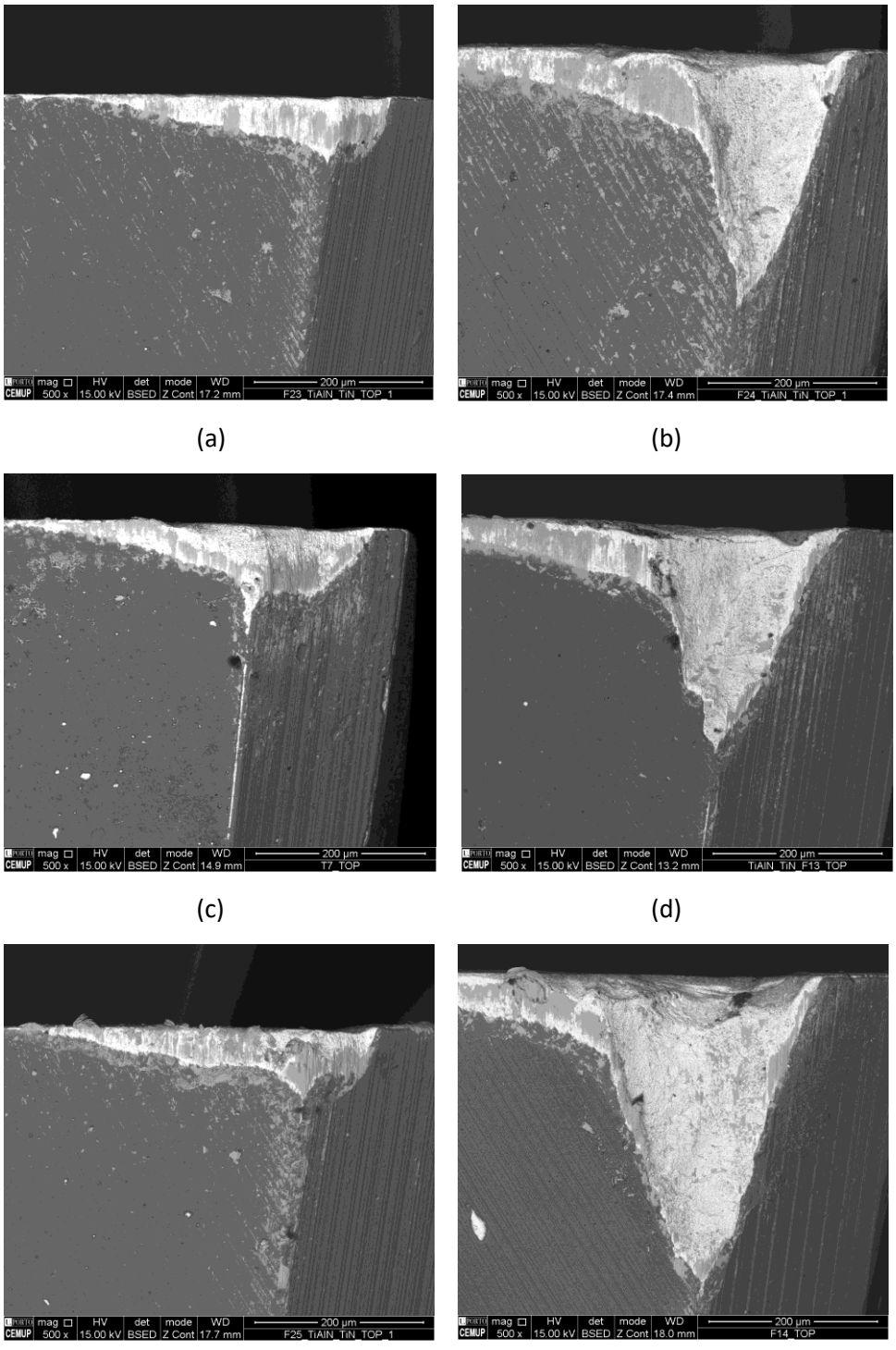

Figure 34 - Top view of the tools tested at 75 m/min of cutting speed at 500x magnification: (a) S75F75L5, (b) S75F75L15, (c) S75F100L5, (d) S75F100L15, (e) S75F150L5, and (f) S75F150L15.

Figure 35 illustrates the rake faces of the tools tested at 75 m/min of cutting speed. It was possible to verify the impact of cutting length on tool-wear, being S75F150L15 condition which resulted in more aggressive wear. In addition, it was observed that the wear mark is deeper for tools tested with higher values of feed per tooth, due to the friction generated in the test and the change in tool geometry. This is more significative in conditions tested at 15 meters of cutting length.

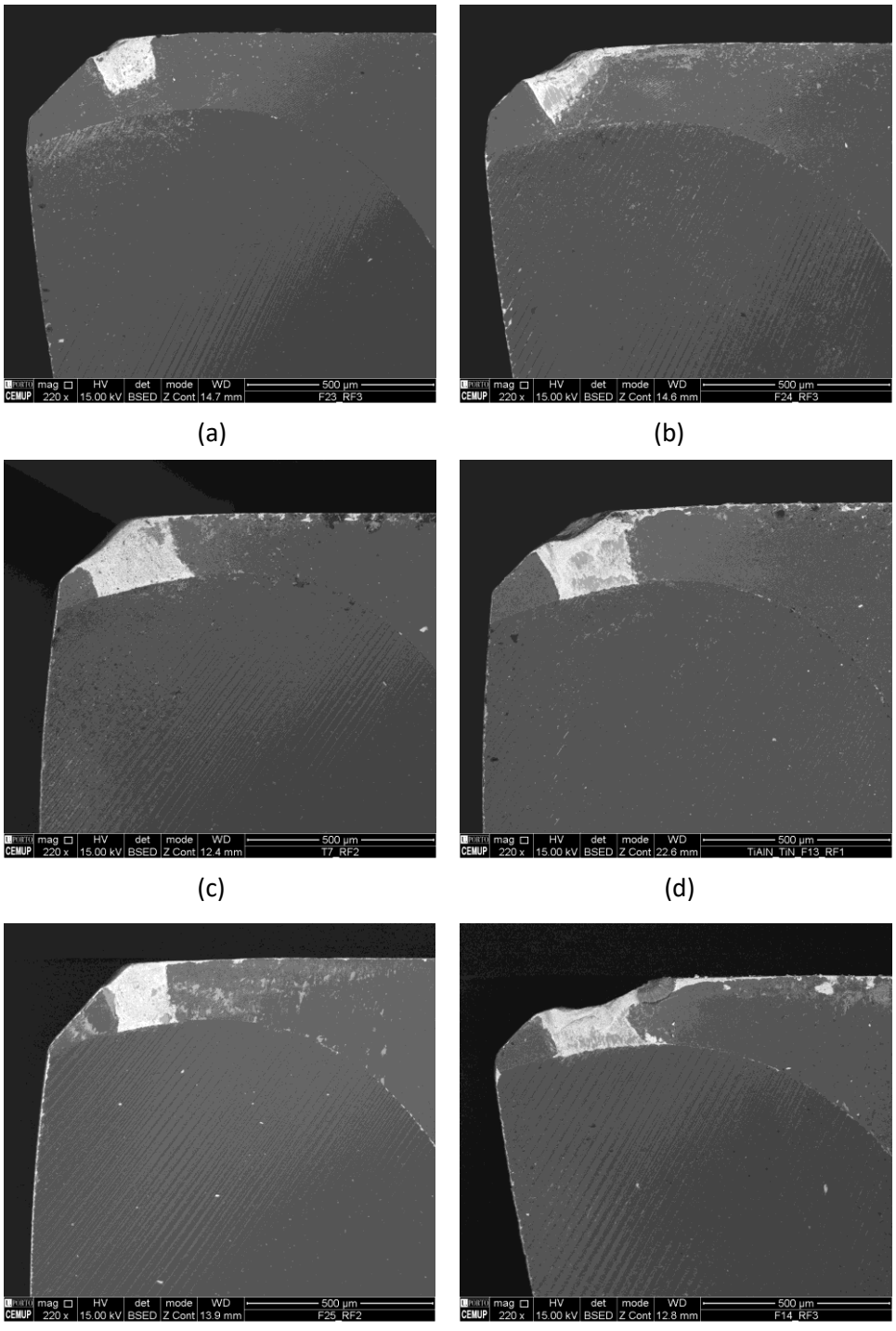

Figure 35 – Rake face view of the tools tested at 75 m/min of cutting speed at 220x magnification: (a) S75F75L5, (b) S75F75L15, (c) S75F100L5, (d) S75F100L15, (e) S75F150L5, and (f) S75F150L15.

Furthermore, Figure 36 illustrates the clearance face of the tools tested under these same conditions. When comparing the figures with 5 meters of cutting length, the influence of the variation in the feed per tooth on the flank wear of the tools is observed, with the S75F100L5 condition being the one that presents the greatest wear, and the S75F75L5 with the least wear. In addition, it is noted that in the conditions at 15 meters of cutting length, the S75F150L15 condition presents the greatest wear, and contrary to what was observed with 5 meters of cutting length, in this case when considering 100% of fz, that is, S75F100L15 the wear was the least.

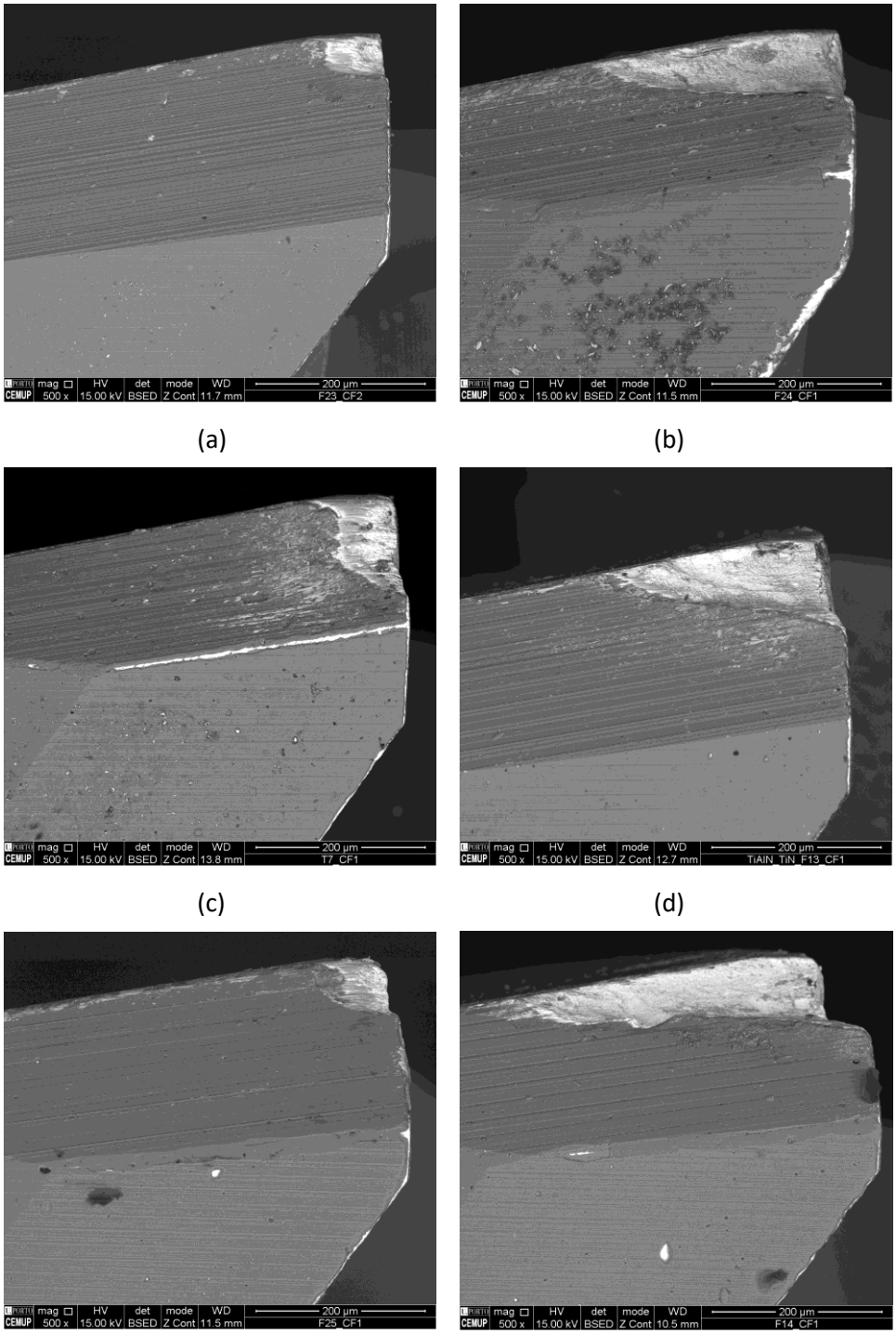

Figure 36 – Clearance face view of the tools tested at 75 m/min of cutting speed at 500x magnification: (a) S75F75L5, (b) S75F75L15, (c) S75F100L5, (d) S75F100L15, (e) S75F150L5, and (f) S75F150L15.

As for the wear mechanism, it can be said that, in the conditions of 75 m/min, were mainly abrasion wear and adhesive wear. As previously observed for the flank wear values (VB3) of the tools, at longer cutting lengths (15 meters), the wear was more severe, which makes the wear mechanism more developed. So, the abrasion wear was detected for all the tests being more significant and more intense for cutting lengths of 15 meters. This type of wear is common when machining Inconel 718 [112]. Figure 37 illustrates the abrasive wear that occurred in the process.

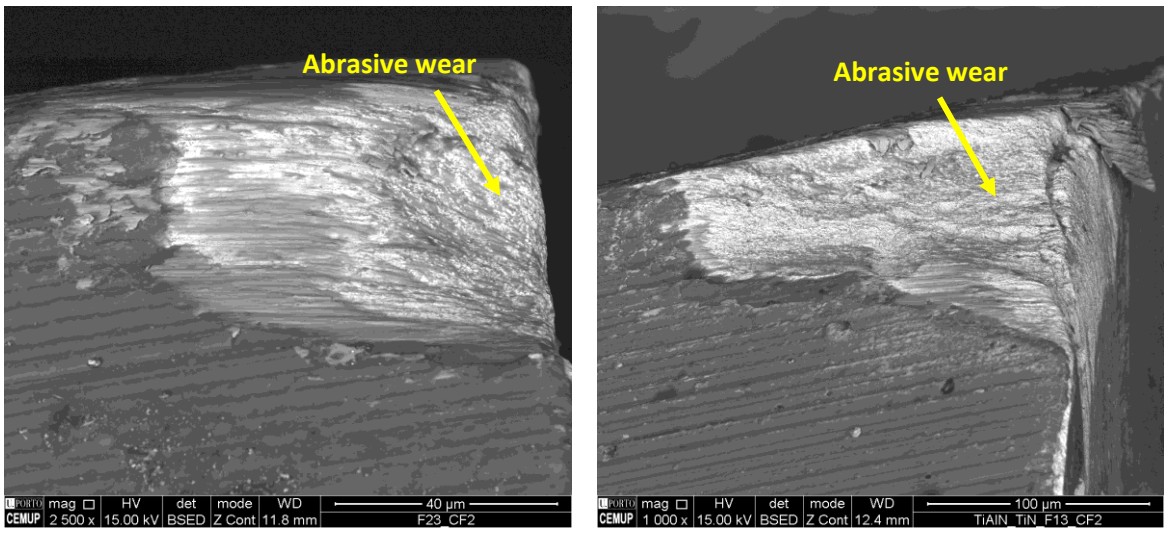

(a) (b)

Figure 37 - Abrasive wear: (a) Clearance face (CF2) of S75F75L5 at 2500x magnification and (b) Clearance face (CF2) of S75F100L15 1000x magnification.

In addition to abrasion, material adhered to the surface of the coating can be observed. As an example, there is the adhesion of the material to the rake face of the S75F75L15 tool (Figure 38). This adhesion causes more abrasive wear and can lead to coating delamination. However, the adhesion observed was of low intensity on the flank and on the edges of the tools, and there seems to be a higher level of adhesion to the substrate of the tools than to the coating. Figure 39 illustrates the adhesion of the material to the tool substrate under conditions S75F100L15 and S75F150L15, being the last one, with the beginning of the formation of a built-up edge.

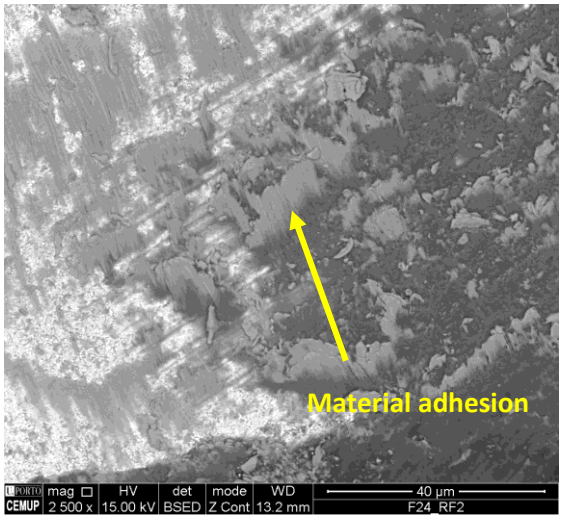

Figure 38 - Rake face (RF2) of S75F75L15 at 2500X magnification showing material adhesion.

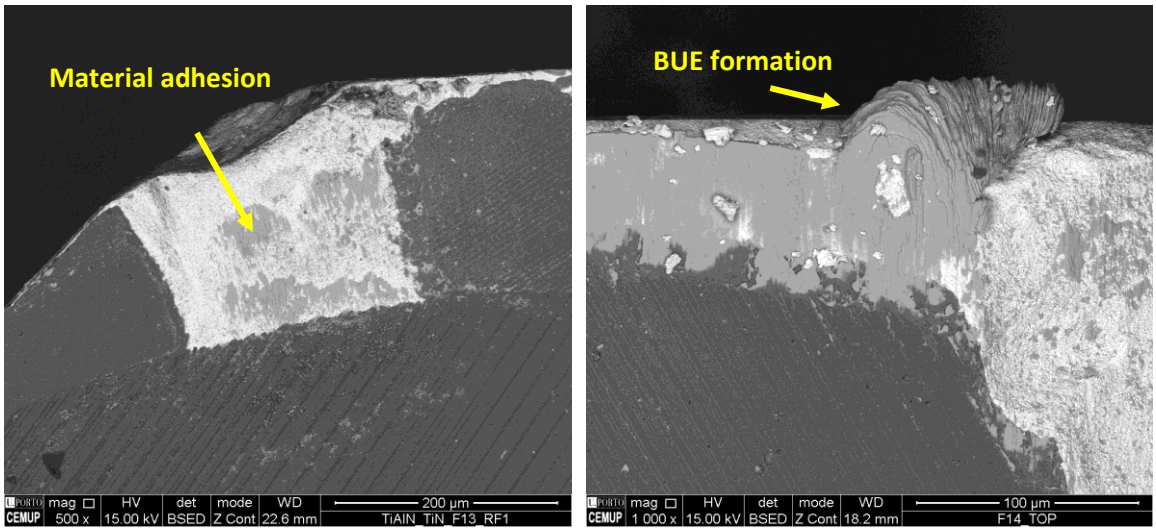

Figure 39 - Adhesion of material to tool substrate: (a) RF1 of S75F100L15 at 500x magnification and (b) Top view of S75F150L15 at 1000x magnification

As said, the adhesion of the material is found both on the surface of the coating and on the substrate of the tool. To exemplify these two cases, and to confirm the presence of adhered material, Figure 40 illustrates the clearance face of the S75F100L5 condition, indicating four zones, which underwent EDS analysis to indicate whether it was the material to be machined (adhesion), coating or tool substrate, according to the chemical composition resulting from this analysis.

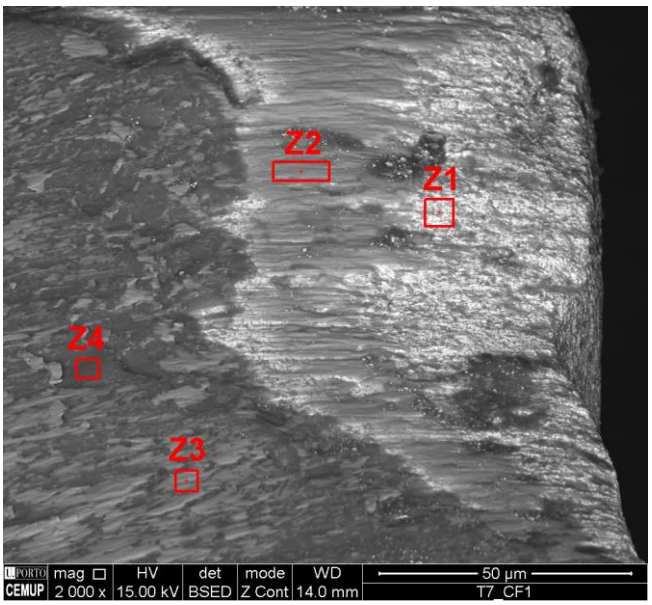

Figure 40 - Clearance face (CF1) of the S75F100L5 at 2000X magnification, indicating four zones, which underwent EDS analysis.

As a result of the EDS analysis, it was verified that zone 1 was the tool substrate, rich in tungsten (W). In zone 2, large amounts of nickel were found, as well as tungsten, which indicated that it was machined material adhered to the surface of the tool substrate. In turn, zone 3, indicated that it was material adhered to the tool coating, and zone 4, proved to be the coating. Figure 41 illustrates the EDS analysis of the four zones.

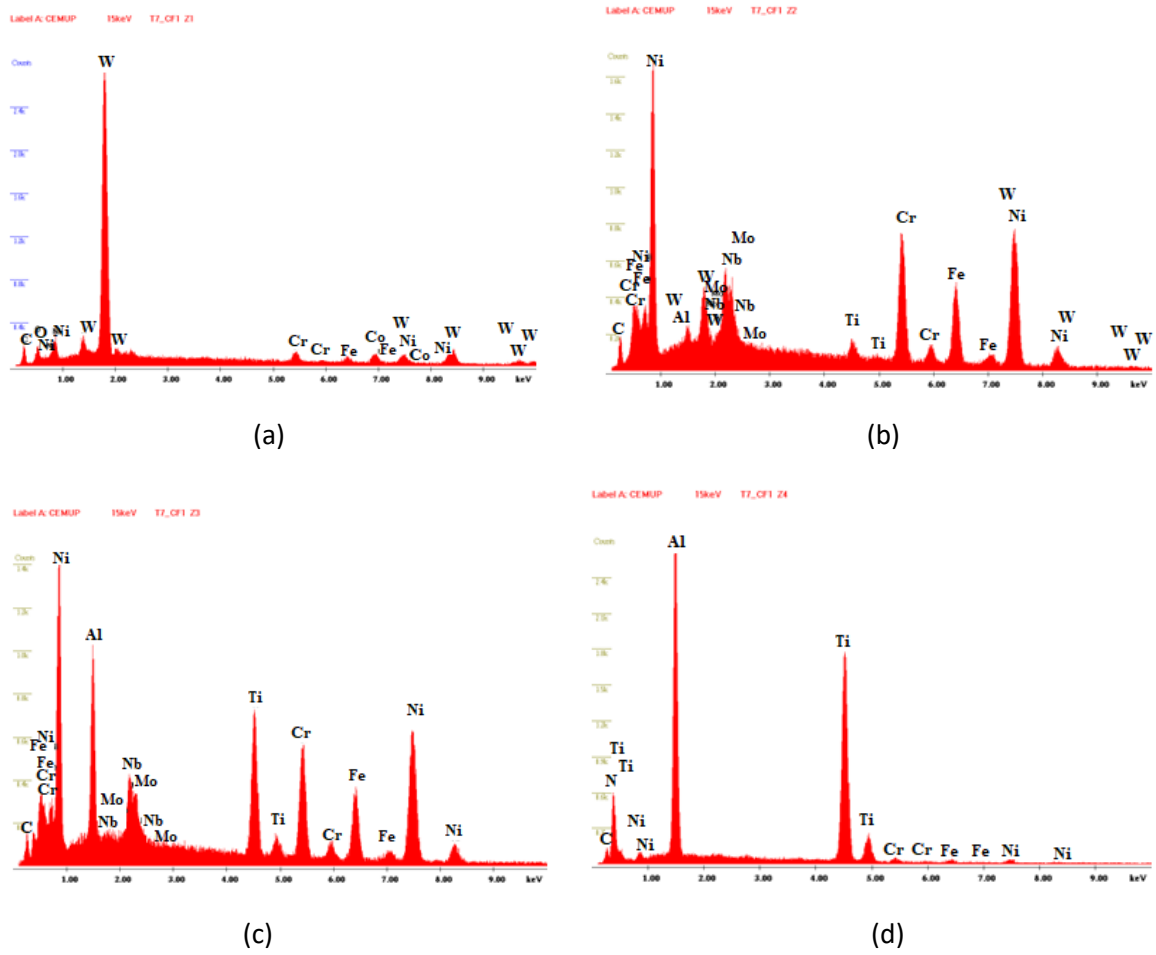

Figure 41 - EDS analysis of the four zones: (a) tool substrate, (b) machined material adhered to the surface of the substrate of the tool, (c) material adhered to the tool coating and (d) coating.

Thus, it can be said that an increase in the cutting length promotes a greater development of wear mechanisms, mainly the adhesion of material to the surface of the tool. This adhesion of material to the surface of the tool is promoted by increasing the length of cut, because as the test progresses, the material accumulates in the grooves left on the surface of the tool, which, in turn, are caused by the tool grinding process and of the substrate. Therefore, at longer cutting lengths, this amount of accumulated material will be greater, which will cause abrasive wear, and eventually result in coating failure. Therefore, as can be seen in Figure 40, with 5 meters of cutting length, some relevant wear mechanisms are already observed, showing adhesion and abrasion marks.

Regarding the coating tool, these seemed to hold quite well, however in the S75F100L15 condition there seems to be delamination on the rake face (RF2), as shown in Figure 42(a) and the occurrence of chipping and cracking, changing the geometry of the tool on the clearance face (CF2), as shown in Figure 42(b). Thus, this condition proved to be aggressive, although its flank wear measure was the smallest of this group of 15 meters cutting length. However, the main wear mechanism of the coating was abrasion (Figure 43).

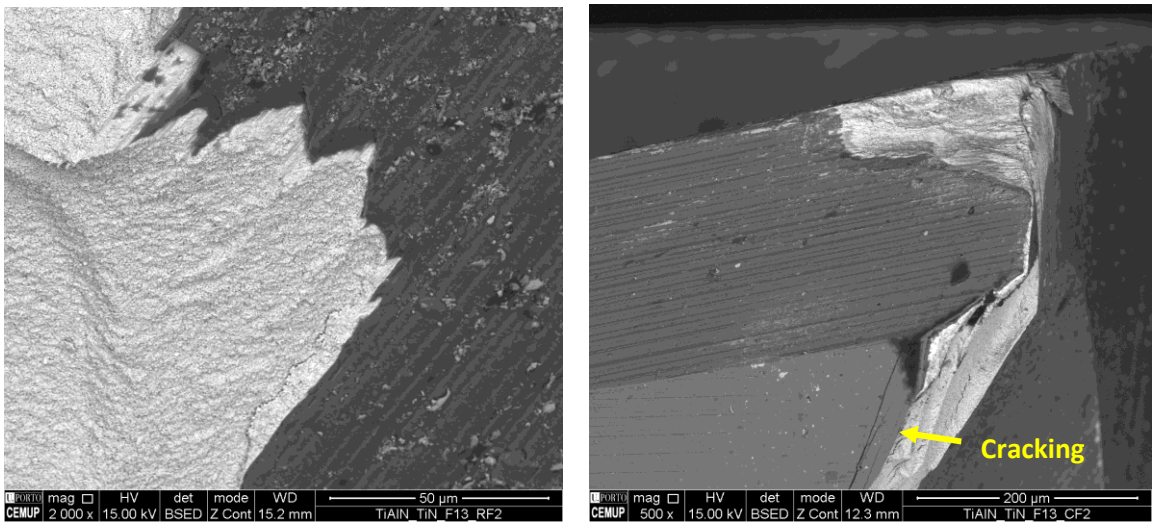

(a) (b)

Figure 42 - S75F100L15 condition: (a) coating delamination in rake face (RF2) at 2000X magnification and (b) Occurrence of chipping and cracking in clearance face (CF2) at 500x magnification

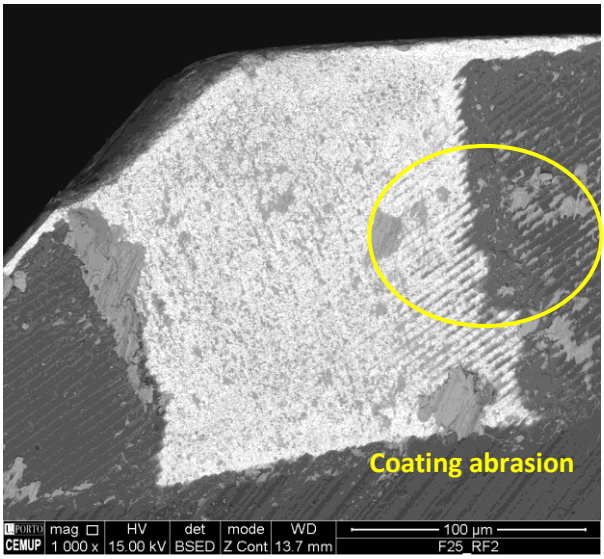

Figure 43 - Coating abrasion in rake face (RF2) of S75F150L5 at 1000x magnification.

In summary, the wear mechanisms observed for the tools tested at 75 m/min of cutting speed are abrasive wear and adhesion of material both on the coating and on the substrate of the tool. And, for condition S75F100L15 also coating delamination, chipping and cracking was observed. In addition, condition S75F150L15 showed the beginning of built-up edge (BUE) development. Furthermore, increasing the feed per tooth did not negatively influence the wear, and both adhesion and abrasion are present for all feed per tooth conditions.

4.5.2. Cutting speed of 100 m/min

Figure 44 illustrates the top view of the tools tested at 100 m/min of cutting speed. As observed in the previous case (75 m/min), in cases where the tools were tested at a cutting speed of 100 m/min, the parameter that most influenced the wear was the cutting length, compared to the feed per tooth.

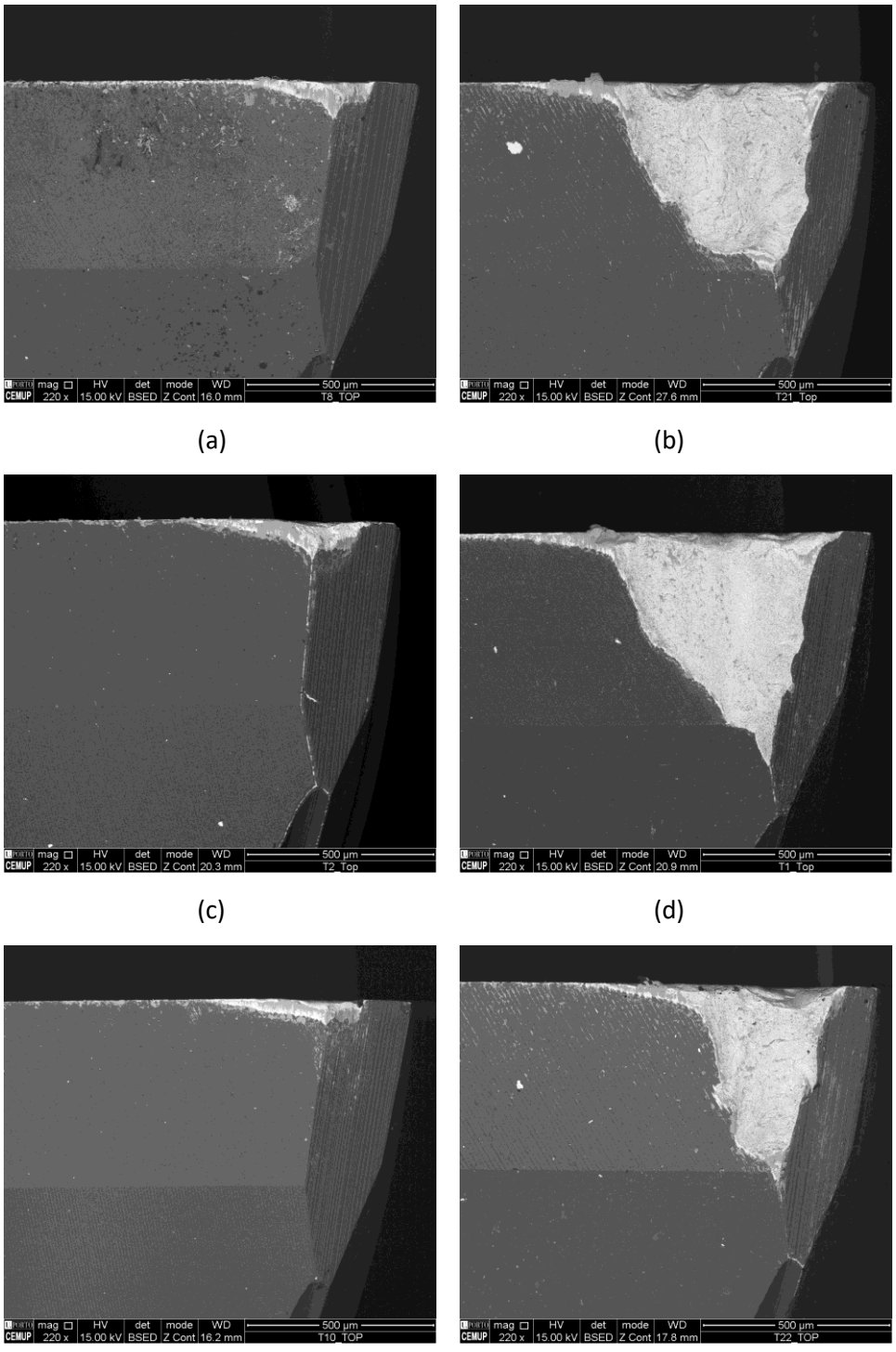

Figure 44 - Top view of the tools tested at 100 m/min of cutting speed at 220x magnification: (a) S100F75L5, (b) S100F75L15, (c) S100F100L5, (d) S100F100L15, (e) S100F150L5, and (f) S100F150L15.

As previously mentioned, the impact of the cutting length seems to increase the wear significantly. As seen in the measurements carried out, it is clear from the generated images that when considering 5 meters of cutting length, and increasing the feed per tooth, the resulting wear tends to be smaller. Furthermore, it is evident that this trend was not the same for 15 meters of cutting length. Figure 45 illustrates the rake faces of the tools tested at 100 m/min of cutting speed, and Figure 46 illustrates the clearance faces of the tools in this same condition.

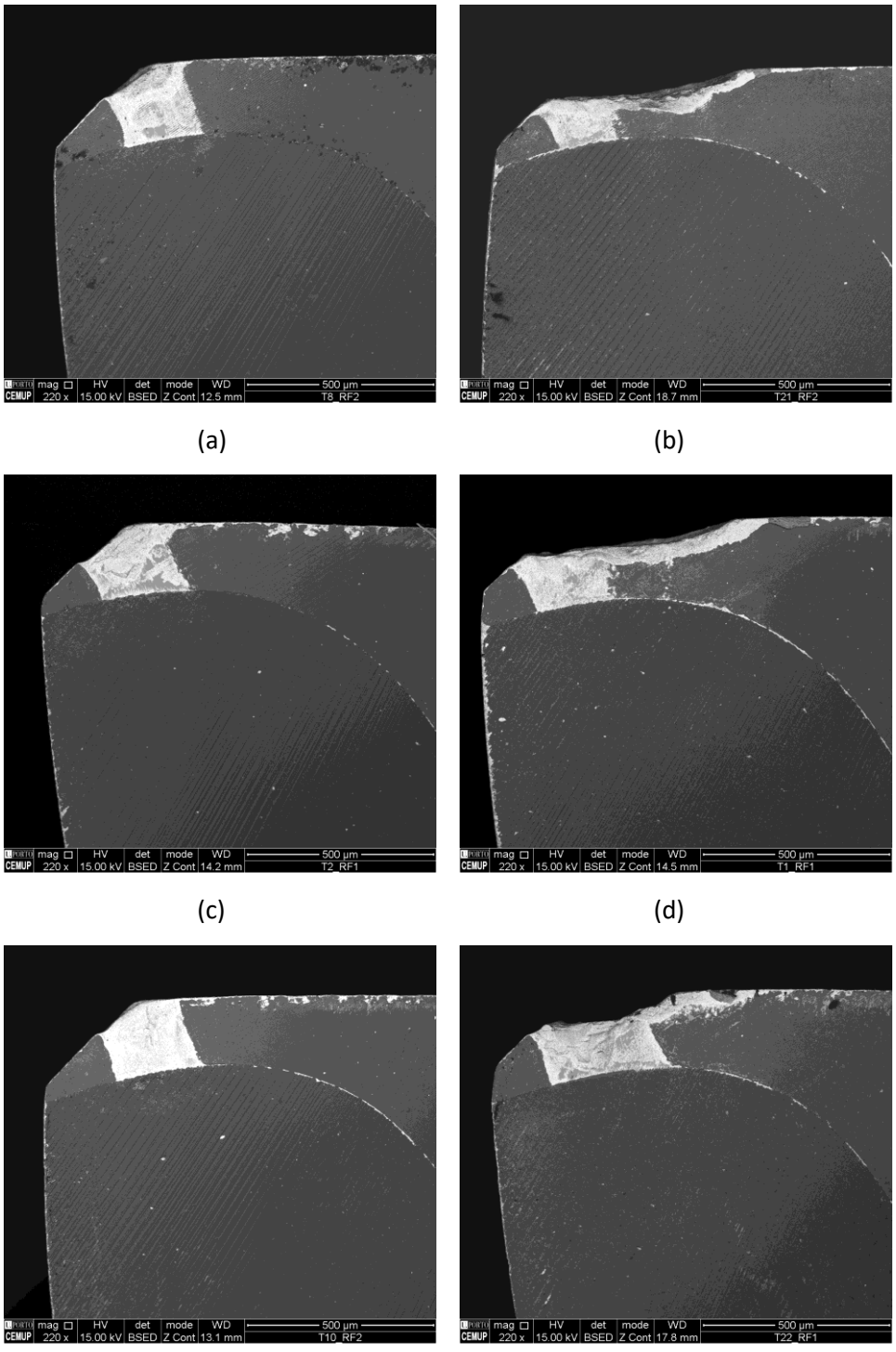

Figure 45 - Rake face view of the tools tested at 100 m/min of cutting speed at 220x magnification: (a) S100F75L5, (b) S100F75L15, (c) S100F100L5, (d) S100F100L15, (e) S100F150L5, and (f) S100F150L15.

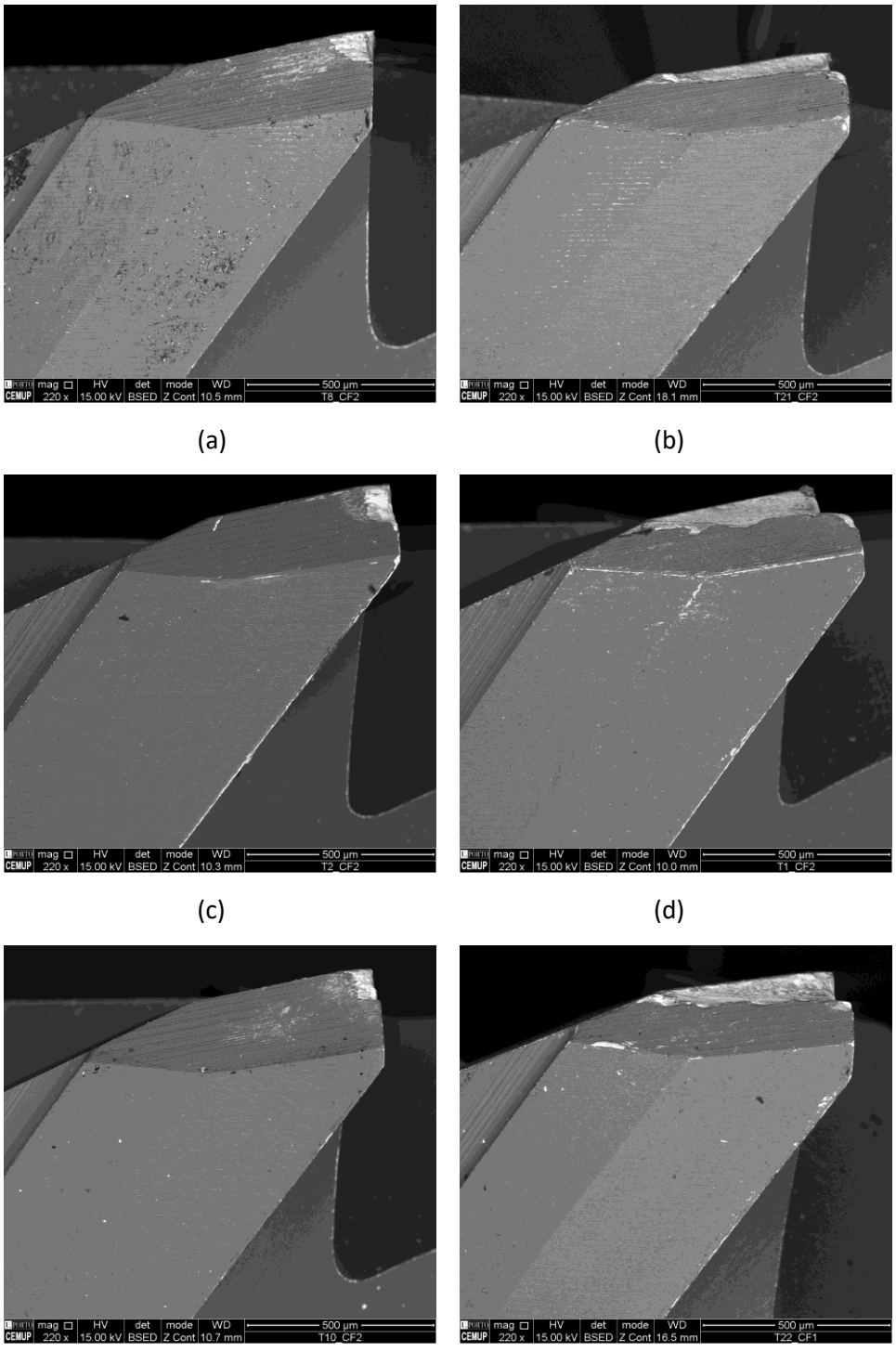

Figure 46 - Clearance face view of the tools tested at 100 m/min of cutting speed at 220x magnification: (a) S100F75L5, (b) S100F75L15, (c) S100F100L5, (d) S100F100L15, (e) S100F150L5, and (f) S100F150L15.

Thus, it can be seen that Figure 45 and Figure 46 clearly show the impact of cutting length on tool wear. Regarding the influence of feed per tooth, it is observed that the wear mark is wider for tools tested with lower feed values, and deeper for tools tested with higher values of this parameter. Possibly this is due to the frictional wear to which the tool is subject at smaller feeds per tooth, which generates more accentuated wear, and which can modify the geometry of the tools. Furthermore, the chip formation mechanism due to friction seems to further accentuate tool wear.

As for the observed wear mechanisms, these were similar to those recorded for 75 m/min of cutting speed, but with different intensities. The predominant wear mechanism is abrasion, as seen in Figure 47, which, as previously stated, is usually observed when machining Inconel 718. As previously mentioned, the tools tested at 15 meters cutting length exhibited considerably higher levels of wear than those tested at 5 meters. Moreover, this abrasive wear was more intense on the clearance face of the tools, as shown in Figure 47.

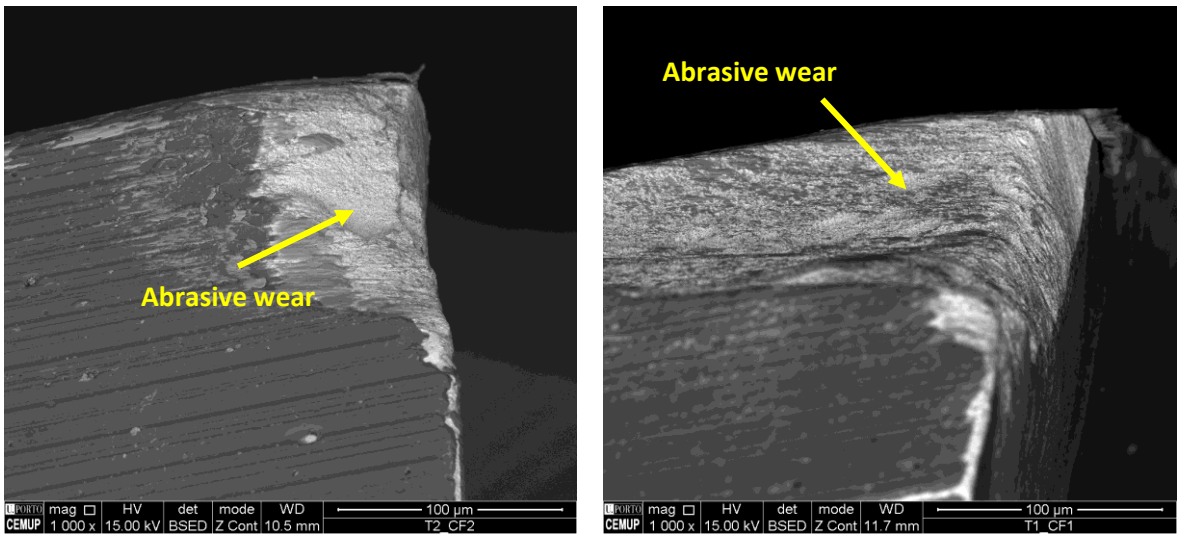

(a) (b)

Figure 47 - Abrasive wear: (a) Clearance face (CF2) of S100F100L5 at 1000x magnification and (b) Clearance face (CF1) of S100F100L15 at 1000x magnification.

In addition to abrasion, higher levels of adhesion can be observed compared to tools at 75 m/min, both on 5 meters and 15 meters lengths. Adhesion is observed both in the substrate of the tool and on the coating, with the level of the first case being higher. This wear was registered on the tools' flank, edges, and rake face; however, this was mainly found on the rake face of the tools. In turn, regarding the influence of the value of feed per tooth on the wear mechanisms presented by the tools tested at 100 m/min, it was verified that the lower the value of this parameter, the greater the adhesion to the substrate of the tool.

To exemplify, Figure 48 illustrates the situation of adhesions to the substrate of the tool, considering two conditions: S100F100L15 and S100F150L15. Thus, it appears that adherence is greater in the first condition, tested with 100% of fz, in comparison with the condition tested with 150% of fz, and keeping equal the other parameters. Furthermore, the formation of build-up edge, in an early and undeveloped stage, was also observed in the conditions with 15 meters of cutting length (Figure 49).

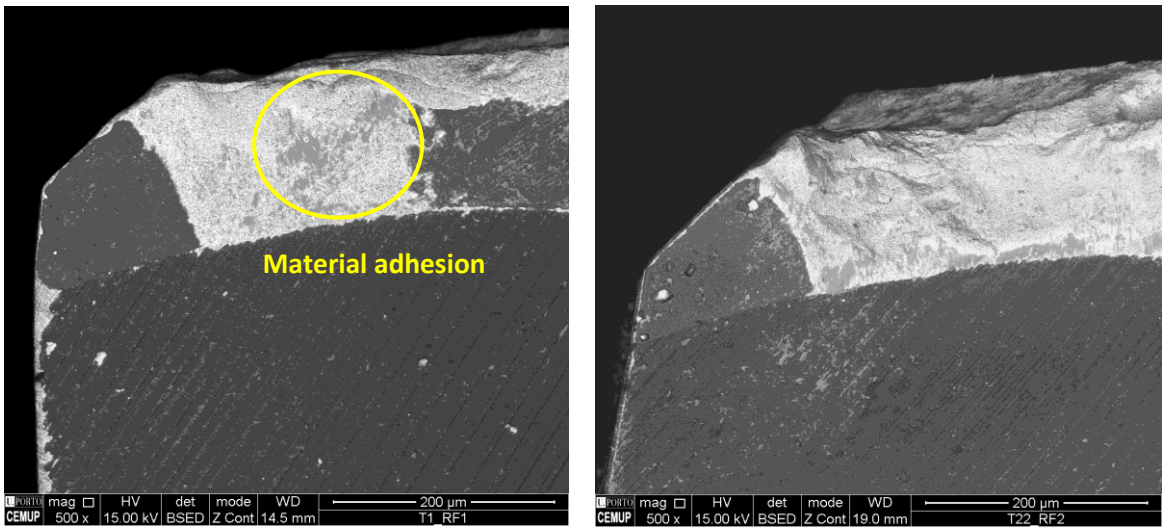

(a) (b)

Figure 48 - Adhesion of material to tool substrate: (a) RF1 of S100F100L15 at 500x magnification and (b) RF2 of S100F150L15 at 500x magnification

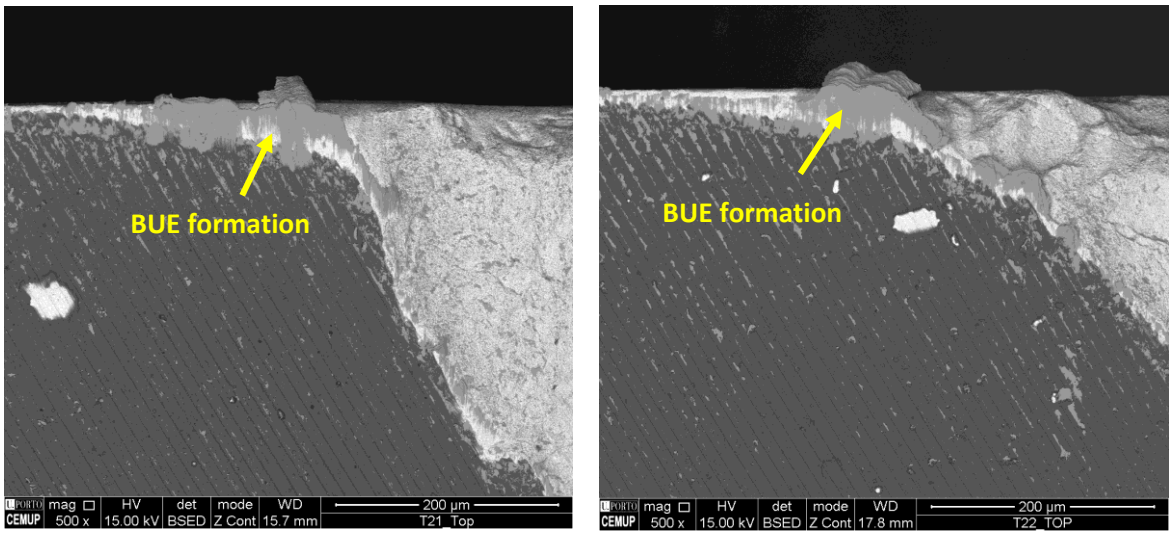

(a) (b)

Figure 49 - Beginning of built-up edge (BUE) formation showing adhesion of material on exposed substrate at 500x magnification: (a) Top view of S100F75L15 and (b) top view of S100F150L15.

Regarding the wear on the coating, this was likewise both abrasion and adhesion, as shown in Figure 50. There was no major evidence of coating delamination, which indicates the good behavior of the coating. Thus, the TiN layer improved the crack resistance of the coatings as no major cracks were identified in the coated tools tested under these conditions.

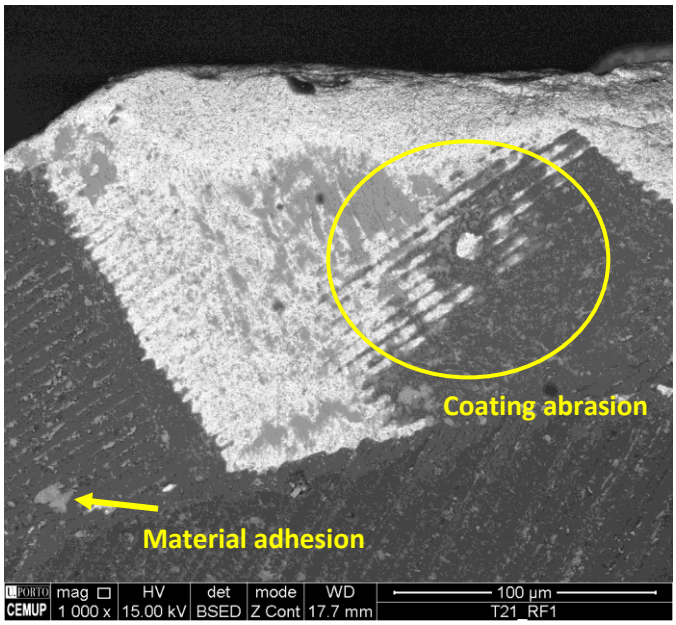

Figure 50 - S100F75L15 showing material adhesion and abrasion on the coating at 1000x magnification.

As in the condition at 75 m/min, an EDS analysis was performed to confirm the presence of adhered material, according to the chemical composition resulting from the analysis. Figure 51 illustrates the condition S100F75L5 with three zones for which the analysis was carried out, and Figure 52 the result of the EDS analysis for the three corresponding zones.

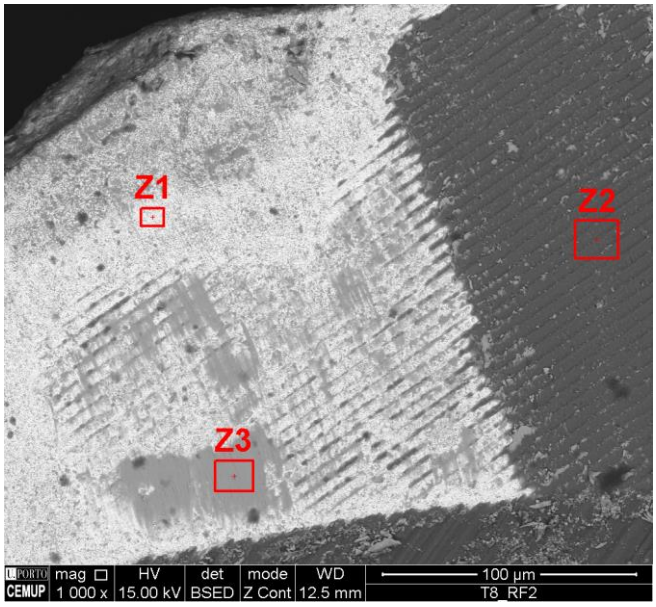

Figure 51 - Condition S100F75L5 with three zones marked for EDS analysis.

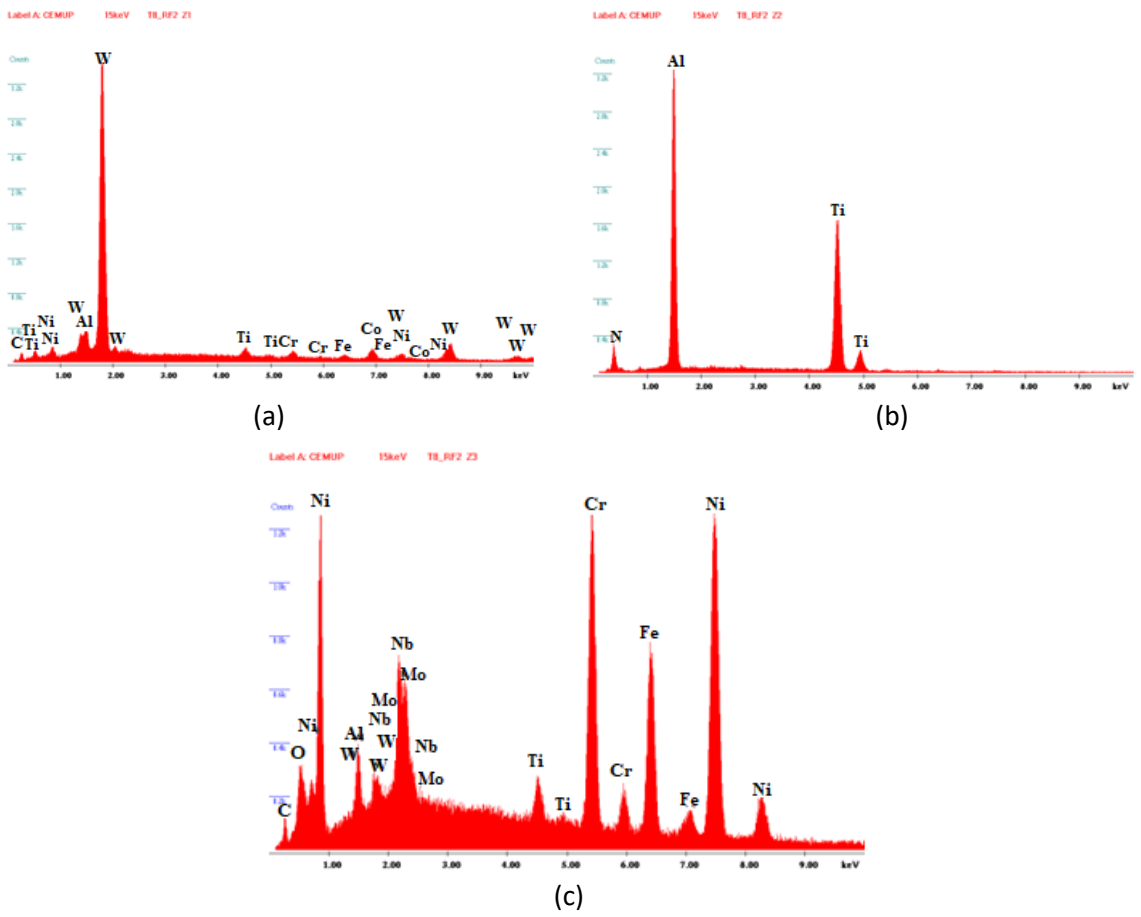

Figure 52 - EDS analysis of the three zones for S100F75L5: (a) tool substrate, (b) coating and (c) machined material adhered to the surface of the substrate of the tool.

Therefore, according to the analysis, zone 1, rich in tungsten, refers to the substrate of the tool, zone 2, in turn, has titanium, aluminum and nitrogen in its composition, indicating that it is the coating, and zone 3, rich in nickel, indicates that it is machined material adhered to the substrate of the tool. When comparing the result with the image of the zones, the coherence of the result is observed based on the chemical composition. Thus, the main mechanisms identified under the conditions at 100 m/min of cutting speed were abrasion and adhesion, with the beginning of the formation of built-up edge.

4.5.3. Cutting speed of 125 m/min

Figure 53 illustrates the top view of the tools tested at 125 m/min of cutting speed. As expected, the severity of wear increases for larger values of cutting length, which can intensify and develop more wear mechanisms.

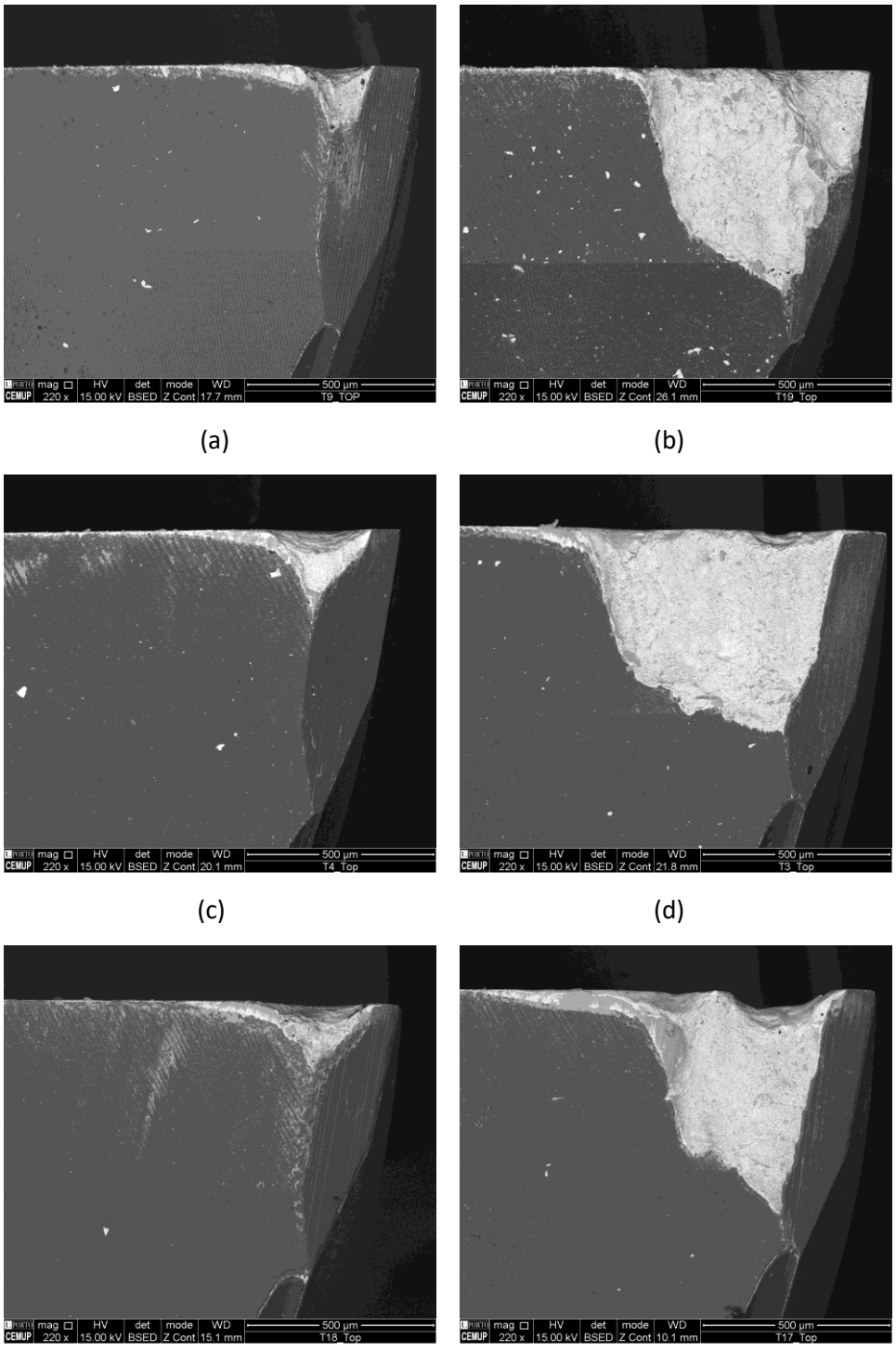

Figure 53 - Top view of the tools tested at 125 m/min of cutting speed at 220x magnification: (a) S125F75L5, (b) S125F75L15, (c) S125F100L5, (d) S125F100L15, (e) S125F150L5, and (f) S125F150L15.

As seen in Figure 53, when increasing the cutting length from 5 meters to 15 meters, the resulting wear increased sharply. In addition, there is also the existing tendency when it comes to 5 meters of cutting length, in which, by increasing the feed per tooth, the wear decreases. However, this trend is registered only for tools tested at 5 meters of cutting length, with the parameter fz not having a great influence on the measured tool wear at 15 meters of cutting length, in which there was a decrease in wear when increasing from 75% fz to 100%, followed by an increase when

increasing to 150% fz. Figure 54 and Figure 55 illustrate the rake face and clearance face of the tools tested at 125 m/min of cutting speed, respectively.

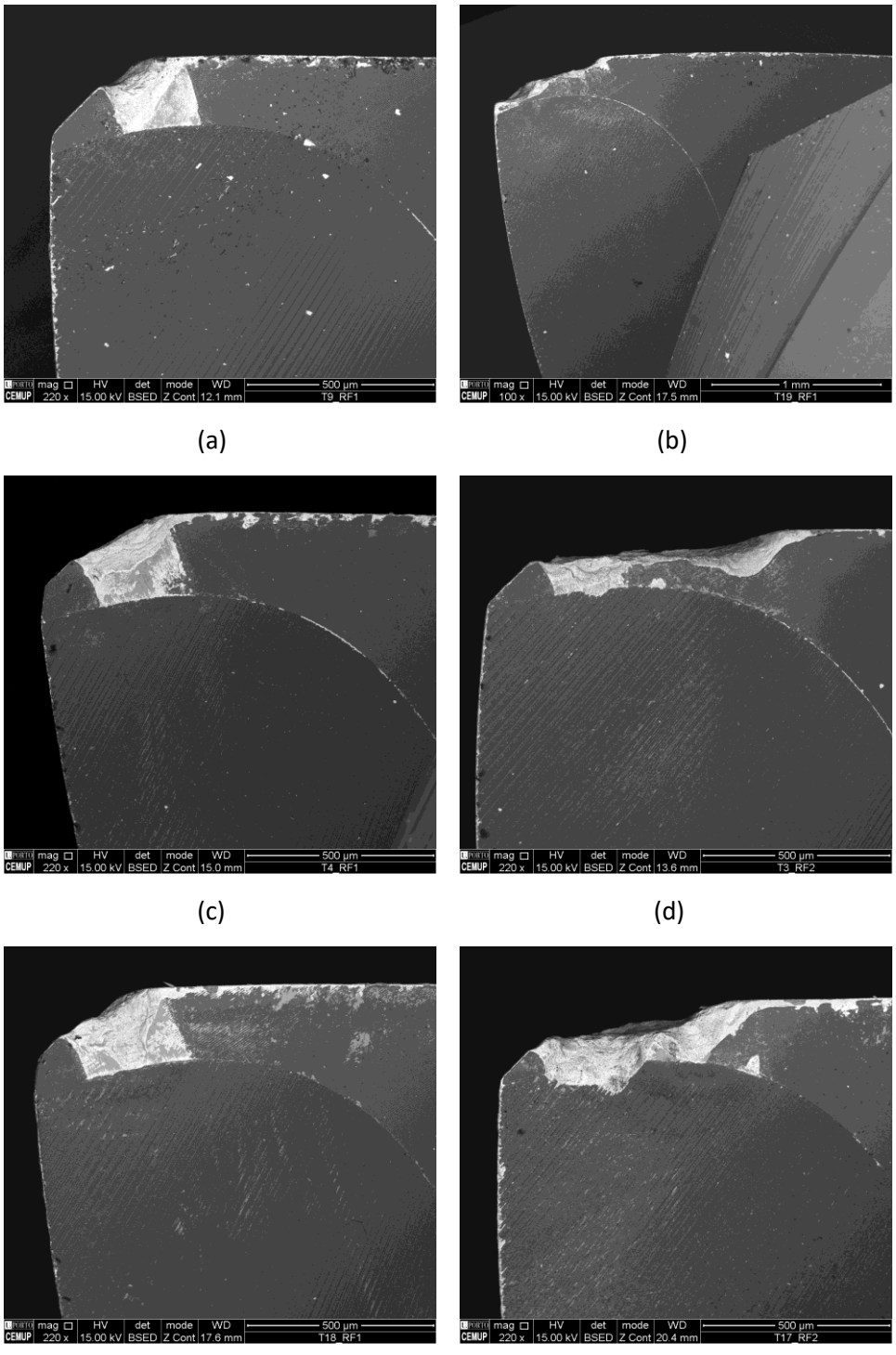

Figure 54 - Rake face view of the tools tested at 125 m/min of cutting speed at 220x magnification: (a) S125F75L5, (b) S125F75L15, (c) S125F100L5, (d) S125F100L15, (e) S125F150L5, and (f) S125F150L15.

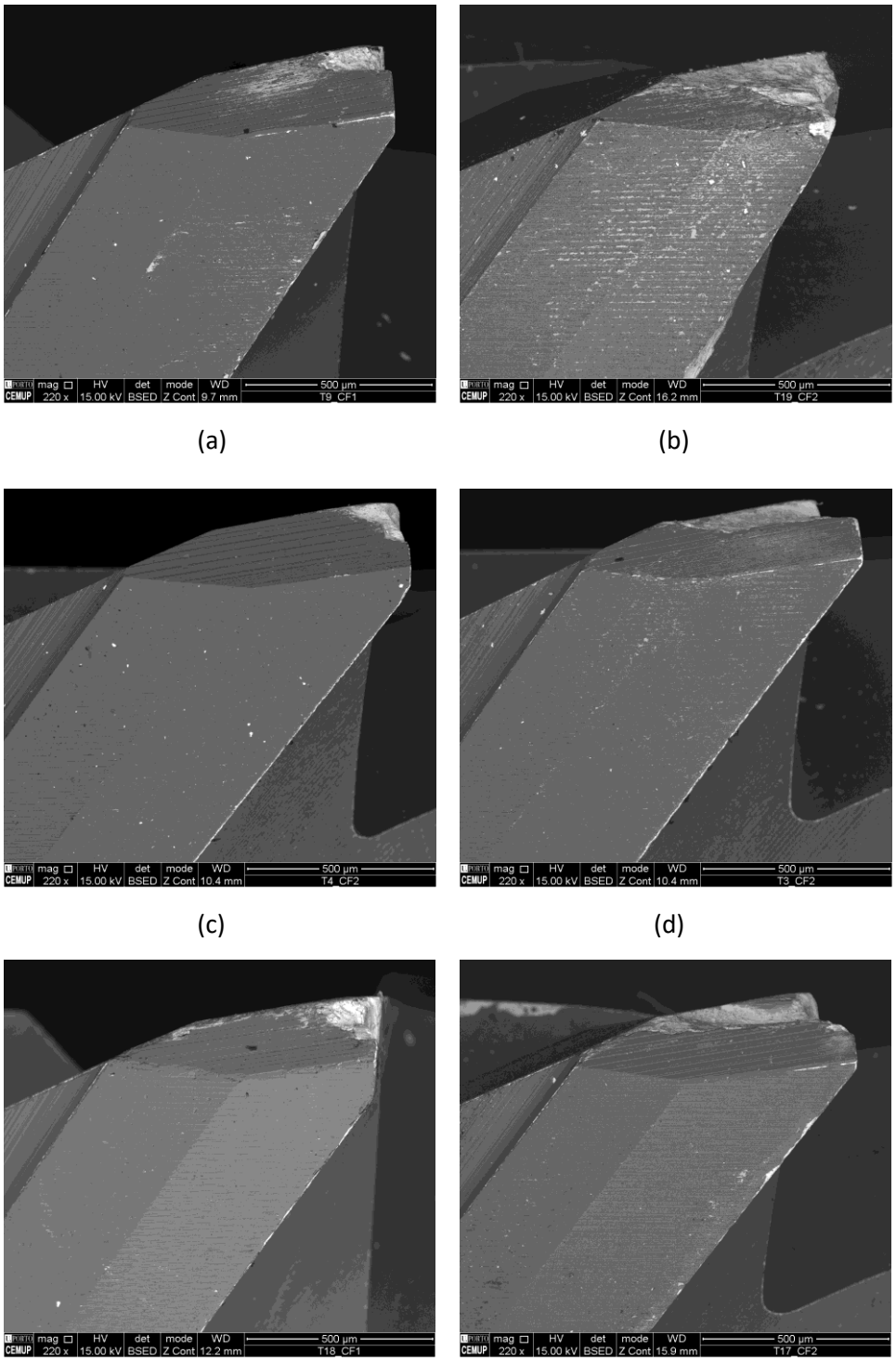

Figure 55 - Clearance face view of the tools tested at 125 m/min of cutting speed at 220x magnification: (a) S125F75L5, (b) S125F75L15, (c) S125F100L5, (d) S125F100L15, (e) S125F150L5, and (f) S125F150L15.

Regarding the influence of tool wear on machined surface quality, it is known that tools with more severe wear tend to produce a worse machined surface quality. However, in the case of tools tested at 125 m/min of cutting speed, and 5 meters of cutting length, it was observed that the wear decreased as the feed per tooth increased, however the quality of the machined surface also decreased with higher mean Ra values.

In turn, in the case of the tools tested at 15 meters of cutting length, the fz parameter did not have a great influence, since there was no trend in the data obtained. In the case of the machined surface quality, it worsened with the increase of fz, however, the wear suffers a decrease when using 100% of fz, and an increase when using 150% of fz.

Regarding the wear mechanisms presented by these tools, abrasion and adhesion both in the substrate of the tool and in the coating, were observed in all cases. In some cases, there was the beginning of the formation of built-up edge and chipping. Note that material adhesion in this case was greater than in previous cases where the tools were tested at 75 and 100 m/min. In addition, it is observed that the increase in the amount of feed per tooth promoted the formation of wear mechanisms at different intensities. For example, under conditions at 75% fz, that is, S125F75L5 and S125F75L15, a large amount of material adhesion was observed on the tool substrate, as well as on the coating but to a lesser extent, and abrasive wear. In addition, the condition with 15 meters of cutting length, had a more accentuated wear, with alteration of the geometry of the tool, which indicates de presence of chipping. Figure 56 illustrates these two conditions with the respective wear mentioned.

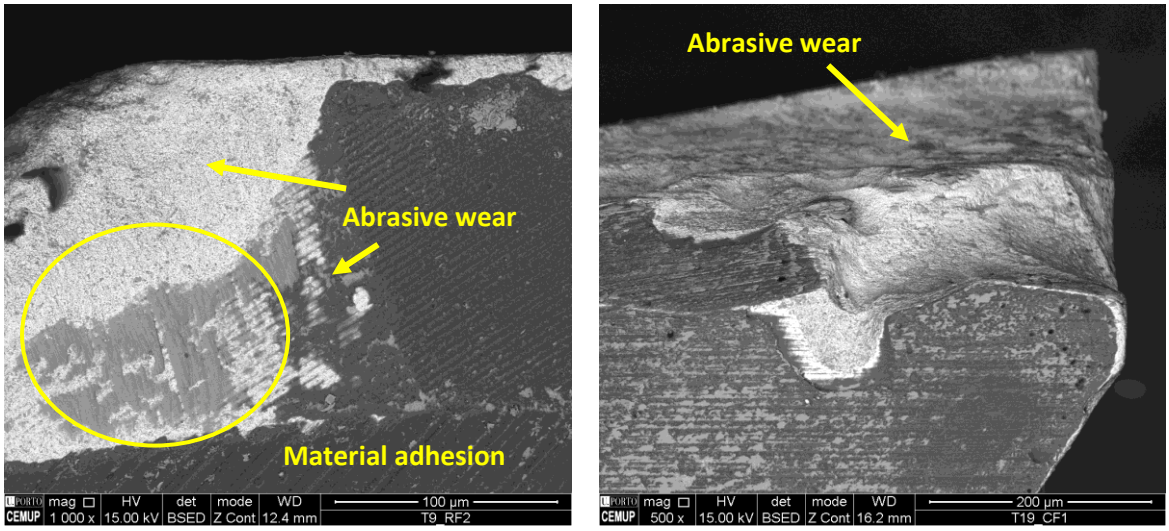

(a) (b)

Figure 56 - Wear at 75% fz: (a) S125F75L5 at 220 magnification showing abrasive a adhesion of material and (b) S125F75L15 at XX magnification showing a large amount of abrasive wear with alteration in the geometry of the tool.

In addition, to confirm the presence of adhered material, the EDS analysis of Figure 57 was performed. The analysis can be found in Figure 58. As a result, it appears that zone 1 corresponds to the substrate, rich in tungsten, zone 2 to the coating and zone 3, with a large amount of nickel, corresponds to the Inconel 718 alloy adhered to the substrate of the tool.

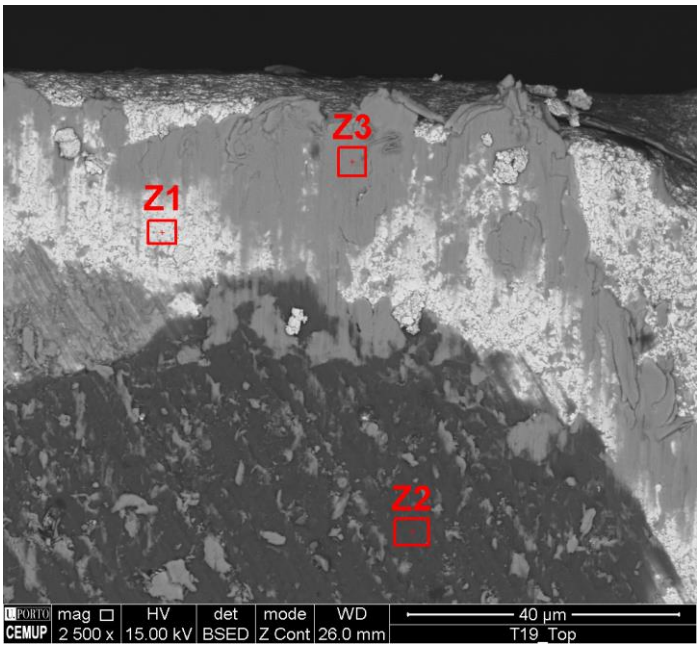

Figure 57 - Condition S125F75L15 with three zones for EDS analysis.

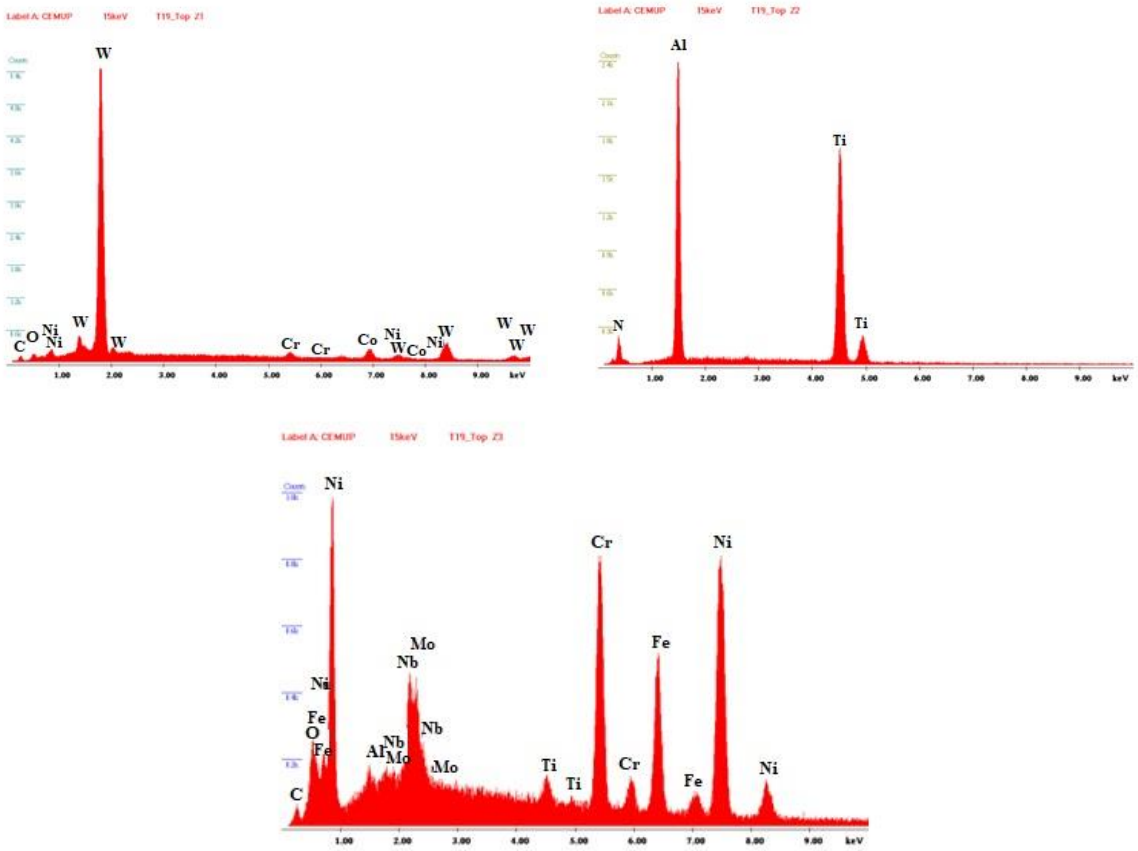

Figure 58 - EDS analysis of the three zones for S125F75L15: (a) tool substrate, (b) coating and (c) machined material adhered to the surface of the substrate of the tool.

In the same way, a greater amount of adhered material was observed, both in the substrate of the tool and in the coating, for the tests carried out at 100% of fz, but in more quantity than in the other conditions. There seems to be a higher level of adhesion to the tools' substrate than to the tool

coating itself. Figure 59 illustrates a rake face of conditions with 100% fz, that is, S125F100L5 and S125F100L15, which have a large amount of adhered material.

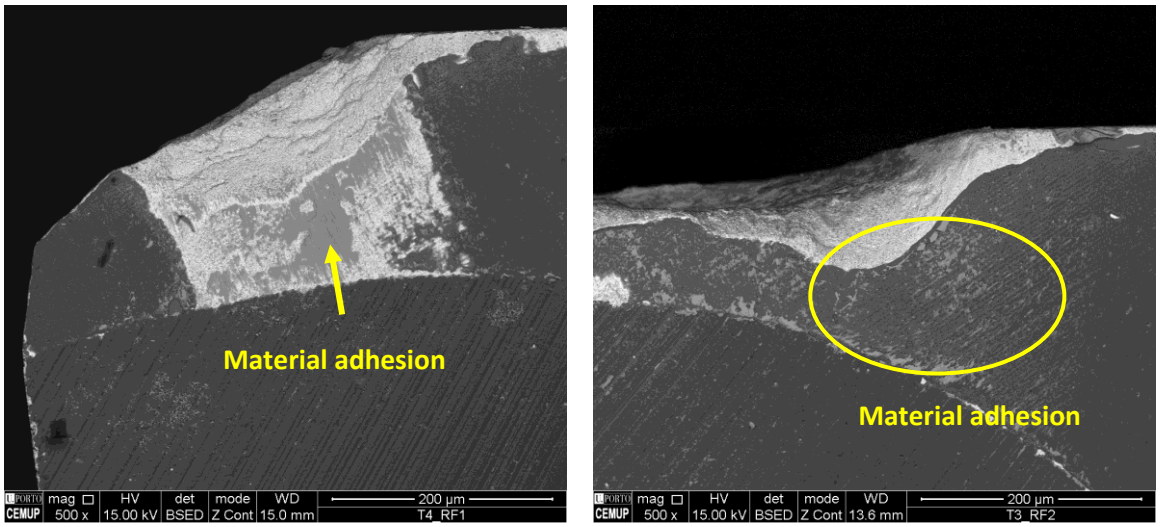

(a) (b)

Figure 59 - Material adhesion: (a) RF1 of S125F100L5 at 500x magnification showing adhered material in the substrate of the tool and (b) RF2 of S125F100L15 at 500x magnification showing material adhered on the coating.

In turn, for the tests carried out at 150% the predominant wear mechanism was abrasive wear together with material adhesion. Figure 60 illustrates the clearance face corresponding to 150% fz, showing abrasive wear and adhered material. In the case with 15 meters of cutting length, the abrasion was greater than in the previous cases.

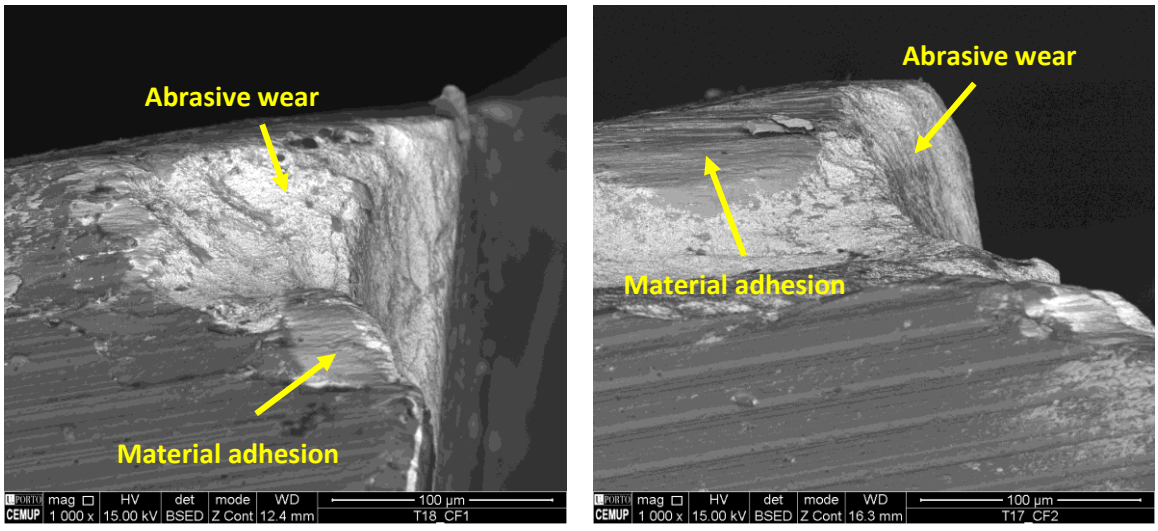

(a) (b)

Figure 60 - Abrasive wear and material adhesion: (a) CF1 of S125F150L5 at 1000x magnification and (b) CF2 of S125F150L15 at 1000x magnification.

In addition, in conditions with greater feed per tooth, that is, 150% of fz, the beginning of the development of built-up edge (BUE) was also observed, as shown in Figure 61. It should be noted that this mechanism is more common at lower cutting speeds, changing the geometry of the tool and possibly causing it to break [13]. Moreover, it can lead to accelerated tool wear.

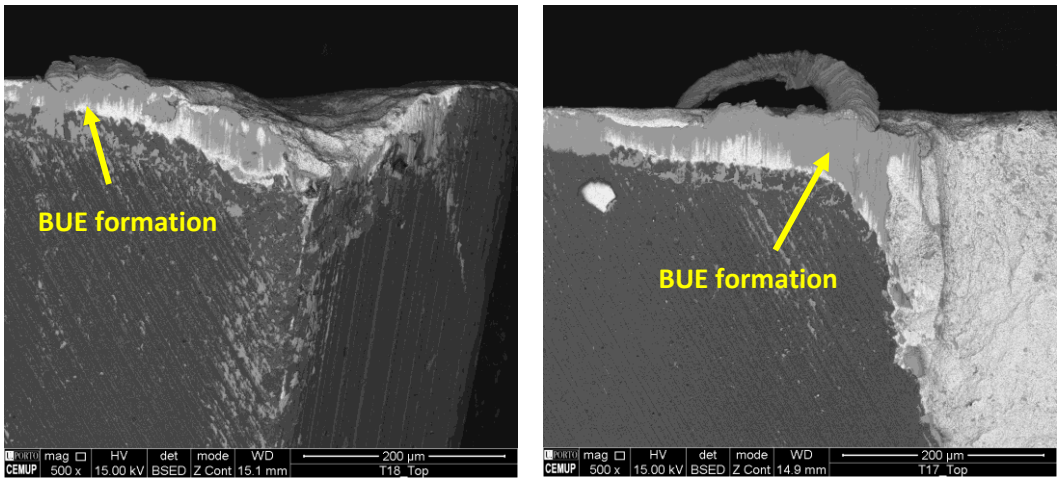

(a) (b)

Figure 61 - BUE formation: (a) top view of S125F150L5 at 500x magnification and (b) top view of S125F150L15 at 500x magnification.

Moreover, under these conditions, a considerable amount of chips was noted, mainly those tested at 15 meters of cutting length. In fact, as previously mentioned, the machining of Inconel 718 can be quite aggressive to cutting tools, promoting high levels of wear [112]. However, the formation of chips impairs the performance of the machining process, since it alters the geometry of the cutting tools, and consequently alters the chip formation mechanism, negatively impacting the quality of the product obtained with the cutting tools with this wear [132]. In addition, it generates higher roughness values for the machined surface, as seen in section 4.2., which the quality of the machined surface for 15 meters of cutting length is worse.

4.5.4. Cutting length of 25 m

As previously mentioned, two conditions were also tested with 25 meters cutting length. These are the conditions with the maximum and minimum parameters: S75F75L25 and S125F150L25. Figure 62 illustrates the top view of the tested tools at 25 meters of cutting length, confirming the similarity between the measurements of the two cases, exposed and analyzed in the section 4.4.4. Also, Figure 63 and Figure 64 illustrate the rake face and clearance face, respectively.

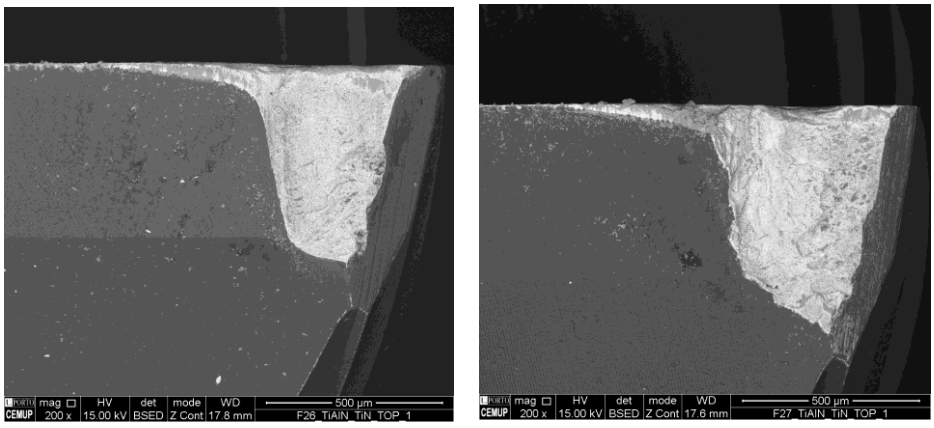

(a) (b)

Figure 62 - Top view of tools tested at 25 meters of cutting length at 200x magnification: (a) S75F75L25 and (b) S125F150L25.

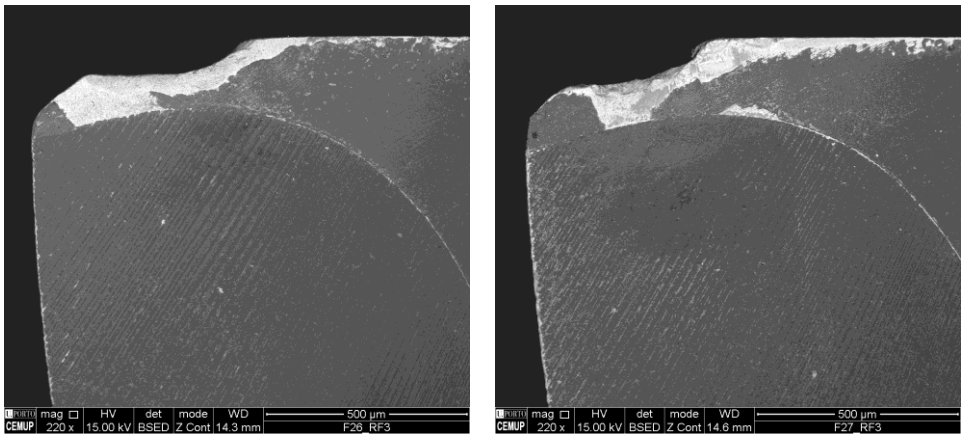

(a) (b)

Figure 63 – Rake face view of tested tools at 25 meters of cutting length at 220x magnification: (a) S75F75L25 and (b) S125F150L25.

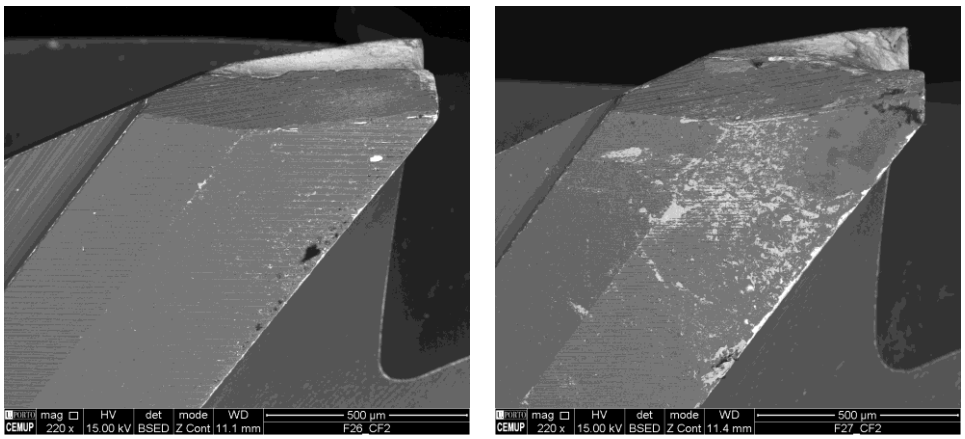

(a) (b)

Figure 64 – Clearance face view of tested tools at 25 meters of cutting length at 220x magnification: (a) S75F75L25 and (b) S125F150L25.

In the two conditions analyzed with 25 meters of cutting length, the following wear mechanisms were mainly observed: abrasion and material adhesion, both on the coating and on the substrate of the tool. Abrasive wear was more intense on the clearance face of the tools, and material adhesion was mainly found on the rake face of the tools. Figure 65 illustrates these wear mechanisms.

Furthermore, it is observed that the condition S125F150L25, being more aggressive, the wear was more severe, and delamination of the coating occurred. This is caused by the high degree of adhesion on the tool, as can be seen in Figure 66, which shows the delamination zone of the coating on the rake face (RF2) of a tool S125F150L25, where the presence of adhered material can also be observed. That is, the rake face exhibited more delamination of the coating, possibly caused by the greater amount of material adhered to these faces. It can also be said that the multilayer coating provided greater resistance to the propagation of cracks, since no cracks developed on it were observed [3].

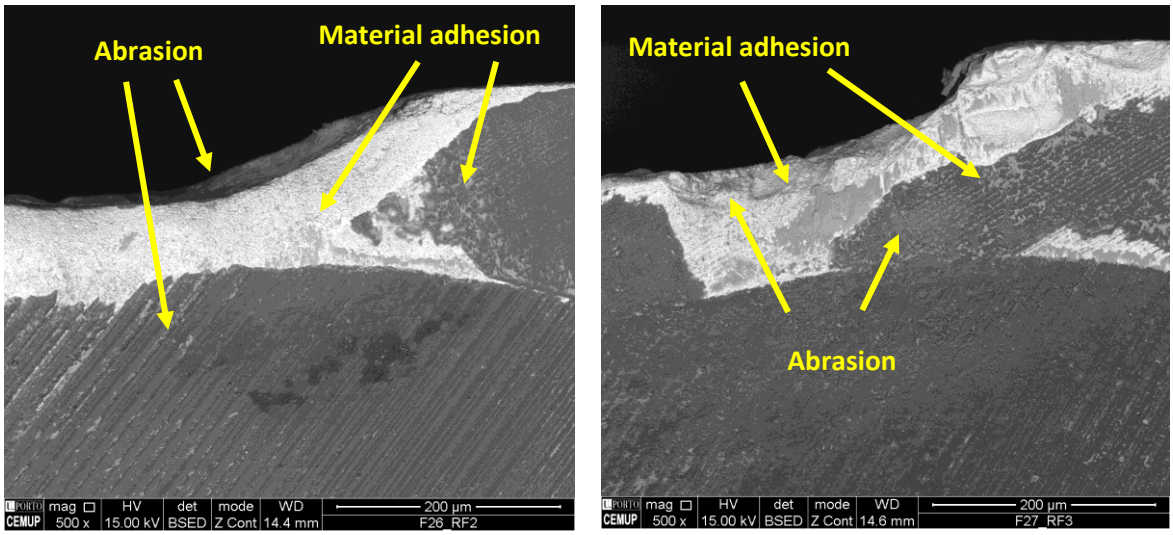

Figure 65 - Wear mechanisms: (a) S75F75L25 (b) S125F150L25

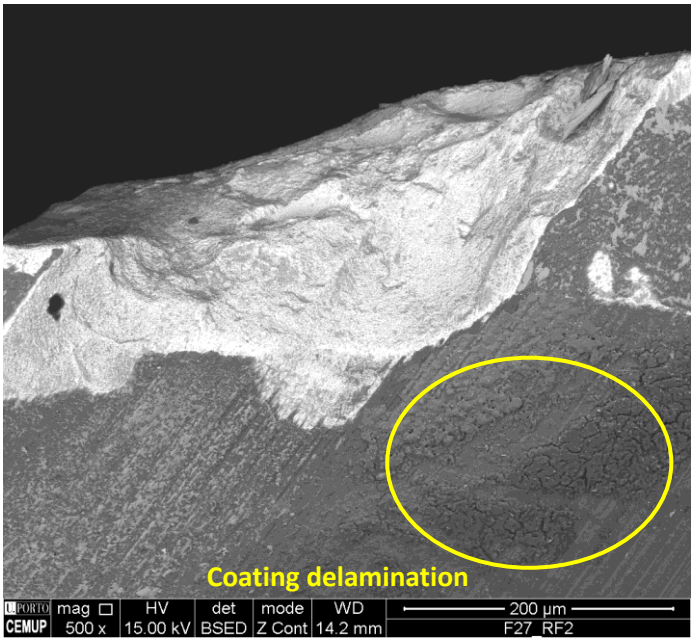

Figure 66 - Coating delamination on rake face (RF2) of S125F150L25 at 500x magnification

4.6. Tool lifespan analysis

As mentioned in section 3.2.7. the end-of-life criterion considered was a maximum VB3 of 0.5 mm on any tooth of the tool. Figure 67 illustrates the progression of the flank wear (VB3) as a function of cutting length.

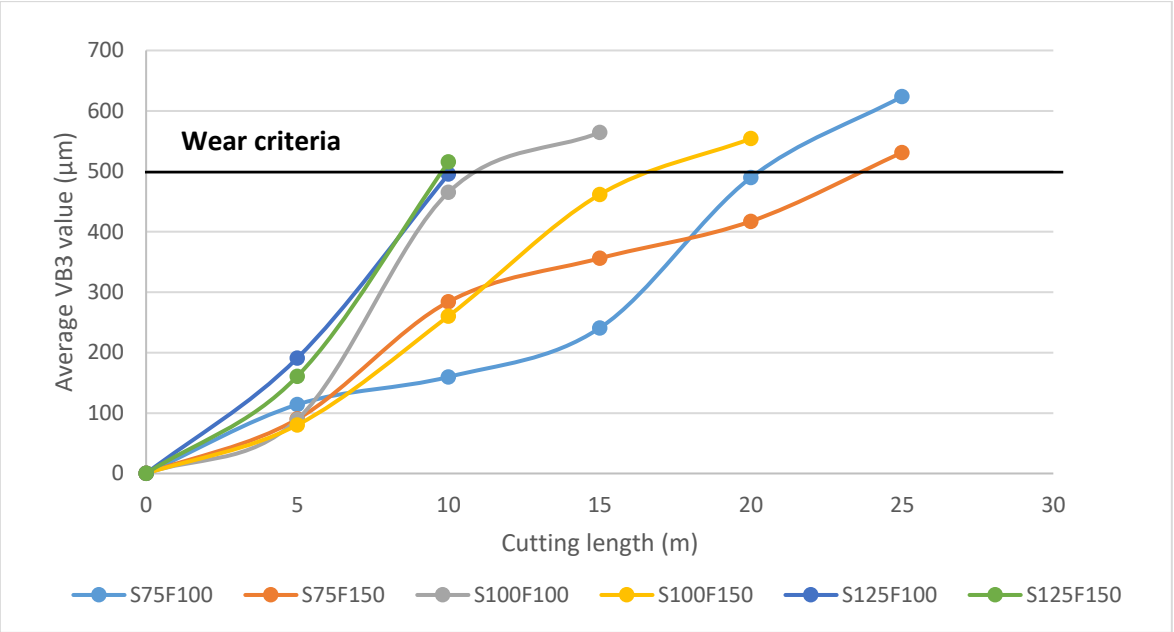

Figure 67 - Progression of flank wear as a function of cutting length.

Firstly, when looking at the figure, it can be seen the increase in wear with increasing cutting length under all conditions. In addition, it appears that conditions S75F100 and S75F150 had their end of life at a cutting length (25 meters) longer than the other conditions, with the second condition being the one that showed less wear in this cutting length. Furthermore, there is a clear influence of cutting speed, since conditions S125F100 and S125F150 had the shortest lifespan. Also, it should be noted that condition S125F100 reached the end of its useful life with an VB3 average of 495.21 µm, as one tooth showed wear of 560.60 µm, and as seen, according to the ISO 8688-2:1986 [119], with only one tooth exceeding 500 µm, the tool's end of life has already been decreed.

Another aspect that is important to point out is that, except for condition S75F100, the flank wear increased sharply from 5 meters of cutting length. In this particular condition, the wear had a slight and more uniform increase until reaching 15 meters of cutting length, with a marked gain from then on. As for the influence of the feed per tooth, this is not as significant as the cutting speed. In general, it is observed that in smaller cutting lengths, and at the same cutting speed, the higher the feed per tooth, the lower the flank wear. However, during the course of the test, this trend is no longer observed, and higher values of feed per tooth may imply greater or lesser flank wear.

Based on this, it can be said that conditions S75F100 and S75F150 had the longest duration in terms of cutting length and flank wear as acceptance criteria. Condition S75F150 reached 500 µm of flank wear (acceptance criterion) with 23.57 meters of cut length, and condition S75F100 with 20.46 meters. Conditions S125F150 and S125F100, on the other hand, had the shortest duration, with 9.82 meters and 10.07 meters (the latter having to be interrupted anyway at 10 meters because one tooth showed flank wear of more than 500 µm), respectively. In addition, conditions S100F100 and S100F150 reached 500 µm of flank wear at 10.54 meters and 16.40 meters, respectively.

Figure 68 illustrates the flank wear in 10 meters of cutting length, in the conditions S75F100 and S125F100, thus emphasizing the influence of the cutting speed in the machining of Inconel 718, since the flank wear of the condition tested at 125 m/min of cutting speed, is much higher than the

tested condition at 75 m/min. Furthermore, as seen, at this cutting length, the condition S125F100 has already reached the maximum of the acceptance criteria.

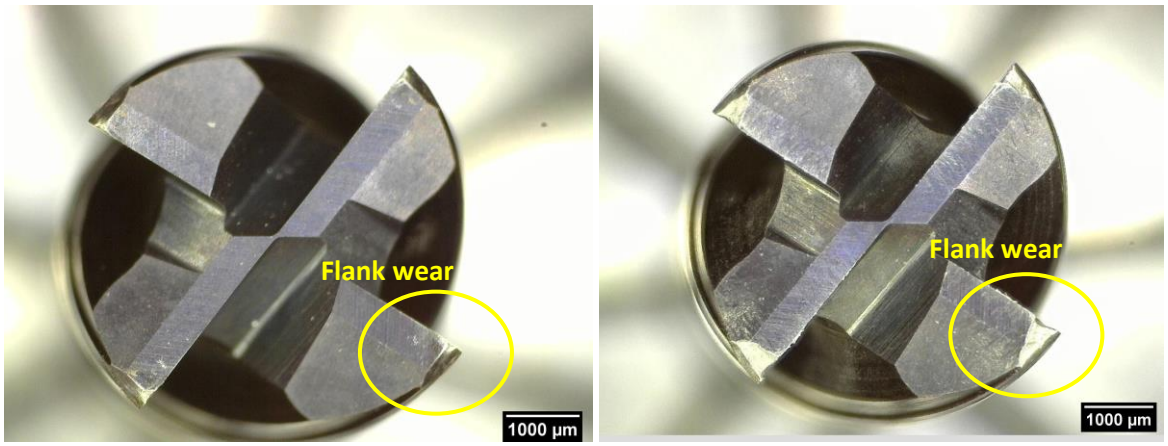

(a) (b)

Figure 68 - Flank wear in 10 meters of cutting length: (a) S75F100 condition and (b) S125F100 condition.

As seen, in 15 meters of cutting length, the S100F100 condition has already exceeded the limits of the acceptance criteria, however, the S100F150 condition still maintained its useful life in this cutting length, indicating that in this case, and in this cutting length, the greater the feed per tooth, the less wear. On the other hand, at this same cutting length, conditions S75F100 and S75F150 showed another trend, in which the second condition had more wear than the first, thus not making clear the influence of feed per tooth on the progression of wear and useful lifespan of the tools. Figure 69 illustrates conditions S100F100 and S100F150, where it shows the highest flank wear of the first one.

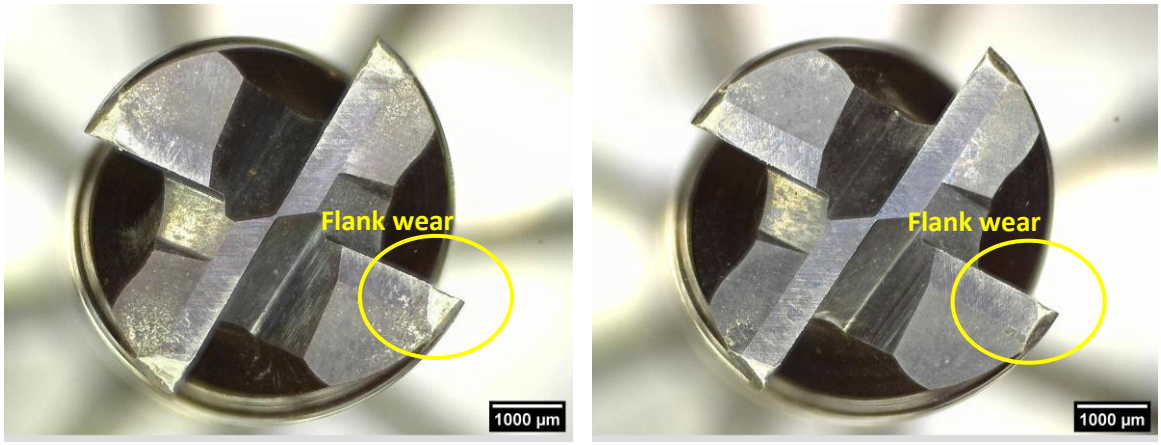

(a) (b)

Figure 69 - Flank wear in 15 meters of cutting length: (a) S100F100 condition and (b) S100F150 condition.

5. DISCUSSION OF THE RESULTS

In this chapter the results obtained in the performed tests will be discussed. For this, the chapter was subdivided into the following subsections: 5.1. Comparison of the surface state obtained on the machined part; 5.2. Comparison of wear generated on tools; 5.3. Tool lifespan comparison and 5.4. Comparison with other coatings used in machining. In this way, the main wear mechanisms will be identified for all tools and test conditions, with a comparison between observed results and tested conditions.

5.1. Comparison of the surface state obtained on the machined part

To compare all test conditions, the values obtained for surface roughness were organized and grouped according to Figure 70. The figure is divided by test conditions, in X axis of the graph, and with three series corresponding to each feed per tooth, in percentage of the initial value (0.07 mm/tooth), in Y axis. It should be noted that according to the identification of the tools, the number after the "S" indicates the cutting speed and the number after the "L" indicates the cutting length value used in the machining test.

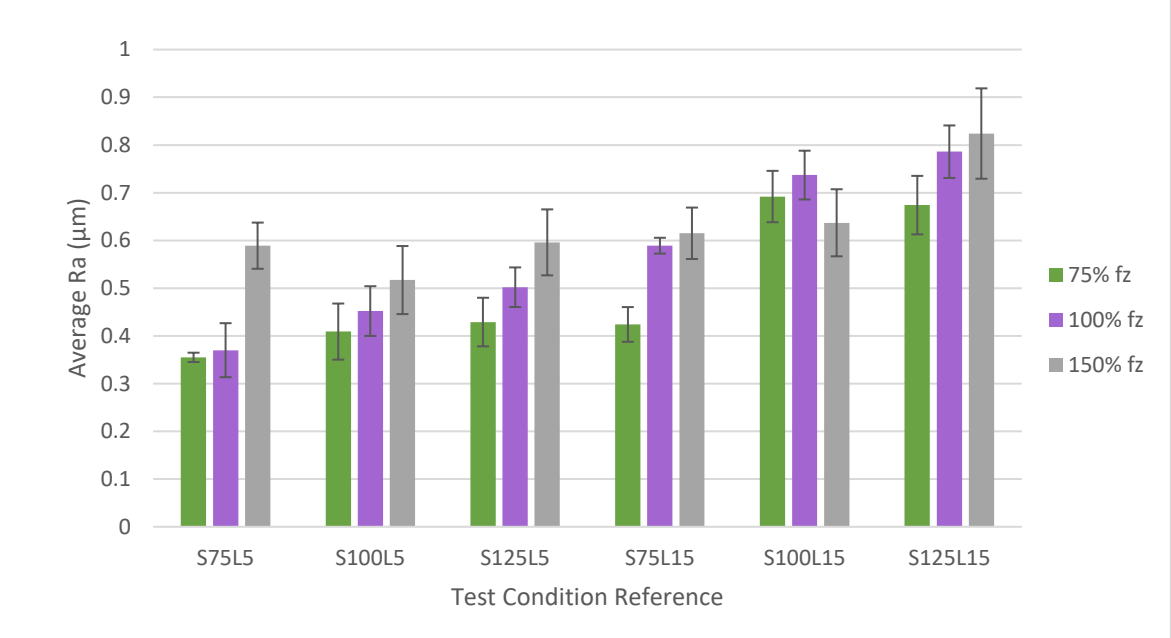

Figure 70 - Comparison of surface roughness values obtained for all conditions tested.

As can be seen in Figure 70, the average values of Ra tend to increase for higher cutting lengths, which is a trend that is registered for all tools conditions. It is also observed that there is a clear influence of the feed per tooth on the roughness of the machined surface. It is noted that this parameter has a clear influence on the surface topography [133]. Thus, when comparing these parameters, it is noticed that higher values result in higher surface roughness values, except in the case of the S100L15 tools, which, when tested at 150% fz, had a lower roughness. That is, they produced a better surface quality than recorded at 75% fz and 100% fz. On the other hand, for conditions S75L5, S100L5, S125L5, S75L15 and S125L15 the minimum mean values of Ra were

recorded for conditions using 75% of feed per tooth. However, in general, increasing the feed per tooth, increases the roughness of the surface [134].

Furthermore, the lowest mean value of Ra for 75% and 100% fz was obtained for the S75L5 condition, and in the case of 150% fz, the lowest mean value was obtained for the S100L5 condition. This shows the clear influence that a shorter cutting length has on the machined surface quality. Moreover, it is observed that the values for S75L5, when increasing the fz from 100% to 150%, there was a marked increase in surface roughness.

In addition, regarding cutting speed, it is observed that the higher this parameter, higher the roughness of the machined surface. This is not commonly observed, as the tendency is for the surface roughness to decrease with increasing cutting speed and depth of cut [135]. This was probably due to the amount of wear sustained by the tools at this cutting speed value [127], and the high abrasive wear that leads to tool-chipping [136]. The only case in which it was observed that increasing the cutting speed, the average roughness was lower, was for 150% of fz, with 5 meters of cutting length, increasing the speed from 75 m/min to 100 m/min.

Regarding the standard deviation recorded for all surface roughness measurements, in almost all conditions this presents a higher value for tests carried out at 150% of the fz value, mainly at 125 m/min and 15 meters of cutting length. This higher standard deviation under these conditions is probably related to the greater sustained abrasive wear of the tool, which leads to a greater difference in surface roughness recorded from the center of the workpiece to its periphery [128].

In general, it can be said that the quality of the machined surface was satisfactory, with good results in terms of its roughness. It is known that the HiPIMS deposition technique produces coatings with significant compressive residual stress values [42], which results in prevention of cohesive failure [137], and makes the presence of compressive stresses one of the main characteristics of surface integrity [138]. This, in turn, is important and beneficial for producing a machined surface with low roughness. Thus, the deposition technique selected to produce the TiN/TiAlN multilayer coating brought a great benefit in terms of the good performance of the tools in producing a good surface quality.

5.2. Comparison of wear generated on tools

To compare all test conditions, the values obtained for flank wear (VB3) were organized and grouped according to Figure 71. The figure is divided into the test conditions in X axis of the graph, and with three series corresponding to each feed per tooth in Y axis, in percentage of the initial value (0.07 mm/tooth). It should be noted that according to the identification of the tools, the number after the "S" indicates the cutting speed and the number after the "L" indicates the cutting length value used in the machining test.

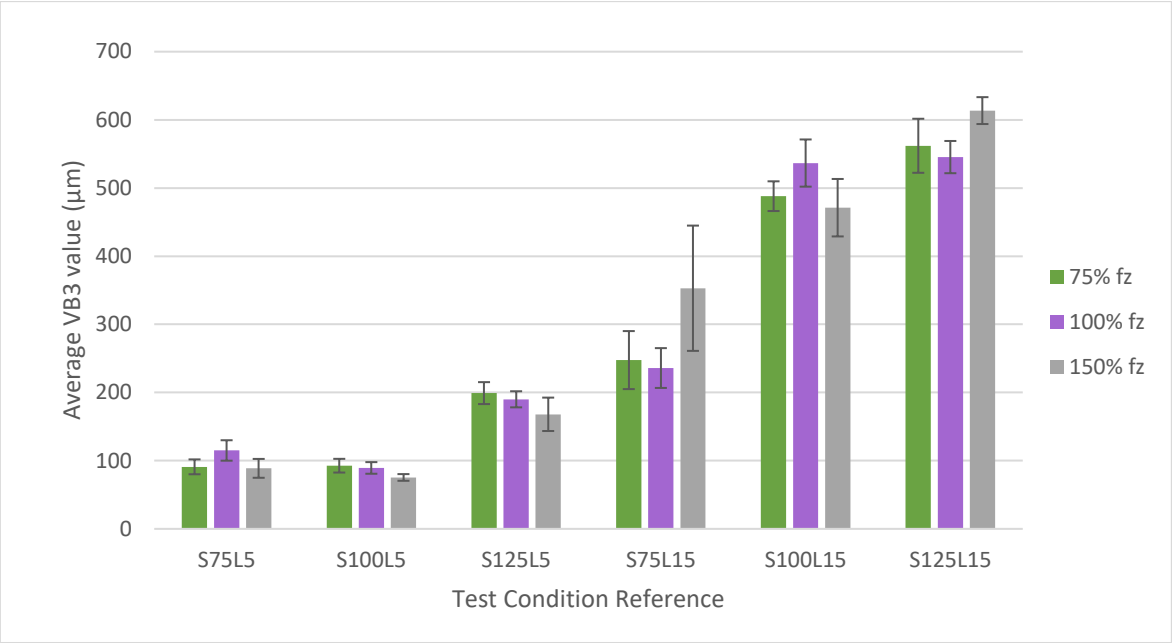

Figure 71 - Comparison of flank wear (VB3) values obtained for all conditions tested.

Analyzing Figure 71, a clear increase in the average value of VB3 is observed with the increase in the cutting length for all conditions. Thus, the impact of this parameter can be seen, which is what most influenced the increase in flank wear. What is commonly observed, since increasing this parameter, the tool wear, tend to increase and the quality of the machined surface tend to decrease [139]. Even under flood lubrication conditions, flank wear increasing with the increase in the cutting length was expected, however, this increase was very significant, showing that even at small distances the Inconel 718 generates great tool wear. This is due to the properties of this alloy, such as the thermomechanical tool load, which generates high abrasive damage [136].

Regarding the feed per tooth, a single trend is not observed for all tools, and its influence is more difficult to be detected. For example, for conditions S100L5, S125L5, flank wear decreased with the increase in feed per tooth, whereas in conditions S75L15 and S125L15, wear decreased when increasing from 75% fz to 100%, but when increasing from 100% of fz to 150% of fz wear increased. On the other hand, the opposite occurred in conditions S75L5 and S100L15, in which wear increased when increasing the feed per tooth from 75% of fz to 100% of fz and decreased when increasing from 100% of fz to 150% of fz. Thus, it seems that the formation of finer chips is the most common cause of poor process performance, as they may break, causing more abrasion and, consequently, higher wear and shorter tool life. Thus, it is more beneficial for the chip section to be thicker, which results in greater integrity and extraction flow, however, if the thickness is too high, it may overload the cutting edge and cause it to break [13]. The feed per tooth is a very important parameter for a productive milling process and is related to the chip formation [140]. In general, in the case of this work, this parameter would be around 0.105 mm/tooth (150% fz), since in this condition, the tendency was for wear to be lower, in four of the six groups of conditions analyzed (S75L5; S100L5; S125L5; S100L15).

As for the cutting speed used in each condition, it appears that when this parameter is increased, the wear also increases, especially when comparing conditions S100L5 with S125L5, and S75L15 with S100L15. This increase in wear is in line with the roughness of the machined surface obtained. However, an increase in cutting speed generally results in a surface with better surface quality and

a smoother cutting behavior by the cutting tools [129], in this case, the opposite was observed, resulting in a more accentuated flank wear.

Regarding the identified wear mechanisms, the most predominant were abrasive wear and adhesion of the material to the tool surface. Mechanical mechanisms such as abrasion and adhesion are predominant when it comes to cutting tool wear [141]. This is in agreement with Inconel 718, which is a difficult-to-machine material, generates excessive wear on the cutting tools, and tends to adhere to the surface of the tool. Furthermore, since Inconel 718 is a material with high heat resistance and hardness, high reactivity with tool materials, and has a strong tendency to form built-up edges (BUE). The presence of this material adhered at the tool tends to generate severe wear [142], as this adhesion of the material to the surface of the tool promotes abrasive wear in these areas, which consequently can promote coating delamination [143]. Thus, only a limited number of tools are capable of being used for machining this alloy [144]. Therefore, it is seen that Inconel 718 commonly adheres to cutting tools [145] and abrasive wear is frequent when machining this alloy [112].

As for the tests carried out at 75 m/min, and considering 5 meters of cutting length, these were the ones that, in general, suffered less wear. However, as it is the condition with the lowest cutting speed, the machining process is less productive [146,147], with possible increases in industrial costs [148,149]. However, when considering 15 meters of cutting length, condition S75F100L15 underwent coating delamination, chipping, and cracking. Furthermore, increasing feed per tooth had no clear influence on the wear, with cutting length being the most significant. Because this condition has a lower speed, it was expected to find other mechanisms, such as built-up edge [13].

For the tests carried out at 100 m/min, it was observed that the wear mark is wider for tools tested with lower feed per tooth values, and deeper for tools tested with higher values of this parameter. This was probably due to the frictional wear which can modify the geometry of the tools and increase the resulting wear. In addition, it was verified that the intensity of wear was greater than in the conditions at 75 m/min, with the influence of the cutting length being significant. It was also verified that abrasive wear was more intense on the clearance face of the tools and the adhesion of material was registered on the tools' flank, edges, and rake face. Furthermore, the formation of build-up edge, in an early and undeveloped stage, was also observed in the conditions with 15 meters of cutting length.

In turn, for the conditions tested at 125 m/min, in the same way, when comparing the cutting length, and 15 meters were used, the resulting wear was greater. For condition S125L5 and varying the feed per tooth value, it was found that the wear decreased as the feed per tooth increased, but the quality of the machined surface also decreased with higher mean Ra values. However, abrasion and adhesion were the predominant mechanisms, with adhesion in this case greater than for 75 and 100 m/min. Moreover, under conditions S125F150L5 and S125F150L15 built-up edge development was observed, and a considerable amount of chips was noticed, mainly those tested at 15 meters of cutting length. This chipping can impair the performance of the machining process, with a decrease in the quality of the machined surface [3]. Thus, the value obtained for the average roughness tends to be higher [2].

It is also noted that, in general, the condition that generated less flank wear was S100F150L5, and the most aggressive condition was S125F150L15, which in turn uses the maximum value of the parameters. Additionally, the presence of cracks was not observed under these conditions,

probably due to the multilayer structure of the coating, which promotes resistance to the propagation of cracks with the TiN layer [3]. In addition, it can be said that the adhesion of the coating was good, since only one condition (S75F100L15) showed delamination, with the main coating wear mechanism being abrasion.

5.3. Tool lifespan comparison

As already stated, Inconel 718 is known as able of inducing high levels of premature wear. It is a difficult to machine alloy, and in many operations cutting tools must be discarded before the end of their useful life to avoid surface damage that may occur, due to the high level of wear developed in the tool. In addition, the fact that Inconel 718 brings short life to cutting tools can be related to its high mechanical resistance and low thermal conductivity [145].

The machining parameters also have a great influence on the tool life. As seen in section 4.6., the condition S75F150 was the one that had the longest tool life according to the acceptance criteria established by the ISO 8688-2:1986 [119], and condition S125F150 was the one that had the flank wear developed more quickly, making its tool life shorter. Thus, the influence of cutting speed on tool life was clear, but on the other hand, no trend was observed in relation to feed per tooth. Kamdani et al. [150] show that selecting the proper machining parameters is crucial to avoid wear and break quickly, with cutting speed and tool geometry being the most important parameters in this matter when considering the Inconel 718. For example, in their work, the authors compared TiAlN and TiN coatings with regard to cutting force variation, surface roughness, tool life and tool wear in end milling of Inconel 718. Thus, it was verified that the TiAlN coating had the greatest tool life, with cutting speed of 50 m/min and feed per tooth of 0.1 mm/tooth. And, when increasing the cutting speed, the resulting wear was higher, and consequently, lower tool life. This is coherent with what was obtained in this work, in which the speeds of 75 m/min, 100 m/min and 125 m/min were used, and the condition at 75 m/min had the highest tool life and at 125 m/min, the lowest. It is noteworthy that the cutting speeds used in the work by Kamdani et al. [150] are 50 m/min, 100 m/min and 150 m/min, that is, the speeds used in the present work are between these values.

Also considering the importance of machining parameters, Motorcu et al. [151], evaluated the effects of cutting speed, milling direction, number of inserts and the use of TiAlN and TiAlN/TiN coating on the surface roughness and tool life in dry milling of Inconel 718. It was verified that the cutting speed has a greater influence on the tool life than the milling method and number of inserts, since in the two tested speeds (50 m/min and 100 m/min), when increasing the cutting speed, tool life had a huge decrease. Regarding the coatings, the best performance was for the TiAlN/TiN coating, which had twice the tool life compared to the other coating.

Based on this, the importance of the correct choice of machining parameters can be observed in order to guarantee a more uniform wear of the tool, and consequently, a greater tool lifespan. In view of this, many researchers consider the flank wear as a criterion for the useful life of a cutting tool, as long as the machining conditions are properly selected [152]. Thus, the tool lifespan is analyzed through the measure of the flank wear, which also impacts the quality of the product obtained, given that if the flank wear increases quickly and sharply, the lifespan decreases drastically [153]. Furthermore, it has been seen in several research, that the flank wear is mainly influenced by the cutting speed, being more significantly than the feed per tooth.

5.4. Comparison with other coatings used in machining

As previously mentioned, Inconel 718 is a difficult to machine material. Thus, the use of coatings on the surface of cutting tools used in the machining process has improved their performance and the surface quality of machined parts. With the analysis carried out, it was possible to verify that the TiN/TiAlN multilayer coating performed well in the tests, with abrasion and material adhesion being the main wear mechanisms identified. Abrasive wear was also identified in the work by Thakur et al. [154], when using the same coating in the machining of Inconel 718, however, in addition to abrasion, the authors also identified plastic deformation and micro chipping as predominant wear mechanisms.

On the other hand, considering the use of another coating, for example, the TiAlSiN/TiSiN/TiAlN coating, analyzed in the work by Kursuncu et al. [96], abrasion and material adhesion were also identified when milling Inconel 718. In this case, the coating was deposited using the magnetron sputtering technique. In the case of the work by Zhao et al. [155], the authors compared two TiAlN coatings, the first with 1 µm thickness (TiAlN-1), and the other with 2 µm thickness (TiAlN-2). About the identified wear mechanisms, adhesion had great prominence, with the formation of built-up edge (BUE), which, in turn, led to the occurrence of coating delamination. Therefore, there is a tendency for both abrasion and material adhesion to occur, or even both mechanisms depending on the coating used, when machining Inconel 718 due to its properties that are characteristic of machining hard-to-machine materials [3].

Another aspect that should be highlighted is the fact that the coating used in this work (TiN/TiAlN) is a multilayer coating, and therefore has greater resistance to the propagation of cracks, and consequently, prevents its delamination [29]. The TiN layer improves the coatings' crack resistance [3]. For example, in the work by Krishnan et al. [156], the TiAlN single-layer coating was used to evaluate its influence on surface roughness, burr formation, and chip formation during machining on Inconel 718. As main wear mechanisms the authors verified that were adhesion, delamination, chipping, cutting edge rounding, and flank wear. Furthermore, it was noted that the main reason for the delamination was the crack propagation. With this, it can be said that the fact that large cracks were not found in the coating in this work was due to its multilayer structure. Moreover, the coatings' adhesion was deemed to be quite good, which also prevented delamination.

Furthermore, as previously seen, the quality of the machined surface was good due to possible residual compressive stresses resulting from the HiPIMS deposition process. Thus, these compressive residual stresses were beneficial for producing a machined surface with good roughness. Thereby, note the importance and advantage of using the PVD HiPIMS technique. To exemplify how the PVD technique generates better results in terms of surface roughness, compared to the CVD technique, there is the work by Gürgen et al. [157], in which the authors compared the behavior of the TiAlN coating deposited using the PVD technique and the TiCN/Al_2O_3/TiN coating deposited by the medium temperature chemical vapor deposition (MT-CVD) in turning operation of Inconel 718. It was verified that the coating deposited by the PVD process obtained a better surface finish in comparison to the coating deposited by MT-CVD method.

Still regarding the comparison between the PVD and CVD methods about surface roughness, there is the work of Ezugwu et al.[158], in which a comparative analysis was made between three coatings used in cutting tools for machining Inconel 718: TiN single layer PVD, TiN/TiCN/TiN multilayer PVD and TiC/Al_2O_3/TiN multilayer CVD. The authors verified that the first coating obtained the best

results in terms of quality of the machined surface, and the last one the worst. Moreover, the work of Yadav et al. [159], similarly showed better performance in terms of roughness of PVD coating than CVD. The authors compared the TiAlN coating deposited by PVD with TiN, TiCN, Al_2O_3 and TiN multilayer coatings deposited by CVD. It was found that the PVD coating in case of flank wear and surface roughness is more efficient, with a better machined surface quality and less flank wear. In turn, Martinho et al. [160], investigated the machining of X2CrNiMoCu25-6-3-3 Duplex Stainless-Steel, using two PALBIT® RDHT-type inserts: PH7930 and PH5740. Both inserts consisted of cemented carbide substrate provided with different coatings, that is, four inserts were PVD-coated with AlTiN, and the other four CVD-coated inserts with TiN/TiCN/Al_2O_3. It was verified that the AlTiN coating showed more failure problems and a more brittle behavior. Thus, the authors note that this coating is more suitable for finishing operations, and the CVD coating for roughing operations, where the surface finish is not so important. Furthermore, the CVD coating showed less wear, but not a better surface finish, and the PVD coating had a better performance in terms of adhesion to the substrate, which, according to the authors, is justified by the fact that the thickness of the PVD coating is smaller.

Therefore, it is clear that the residual stress generated by the deposition method, impact the coating's behavior when cutting [29]. Thus, the choice of the deposition method is crucial for the success of the machining process. Furthermore, it should be noted that PVD coatings are mainly used in finishing operations, as the residual compressive stresses improve the resistance of the coating, which generates sharp edges, and thus produces a better surface finish on the workpiece [161]. On the other hand, CVD coatings are best suited for roughing operations [2].

Thus, the good wear behavior of the TiN/TiAlN coating is verified, with abrasion and material adhesion being the main mechanisms identified, in comparison with other coatings analyzed in recent studies. This is observed mainly regarding resistance to crack propagation related to the multilayer coating and the presence of TiN, and to the PVD deposition method, which generates better quality of the machined surface.

6. CONCLUSION

The elaboration of this thesis resulted in the development of two articles:

- Review article about hybrid manufacturing, which includes the machining process: Hybrid Manufacturing Processes Used in the Production of Complex Parts: A Comprehensive Review [9];
- Article for the FAIM'2023 conference with the analysis of the parameters of this thesis in which 0.07 mm/tooth was used: Wear behavior analysis of TiN/TiAlN coated tools in milling of Inconel 718 [in press].

In addition, the extended article will be prepared for publication, as well.

Then, in this chapter, conclusions regarding the work will be presented, as well as proposals for future work.

6.1. Final conclusions

The tests carried out in this study allowed evaluating the influence on the wear behavior and on the quality of the surface produced in the milling of Inconel 718 using end mills coated with TiN/TiAlN. For this, machining parameters were varied, such as cutting speed, feed per tooth and cutting length. As for the developed cutting forces, these were recorded for the feed values per tooth analyzed in this work, and for the conditions with 100 and 125 m/min of cutting speed. A tendency for the cutting force values to be higher for higher values of feed per tooth was verified. Furthermore, the cutting forces were greater at the end of the test than at the beginning of the test, due to the increase in tool wear during the process. In addition, the parameter that had a greater influence was the feed per tooth in the variation of the cutting forces. Regarding the results of the remaining analyses, these will be presented according to the cutting speed used and for the conditions at 25 meters of cutting length, separately, as was done in the analyzes. Thus, the following conclusions can be drawn for each test group:

- Tests carried out at 75 m/min of cutting speed: regarding the roughness of the machined surface, it was verified that when increasing the cutting length, the surface roughness values also increased. In addition, the measurements in the center of the workpiece were a little smaller than in its periphery, which explains the standard deviation of the measurements, and is directly related to the increase in wear over the course of the test, since it started in the center part and ended on its periphery. Under these conditions, the maximum value of Ra was found for the S75F150L15 condition and the lowest for the S75F75L5 condition, which confirmed the influence of feed per tooth and cutting length on the roughness of the machined surface. That is, by increasing the feed per tooth and the cutting length, the roughness of the machined surface decreased. This is consistent, because generally, for smaller values of feed per tooth, the quality of the machined surface is better than that obtained for larger values of this parameter [125]. As for the wear mechanisms, these were mainly abrasion and adhesion, both related to the tool substrate and to the coating. Condition S75F150L15 showed the beginning of built-up edge

development and condition S75F100L15 observed delamination of the coating, cracking, and chipping.

- Tests carried out at 100 m/min of cutting speed: in this case, regarding the roughness of the machined surface, the lowest value obtained, as in the previous case, was related to 75% of feed per tooth and 5 meters of cutting length, that is, for condition S100F75L5. On the other hand, the highest value found was for the S100F100L15 condition, showing that the cutting length is the parameter with the greatest influence on the process, since Inconel 718 is a difficult-to-machine material that, even at a few meters of cutting length, suffers considerable wear. Regarding flank wear, a tendency was identified for 5 meters of cutting length that the values of VB3 are higher for the tests carried out at 75% of the feed per tooth, decreasing with the increase of this parameter, being the condition S100F150L5 with the lowest value obtained in this test group. However, this was not verified for the tests carried out at 15 meters of cutting length, in which the condition that had the most wear was S100F100L15, and the least S100F150L15, being consistent with the roughness of the machined surface, in which the greater the wear of the tool, the worse is the surface quality obtained on the part. Thus, as for 75 m/min, the main wear mechanisms were abrasion and material adhesion, with the beginning of development of built-up edge for conditions S100F75L15 and S100F150L15, indicating that this develops for longer cutting lengths.
- Tests carried out at 125 m/min of cutting speed: for the conditions within this test group, regarding the surface roughness obtained, the condition with the best quality of the machined surface was S125F75L5, and the worst S125F150L15, and in these cases, at increasing both the cutting length and the feed per tooth resulted in an increase in surface roughness, which shows the clear influence of these parameters on the process. However, for 5 meters of cutting length, the wear decreased as the feed per tooth increased, but the quality of the machined surface also decreased, consequently, showing the higher Ra values. Regarding the wear mechanisms presented by these tools, abrasion and adhesion both in the substrate of the tool and in the coating, were observed in all cases. Under the conditions S125F150L5 and S125F150L15, a built-up edge started to develop, which shows that by increasing the cutting speed to 125 m/min, even at a cutting length of 5 meters, this phenomenon can already be observed.
- Tests carried out at 25 m of cutting length: under these conditions, the roughness of the machined surface, as expected, was higher, resulting in worse surface quality for Inconel 718, and the flank wear had high values. As wear mechanisms, abrasion, material adhesion was identified and for condition S100F150L25 (maximum condition tested) coating delamination was verified.

In general, as for the roughness of the machined surface, the condition that allowed the best result was S75F75L5 (minimum parameters), and when increasing the cutting length, the surface roughness values also increased. In addition, due to the sustained wear of cutting tools, when comparing the cutting speed to the roughness values of the machined surface, the results obtained at 125 m/min tend to be slightly higher than those recorded at 100/min, which in turn are higher than those at 75 m/min. And, the standard deviation registered in the surface roughness measurements is related to the differences in the measurements at the center and at the periphery of the part (end of the tool path), which is indicative of greater sustained tool wear.

As for wear, less flank wear was recorded for test conditions S100F150L5, with a decrease in the value of fz resulting in a greater amount of recorded tool wear, and an increase in cutting speed has promoted an increase in tool wear. So, the parameter with the greatest influence on flank wear was the cutting length, due to the Inconel 718 properties, causing high amounts of abrasive wear. Furthermore, only one condition showed cracking, as the resistance to crack propagation was achieved due to the TiN layer, which enhances the coatings' crack resistance and its adhesion. With this, it was verified that the coating performed well in the process but is not suitable for use in operations with high cutting lengths, due to the considerable amount of wear suffered only after a few meters. Furthermore, regarding tool lifespan, it was verified that the higher the cutting speed, the greater the flank wear, and the shorter the tool life. The S75F150 condition had the longest duration, reaching 23.57 meters of cutting length, and the S125F150 condition had the shortest duration with only 9.82 meters of cutting length. Thus, the cutting speed showed to have greater influence than the feed per tooth.

Thus, the results obtained showed the advantages of using TiAlN-based coatings to obtain a satisfactory machined surface quality in finishing operations applied to Inconel 718. As well as the relevance of using multilayer coatings, which in this case resulted greater resistance to crack propagation, was confirmed. So, this shows the importance of using the TiN/TiAlN coating, with regard its advantages in the wear behavior of cutting tools when machining Inconel 718, that is, a material that is difficult to machine, which induces high levels of wear in the cutting tools.

6.2. Future work proposals

Throughout the project and after analyzing the results, viable ideas for future work emerged, to expand the results acquired so far, they are:

- Analyze the wear behavior of this same coating in cutting tools of different geometries;
- Analyze the influence of the lubrication regime on the wear behavior, in order to carry out a comparative analysis of dry and lubricated performance;
- Compare the performance of this coating with other multilayer and monolayer coatings;
- Analyze the influence of other machining parameters, as well as compare the behavior of uncoated milling cutting tools;
- Perform Taguchi analysis with regard to optimization of machining parameters.

REFERENCES

[1] R. Batista, "Tendências do Corte por Arranque de Apara - Maquinagem," Dissertação de Mestrado, Faculdade de Engenharia da Universidade do Porto, Porto, 2010.

[2] V. F. C. Sousa and F. J. G. Silva, "Recent Advances in Turning Processes Using Coated Tools—A Comprehensive Review," *Metals*, vol. 10, no. 2, p. 170, Jan. 2020, doi: 10.3390/met10020170.

[3] V. F. C. Sousa, F. J. G. Da Silva, G. F. Pinto, A. Baptista, and R. Alexandre, "Characteristics and Wear Mechanisms of TiAlN-Based Coatings for Machining Applications: A Comprehensive Review," *Metals*, vol. 11, no. 2, p. 260, Feb. 2021, doi: 10.3390/met11020260.

[4] W. Mersni, M. Boujelbene, S. Ben Salem, and H. P. Singh, "Machining time and quadratic mean roughness optimization in ball end milling of titanium alloy Ti-6Al-4V – Aeronautic field," *Mater. Today Proc.*, vol. 26, pp. 2619–2624, 2020, doi: 10.1016/j.matpr.2020.02.553.

[5] H. B. Kulkarni, M. M. Nadakatti, S. C. Kulkarni, and R. M. Kulkarni, "Investigations on effect of nanofluid based minimum quantity lubrication technique for surface milling of Al7075-T6 aerospace alloy," *Mater. Today Proc.*, vol. 27, pp. 251–256, 2020, doi: 10.1016/j.matpr.2019.10.127.

[6] V. F. C. Sousa, F. J. G. Da Silva, J. S. Fecheira, H. M. Lopes, R. P Martinho, R. B. Casais, L. P. Ferreira., "Cutting Forces Assessment in CNC Machining Processes: A Critical Review," *Sensors*, vol. 20, no. 16, p. 4536, Aug. 2020, doi: 10.3390/s20164536.

[7] Y. Zhu, Z.-T. Chen, T. Ning, and R.-F. Xu, "Tool orientation optimization for 3 + 2 -axis CNC machining of sculptured surface," *Comput.-Aided Des.*, vol. 77, pp. 60–72, Aug. 2016, doi: 10.1016/j.cad.2016.02.007.

[8] A. Hay, "Ultimate Guide to CNC Machining," Sep. 06, 2021. https://jiga.io/resource-center/cnc-machining/what-is-cnc-machining-guide/ (accessed Oct. 29, 2022).

[9] N. P. V. Sebbe, F. Fernandes, V. F. C. Sousa, and F. J. G. Silva, "Hybrid Manufacturing Processes Used in the Production of Complex Parts: A Comprehensive Review," *Metals*, vol. 12, no. 11, p. 1874, Nov. 2022, doi: 10.3390/met12111874.

[10] S. Lakshmanan and M. A. Xavior, "Performance of Coated and Uncoated Inserts during Intermittent Cut Milling of AISI 1030 Steel," *Procedia Eng.*, vol. 97, pp. 372–380, 2014, doi: 10.1016/j.proeng.2014.12.261.

[11] W. Baohai, Y. Xue, L. Ming, and G. Ge, "Cutting force prediction for circular end milling process," p. 7.

[12] "Groover, M.P. (2019) 'Fundamentals of modern manufacturing: materials, processes, and systems, 7th Edition'. John Wiley & Sons, Nova Jersey - EUA. ISBN: 978-1-119-47521-7."

[13] "S. Coromant (2010) 'Manual técnico de usinagem, torneamento, fresamento, furação, mandrilamento e sistemas de fixação'. Sandvik Coromant, São Paulo – Brasil."

[14] P. Gray, S. Bedi, F. Ismail, N. Rao, and G. Morphy, "Comparison of 5-Axis and 3-Axis Finish Machining of Hydroforming Die Inserts," *Int. J. Adv. Manuf. Technol.*, vol. 17, no. 8, pp. 562–569, Apr. 2001, doi: 10.1007/s001700170139.

[15] F. J. G. Silva, R. D. S. G. Campilho, V. F. C. Sousa, L. F. P. Coelho, L. P. Ferreira, and J. Matos, "A New Concept of Jig Rotary Holder System for 3-Axis CNC Milling Machine Operated by the Main Machine Control," *J Test Eval*, vol. 50(5), pp. 2295–2309, 2022, doi: 10.1520/JTE20210723.

[16] A. F. de Souza, L. G. Camargo, H. da S. Gaspar, F. Marin, A. Calleja Ochoa, and L. N. López de Lacalle, "New mechanistic model to predict machining time for milling free form geometries using 4-axis milling," *Procedia CIRP*, vol. 101, pp. 34–37, 2021, doi: 10.1016/j.procir.2020.09.187.

[17] O. Bologa, R. E. Breaz, S. G. Racz, and M. Crenganiş, "Decision-making Tool for Moving from 3-axes to 5-axes CNC Machine-tool," *Procedia Comput. Sci.*, vol. 91, pp. 184–192, 2016, doi: 10.1016/j.procs.2016.07.056.

[18] C. A. My and E. L. J. Bohez, “A novel differential kinematics model to compare the kinematic performances of 5-axis CNC machines,” *Int. J. Mech. Sci.*, vol. 163, p. 105117, Nov. 2019, doi: 10.1016/j.ijmecsci.2019.105117.

[19] J. Zajac, J. Duplak, D. Duplakova, P. Cizmar, I. Olexa, and A. Bittner, “Prediction of Cutting Material Durability by T = f(vc) Dependence for Turning Processes,” *Processes*, vol. 8, no. 7, p. 789, Jul. 2020, doi: 10.3390/pr8070789.

[20] R. E. Breaz, S. G. Racz, and O. C. Bologa, “5-axes modular CNC machining center,” *MATEC Web Conf.*, vol. 112, p. 06004, 2017, doi: 10.1051/matecconf/201711206004.

[21] A. Lasemi, D. Xue, and P. Gu, “Recent development in CNC machining of freeform surfaces: A state-of-the-art review,” *Comput.-Aided Des.*, vol. 42, no. 7, pp. 641–654, Jul. 2010, doi: 10.1016/j.cad.2010.04.002.

[22] Q. Chen, W. Li, C. Jiang, Z. Zhou, and S. Min, “Separation and compensation of geometric errors of rotary axis in 5-axis ultra-precision machine tool by empirical mode decomposition method,” *J. Manuf. Process.*, vol. 68, pp. 1509–1523, Aug. 2021, doi: 10.1016/j.jmapro.2021.06.057.

[23] M. Wiessner, P. Blaser, S. Böhl, J. Mayr, W. Knapp, and K. Wegener, “Thermal test piece for 5-axis machine tools,” *Precis. Eng.*, vol. 52, pp. 407–417, Apr. 2018, doi: 10.1016/j.precisioneng.2018.01.017.

[24] A. Mudcharoen and S. S. Makhanov, “Optimization of rotations for six-axis machining,” *Int. J. Adv. Manuf. Technol.*, vol. 53, no. 5–8, pp. 435–451, Mar. 2011, doi: 10.1007/s00170-010-2864-3.

[25] J. Mahmood, G. Mustafa, and M. Ali, “Accurate estimation of tool wear levels during milling, drilling and turning operations by designing novel hyperparameter tuned models based on LightGBM and stacking,” *Measurement*, vol. 190, p. 110722, Feb. 2022, doi: 10.1016/j.measurement.2022.110722.

[26] W. Ji, B. Zou, S. Zhang, H. Xing, H. Yun, and Y. Wang, “Design and fabrication of gradient cermet composite cutting tool, and its cutting performance,” *J. Alloys Compd.*, p. 7, 2018.

[27] M. S. I. Chowdhury, B. Bose, K. Yamamoto, L. S. Shuster, J. Paiva, G. S. Fox-Rabinovich, S. C. Veldhuis, “Wear performance investigation of PVD coated and uncoated carbide tools during high-speed machining of TiAl6V4 aerospace alloy,” *Wear*, vol. 446–447, p. 203168, Apr. 2020, doi: 10.1016/j.wear.2019.203168.

[28] P. Eh. Hovsepian, Q. Luo, G. Robinson, M. Pittman, M. Howarth, D. Doerwald, R. Tietema, W. M. Sim, A. Deeming, T. Zeus, “TiAlN/VN superlattice structured PVD coatings: A new alternative in machining of aluminium alloys for aerospace and automotive components,” *Surf. Coat. Technol.*, vol. 201, no. 1–2, pp. 265–272, Sep. 2006, doi: 10.1016/j.surfcoat.2005.11.106.

[29] V. F. C. Sousa and F. J. G. Silva, “Recent Advances on Coated Milling Tool Technology—A Comprehensive Review,” *Coatings*, vol. 10, no. 3, p. 235, Mar. 2020, doi: 10.3390/coatings10030235.

[30] A. F. D. Costa, “Análise Comparativa de Ferramentas Revestidas por PVD e CVD no Torneamento do Aço ABNT 8620,” Dissertação de Mestrado, Universidade Estadual Paulista “Júlio de Mesquita Filho,” Guaratinguetá, 2016.

[31] A. Baptista, F. J. G. Silva, J. Porteiro, J. L. Míguez, G. Pinto, and L. Fernandes, “On the Physical Vapour Deposition (PVD): Evolution of Magnetron Sputtering Processes for Industrial Applications,” *Procedia Manuf.*, vol. 17, pp. 746–757, 2018, doi: 10.1016/j.promfg.2018.10.125.

[32] D. M. Mattox, *Handbook of physical vapor deposition (PVD) processing*, 2nd ed. Oxford, UK: William Andrew, 2010.

[33] D. Depla, S. Mahieu, and J. E. Greene, “Handbook of Deposition Technologies for Films and Coatings (Third Edition) - Sputter Deposition Processes,” *Science, Applications and Technology*, pp. 253–296, 2010, doi: 10.1016/B978-0-8155-2031-3.00005-3.

[34] “Mattox, D.M. (2003). Deposition Processes. In: The Foundations of Vacuum Coating Technology. Springer, Berlin, Heidelberg. doi: 10.1007/978-3-662-10329-6_7.”

[35] Mohd. Z. B. Abdullah, M. A. Ahmad, A. N. Abdullah, M. H. Othman, P. Hussain, and A. Zainuddin, “Metal Release of Multilayer Coatings by Physical Vapour Deposition (PVD),” *Procedia Eng.*, vol. 148, pp. 254–260, 2016, doi: 10.1016/j.proeng.2016.06.612.

[36] A. Baptista, F. Silva, J. Porteiro, J. Míguez, and G. Pinto, “Sputtering Physical Vapour Deposition (PVD) Coatings: A Critical Review on Process Improvement and Market Trend Demands,” *Coatings*, vol. 8, no. 11, p. 402, Nov. 2018, doi: 10.3390/coatings8110402.

[37] V. F. C. Sousa, F. J. G. Silva, H. Lopes, R. C. B. Casais, A. Baptista, G. Pinto, R. Alexandre, “Wear Behavior and Machining Performance of TiAlSiN-Coated Tools Obtained by dc MS and HiPIMS: A Comparative Study,” *Materials*, vol. 14, no. 18, p. 5122, Sep. 2021, doi: 10.3390/ma14185122.

[38] Z. Wang, B. Zhang, K. Gao, and R. Liu, “Adjustable TiN coatings deposited with HiPIMS on titanium bipolar plates for PEMFC,” *Int. J. Hydrog. Energy*, p. S0360319922041817, Sep. 2022, doi: 10.1016/j.ijhydene.2022.09.066.

[39] C. Promjantuk, T. Lertvanithphol, N. Limsuwan, S. Limwichean, N. Wongdamnern, T. Sareein, W. Phae-ngam, H. Nakajima, P. Poolcharuansin, M. Horprathum, A. Klamchuen, “Spectroscopic study on alternative plasmonic TiN-NRs film prepared by R-HiPIMS with GLAD technique,” *Radiat. Phys. Chem.*, vol. 202, p. 110589, Jan. 2023, doi: 10.1016/j.radphyschem.2022.110589.

[40] S. Azim, S. Gangopadhyay, S. S. Mahapatra, and R. K. Mittal, “Performance evaluation of CrAlN and TiAlN coatings deposited by HiPIMS in micro drilling of a Ni-based superalloy,” *Surf. Coat. Technol.*, vol. 449, p. 128980, Nov. 2022, doi: 10.1016/j.surfcoat.2022.128980.

[41] B. Zhao, X. Zhao, L. Lin, and L. Zou, “Effect of bias voltage on mechanical properties, milling performance and thermal crack propagation of cathodic arc ion-plated TiAlN coatings,” *Thin Solid Films*, vol. 708, p. 138116, Aug. 2020, doi: 10.1016/j.tsf.2020.138116.

[42] W. Tillmann, D. Grisales, D. Stangier, C. A. Thomann, J. Debus, A. Nienhaus, D. Apel, “Residual stresses and tribomechanical behaviour of TiAlN and TiAlCN monolayer and multilayer coatings by DCMS and HiPIMS,” *Surf. Coat. Technol.*, vol. 406, p. 126664, Jan. 2021, doi: 10.1016/j.surfcoat.2020.126664.

[43] L. Zauner, Ph. Ertelthaler, T. Wojcik, H. Bolvardi, S. Kolozsvári, P.H. Mayrhofer, H. Riedl, “Reactive HiPIMS deposition of Ti-Al-N: Influence of the deposition parameters on the cubic to hexagonal phase transition,” *Surf. Coat. Technol.*, vol. 382, p. 125007, Jan. 2020, doi: 10.1016/j.surfcoat.2019.125007.

[44] J. Alami, S. Bolz, and K. Sarakinos, “High power pulsed magnetron sputtering: Fundamentals and applications,” *J. Alloys Compd.*, vol. 483, no. 1–2, pp. 530–534, Aug. 2009, doi: 10.1016/j.jallcom.2008.08.104.

[45] C. L. Chang and F. C. Yang, “Effect of target composition on the microstructural, mechanical, and corrosion properties of TiAlN thin films deposited by high-power impulse magnetron sputtering,” *Surf. Coat. Technol.*, vol. 352, pp. 330–337, Oct. 2018, doi: 10.1016/j.surfcoat.2018.08.023.

[46] E. Contreras Romero, A. Hurtado Macías, J. Méndez Nonell, O. Solís Canto, and M. Gómez Botero, “Mechanical and tribological properties of nanostructured TiAlN/TaN coatings deposited by DC magnetron sputtering,” *Surf. Coat. Technol.*, vol. 378, p. 124941, Nov. 2019, doi: 10.1016/j.surfcoat.2019.124941.

[47] L. Liu, L. Zhou, W. Tang, Q. Ruan, X. Li, Z. Wu, A. M. Qasin, S. Cui, T. Li, X. Tian, R. K. Y. Fu, Z. Wu, P. K. Chu, “Study of TiAlN coatings deposited by continuous high power magnetron sputtering (C-HPMS),” *Surf. Coat. Technol.*, vol. 402, p. 126315, Nov. 2020, doi: 10.1016/j.surfcoat.2020.126315.

[48] J. O. Carlsson and P. M. Martin, “Handbook of Deposition Technologies for Films and Coatings - Chemical Vapor Deposition,” *Science, Applications and Technology*, no. Third Edition, pp. 314–363, 2010, doi: 10.1016/B978-0-8155-2031-3.00007-7.

[49] J. E. Crowell, “Chemical methods of thin film deposition: Chemical vapor deposition, atomic layer deposition, and related technologies,” *J. Vac. Sci. Technol. Vac. Surf. Films*, vol. 21, no. 5, pp. S88–S95, Sep. 2003, doi: 10.1116/1.1600451.

[50] K. H. J. Buschow, Ed., *Encyclopedia of materials: science and technology*. Amsterdam; New York: Elsevier, 2001.

[51] F. J. G. Silva, A. J. S. Fernandes, F. M. Costa, V. Teixeira, A. P. M. Baptista, and E. Pereira, “Tribological behaviour of CVD diamond films on steel substrates,” *Wear*, vol. 255, no. 7–12, pp. 846–853, Aug. 2003, doi: 10.1016/S0043-1648(03)00145-5.

[52] F. J. G. Silva, R. P. Martinho, R. J. D. Alexandre, and A. P. M. Baptista, “Wear Resistance of TiAlSiN Thin Coatings,” *J. Nanosci. Nanotechnol.*, vol. 12, no. 12, pp. 9094–9101, Dec. 2012, doi: 10.1166/jnn.2012.6760.

[53] J. P. Davim and F. Mata, “Chemical vapour deposition (CVD) diamond coated tools performance in machining of PEEK composites,” *Mater. Des.*, vol. 29, no. 8, pp. 1568–1574, Jan. 2008, doi: 10.1016/j.matdes.2007.11.002.

[54] N. Schalk, J. Keckes, C. Czettl, M. Burghammer, M. Penoy, C. Michotte, C. Mitterer, “Investigation of the origin of compressive residual stress in CVD TiB 2 hard coatings using synchrotron X-ray nanodiffraction,” *Surf. Coat. Technol.*, vol. 258, pp. 121–126, Nov. 2014, doi: 10.1016/j.surfcoat.2014.09.050.

[55] C. Kainz, N. Schalk, M. Tkadletz, C. Mitterer, and C. Czettl, “The effect of B and C addition on microstructure and mechanical properties of TiN hard coatings grown by chemical vapor deposition,” *Thin Solid Films*, vol. 688, p. 137283, Oct. 2019, doi: 10.1016/j.tsf.2019.05.002.

[56] X. Shen, X. Wang, and F. Sun, “Fabrication and evaluation of monolayer diamond grinding tools by hot filament chemical vapor deposition method,” *J. Mater. Process. Technol.*, vol. 265, pp. 1–11, Mar. 2019, doi: 10.1016/j.jmatprotec.2018.10.001.

[57] A. M. Jetpurwala and M. Dikshit, “Chemical vapor deposition diamond dental burs for high speed air turbine handpieces,” *Surf. Coat. Technol.*, vol. 418, p. 127244, Jul. 2021, doi: 10.1016/j.surfcoat.2021.127244.

[58] F. Silva, R. Martinho, C. Martins, H. Lopes, and R. Gouveia, “Machining GX2CrNiMoN26-7-4 DSS Alloy: Wear Analysis of TiAlN and TiCN/Al_2O_3/TiN Coated Carbide Tools Behavior in Rough End Milling Operations,” *Coatings*, vol. 9, no. 6, p. 392, Jun. 2019, doi: 10.3390/coatings9060392.

[59] H. Caliskan, P. Panjan, and C. Kurbanoglu, “3.16 Hard Coatings on Cutting Tools and Surface Finish,” in *Comprehensive Materials Finishing*, Elsevier, 2017, pp. 230–242. doi: 10.1016/B978-0-12-803581-8.09178-5.

[60] K. Bobzin, “High-performance coatings for cutting tools,” *CIRP J. Manuf. Sci. Technol.*, vol. 18, pp. 1–9, Aug. 2017, doi: 10.1016/j.cirpj.2016.11.004.

[61] C. Kainz, N. Schalk, M. Tkadletz, C. Mitterer, and C. Czettl, “Microstructure and mechanical properties of CVD TiN/TiBN multilayer coatings,” *Surf. Coat. Technol.*, vol. 370, pp. 311–319, Jul. 2019, doi: 10.1016/j.surfcoat.2019.04.086.

[62] S. PalDey and S. C. Deevi, “Single layer and multilayer wear resistant coatings of (Ti,Al)N: a review,” *Mater. Sci. Eng. A*, vol. 342, no. 1–2, pp. 58–79, Feb. 2003, doi: 10.1016/S0921-5093(02)00259-9.

[63] Z. Lei, X. Zhu, Y. Li, Z. Song, H. Liu, and Y. Q. Fu, “Characterization and Tribological Behavior of TiAlN/TiAlCN Multilayer Coatings,” *J. Tribol.*, vol. 140, no. 5, p. 051301, Sep. 2018, doi: 10.1115/1.4039723.

[64] A. A. Vereschaka, S. N. Grigoriev, A. S. Vereschaka, A. Yu. Popov, and A. D. Batako, “Nano-scale Multilayered Composite Coatings for Cutting Tools Operating under Heavy Cutting Conditions,” *Procedia CIRP*, vol. 14, pp. 239–244, 2014, doi: 10.1016/j.procir.2014.03.070.

[65] İ. Ucun, K. Aslantas, and F. Bedir, “The performance of DLC-coated and uncoated ultra-fine carbide tools in micromilling of Inconel 718,” *Precis. Eng.*, vol. 41, pp. 135–144, Jul. 2015, doi: 10.1016/j.precisioneng.2015.01.002.

[66] Y. M. Durmaz and F. Yildiz, “The wear performance of carbide tools coated with TiAlSiN, AlCrN and TiAlN ceramic films in intelligent machining process,” *Ceram. Int.*, vol. 45, no. 3, pp. 3839–3848, Feb. 2019, doi: 10.1016/j.ceramint.2018.11.055.

[67] M. Bohley, S. Kieren-Ehses, L. Heberger, B. Kirsch, and J. C. Aurich, “Size limitations and wear behavior of TiB 2 coated micro end mills (Ø < 50 µm) when machining cp-titanium,” *Procedia CIRP*, vol. 71, pp. 187–191, 2018, doi: 10.1016/j.procir.2018.05.095.

[68] A. Bjerke, F. Lenrick, S. Norgren, H. Larsson, A. Markström, R. M’Saoubi, I. Petrusha, V. Bushlya, “Understanding wear and interaction between CVD α-Al_2O_3 coated tools, steel, and non-metallic inclusions in machining,” *Surf. Coat. Technol.*, vol. 450, p. 128997, Nov. 2022, doi: 10.1016/j.surfcoat.2022.128997.

[69] K. Gobivel and K. S. Vijay Sekar, “Investigation on the effect of TiN and Al_2O_3 coated tools in the Machining of Ti-6Al-4 V alloy,” *Mater. Today Proc.*, vol. 62, pp. 920–924, 2022, doi: 10.1016/j.matpr.2022.04.071.

[70] S. Grigoriev, A. Vereschaka, V. Uglov, F. Milovich, N. Cherenda, N. Andreev, M. Migranov, A. Seleznev, “Influence of tribological properties of Zr-ZrN-(Zr,Cr,Al)N and Zr-ZrN-(Zr,Mo,Al)N multilayer nanostructured coatings on the cutting properties of coated tools during dry turning of Inconel 718 alloy,” *Wear*, vol. 512–513, p. 204521, Jan. 2023, doi: 10.1016/j.wear.2022.204521.

[71] S. H. Kim, H. Park, K. H. Lee, S. H. Jee, D. J. Kim, Y. S. Yoon, H. B. Chae, “Structure and mechanical properties of titanium nitride thin films grown by reactive pulsed laser deposition,” p. 5.

[72] A. Mitsuo, S. Uchida, N. Nihira, and M. Iwaki, “Improvement of high-temperature oxidation resistance of titanium nitride and titanium carbide films by aluminum ion implantation,” *Surf. Coat. Technol.*, vol. 103–104, pp. 98–103, May 1998, doi: 10.1016/S0257-8972(98)00380-6.

[73] R. Aninat, N. Valle, J-B. Chemin, D. Duday, C. Michotte, M. Penoy, L. Bourgeois, P. Choquet, “Addition of Ta and Y in a hard Ti-Al-N PVD coating: Individual and conjugated effect on the oxidation and wear properties,” *Corros. Sci.*, vol. 156, pp. 171–180, Aug. 2019, doi: 10.1016/j.corsci.2019.04.042.

[74] K. Yang, G. Xian, H. Zhao, H. Fan, J. Wang, H. Wang, H. Du, “Effect of Mo content on the structure and mechanical properties of TiAlMoN films deposited on WC–Co cemented carbide substrate by magnetron sputtering,” *Int. J. Refract. Met. Hard Mater.*, vol. 52, pp. 29–35, Sep. 2015, doi: 10.1016/j.ijrmhm.2015.04.016.

[75] J. Yi, S. Chen, K. Chen, Y. Xu, Q. Chen, C. Zhu, Li Liu, “Effects of Ni content on microstructure, mechanical properties and Inconel 718 cutting performance of AlTiN-Ni nanocomposite coatings,” *Ceram. Int.*, vol. 45, no. 1, pp. 474–480, Jan. 2019, doi: 10.1016/j.ceramint.2018.09.192.

[76] Z. R. Liu, L. Chen, Y. Du, and S. Zhang, “Influence of Ru-addition on thermal decomposition and oxidation resistance of TiAlN coatings,” *Surf. Coat. Technol.*, vol. 401, p. 126234, Nov. 2020, doi: 10.1016/j.surfcoat.2020.126234.

[77] V. Nunes, F. J. G. Silva, M. F. Andrade, R. Alexandre, and A. P. M. Baptista, “Increasing the lifespan of high-pressure die cast molds subjected to severe wear,” *Surf. Coat. Technol.*, vol. 332, pp. 319–331, Dec. 2017, doi: 10.1016/j.surfcoat.2017.05.098.

[78] G. Li, J. Sun, Y. Xu, Y. Xu, J. Gu, L. Wang, K. Huang, K. Liu, L. Li, “Microstructure, mechanical properties, and cutting performance of TiAlSiN multilayer coatings prepared by HiPIMS,” *Surf. Coat. Technol.*, vol. 353, pp. 274–281, Nov. 2018, doi: 10.1016/j.surfcoat.2018.06.017.

[79] O. Çomaklı, “Improved structural, mechanical, corrosion and tribocorrosion properties of Ti45Nb alloys by TiN, TiAlN monolayers, and TiAlN/TiN multilayer ceramic films,” *Ceram. Int.*, vol. 47, no. 3, pp. 4149–4156, Feb. 2021, doi: 10.1016/j.ceramint.2020.09.292.

[80] G. Li, L. Zhang, F. Cai, Y. Yang, Q. Wang, and S. Zhang, “Characterization and corrosion behaviors of TiN/TiAlN multilayer coatings by ion source enhanced hybrid arc ion plating,” *Surf. Coat. Technol.*, vol. 366, pp. 355–365, May 2019, doi: 10.1016/j.surfcoat.2019.03.027.

[81] V. Varghese, D. Chakradhar, and M. R. Ramesh, “Micro-mechanical characterization and wear performance of TiAlN/NbN PVD coated carbide inserts during End milling of AISI 304 Austenitic Stainless Steel,” *Mater. Today Proc.*, vol. 5, no. 5, pp. 12855–12862, 2018, doi: 10.1016/j.matpr.2018.02.270.

[82] G. Zheng, G. Zhao, X. Cheng, R. Xu, J. Zhao, and H. Zhang, “Frictional and wear performance of TiAlN/TiN coated tool against high-strength steel,” *Ceram. Int.*, vol. 44, no. 6, pp. 6878–6885, Apr. 2018, doi: 10.1016/j.ceramint.2018.01.113.

[83] J. Wang, M. A. P. Yazdi, F. Lomello, A. Billard, A. Kovács, F. Schuster, C. Guet, T. J. White, F. Sanchette, Z. Dong, “Influence of microstructures on mechanical properties and tribology behaviors of TiN/TiXAl1−XN multilayer coatings,” *Surf. Coat. Technol.*, vol. 320, pp. 441–446, Jun. 2017, doi: 10.1016/j.surfcoat.2016.11.101.

[84] A. V. Pshyk, Y. Kravchenko, E. Coy, M. Kempiński, I. Iatsunskyi, K. Załęski, A. D. Pogrebnjak, S. Jurga, “Microstructure, phase composition and mechanical properties of novel nanocomposite (TiAlSiY)N and nano-scale (TiAlSiY)N/MoN multifunctional heterostructures,” *Surf. Coat. Technol.*, vol. 350, pp. 376–390, Sep. 2018, doi: 10.1016/j.surfcoat.2018.07.010.

[85] D. Geng, R. Zeng, Z. Wu, and Q. Wang, “An investigation on microstructure and milling performance of arc-evaporated TiSin/AlTiN film,” *Thin Solid Films*, vol. 709, p. 138243, Sep. 2020, doi: 10.1016/j.tsf.2020.138243.

[86] LAUS Laboratório de Automação em Usinagem. https://www.ufrgs.br/laus/ (accessed Oct. 31, 2022).

[87] C. Bandapalli, B. M. Sutaria, D. V. Prasad Bhatt, and K. K. Singh, “Tool Wear Analysis of Micro End Mills - Uncoated and PVD Coated TiAlN & AlTiN in High Speed Micro Milling of Titanium Alloy - Ti-0.3Mo-0.8Ni,” *Procedia CIRP*, vol. 77, pp. 626–629, 2018, doi: 10.1016/j.procir.2018.08.191.

[88] R. P. Martinho, F. J. G. Silva, and A. P. M. Baptista, “Wear behaviour of uncoated and diamond coated Si3N4 tools under severe turning conditions,” *Wear*, vol. 263, no. 7–12, pp. 1417–1422, Sep. 2007, doi: 10.1016/j.wear.2007.01.048.

[89] W. Liu, Q. Chu, J. Zeng, R. He, H. Wu, Z. Wu, S. Wu, “PVD-CrAlN and TiAlN coated Si_3N_4 ceramic cutting inserts-2. High speed face milling performance and wear mechanism study,” *Ceram. Int.*, vol. 43, no. 12, pp. 9488–9492, Aug. 2017, doi: 10.1016/j.ceramint.2017.04.127.

[90] J. Zuo, Y. Lin, J. Zheng, P. Zhong, and M. He, “An investigation of thermal-mechanical interaction effect on PVD coated tool wear for milling Be/Cu alloy,” *Vacuum*, vol. 167, pp. 271–279, Sep. 2019, doi: 10.1016/j.vacuum.2019.06.017.

[91] V. F. C. Sousa, J. Castanheira, F. J. G. Silva, J. S. Fecheira, G. Pinto, and A. Baptista, “Wear Behavior of Uncoated and Coated Tools in Milling Operations of AMPCO (Cu-Be) Alloy,” *Appl. Sci.*, vol. 11, no. 16, p. 7762, Aug. 2021, doi: 10.3390/app11167762.

[92] C. Ni, L. Zhu, and Z. Yang, “Comparative investigation of tool wear mechanism and corresponding machined surface characterization in feed-direction ultrasonic vibration assisted milling of Ti–6Al–4V from dynamic view,” *Wear*, vol. 436–437, p. 203006, Oct. 2019, doi: 10.1016/j.wear.2019.203006.

[93] M. Kumar, S. N. Melkote, and R. M’Saoubi, “Wear behavior of coated tools in laser assisted micro-milling of hardened steel,” *Wear*, vol. 296, no. 1–2, pp. 510–518, Aug. 2012, doi: 10.1016/j.wear.2012.08.011.

[94] H. Çalışkan, C. Kurbanoğlu, P. Panjan, M. Čekada, and D. Kramar, “Wear behavior and cutting performance of nanostructured hard coatings on cemented carbide cutting tools in hard milling,” *Tribol. Int.*, vol. 62, pp. 215–222, Jun. 2013, doi: 10.1016/j.triboint.2013.02.035.

[95] Y.-Y. Chang and H.-M. Lai, “Wear behavior and cutting performance of CrAlSiN and TiAlSiN hard coatings on cemented carbide cutting tools for Ti alloys,” *Surf. Coat. Technol.*, vol. 259, pp. 152–158, Nov. 2014, doi: 10.1016/j.surfcoat.2014.02.015.

[96] B. Kursuncu, H. Caliskan, S. Y. Guven, and P. Panjan, “Wear Behavior of Multilayer Nanocomposite TiAlSiN/TiSiN/TiAlN Coated Carbide Cutting Tool during Face Milling of

Inconel 718 Superalloy," *J. Nano Res.*, vol. 47, pp. 11–16, May 2017, doi: 10.4028/www.scientific.net/JNanoR.47.11.

[97] A. Dadgari, D. Huo, and D. Swailes, "Investigation on tool wear and tool life prediction in micro-milling of Ti-6Al-4V," *Nanotechnol. Precis. Eng.*, vol. 1, no. 4, pp. 218–225, Dec. 2018, doi: 10.1016/j.npe.2018.12.005.

[98] T. Mohanraj, S. Shankar, R. Rajasekar, N. R. Sakthivel, and A. Pramanik, "Tool condition monitoring techniques in milling process — a review," *J. Mater. Res. Technol.*, vol. 9, no. 1, pp. 1032–1042, Jan. 2020, doi: 10.1016/j.jmrt.2019.10.031.

[99] A. Vereschaka, V. Gurin, M. Oganyan, G. Oganyan, J. Bublikov, and A. Shein, "Increase in tool life for end milling titanium alloys using tools with multilayer composite nanostructured modified coatings," *Procedia CIRP*, vol. 81, pp. 1412–1416, 2019, doi: 10.1016/j.procir.2019.04.173.

[100] C. Wang, X. Wang, and F. Sun, "Tribological behavior and cutting performance of monolayer, bilayer and multilayer diamond coated milling tools in machining of zirconia ceramics," *Surf. Coat. Technol.*, vol. 353, pp. 49–57, Nov. 2018, doi: 10.1016/j.surfcoat.2018.08.074.

[101] M. Sortino, S. Belfio, G. Totis, E. Kuljanic, and G. Fadelli, "Innovative Tool Coatings for Increasing Tool Life in Milling Nickel-coated Nickel-silver Alloy," *Procedia Eng.*, vol. 100, pp. 946–952, 2015, doi: 10.1016/j.proeng.2015.01.453.

[102] A. Vereschaka, S. Grigoriev, N. Sitnikov, G. Oganyan, and C. Sotova, "Influence of thickness of multilayer composite nano-structured coating Ti-TiN-(Ti,Al,Cr)N on tool life of metal-cutting tool," *Procedia CIRP*, vol. 77, pp. 545–548, 2018, doi: 10.1016/j.procir.2018.08.237.

[103] M. Oganyan, A. Vereschaka, M. Volosova, and V. Gurin, "Influence of the application of wear-resistant coatings on force parameters of the cutting process and the tool life during end milling of titanium alloys," *Mater. Today Proc.*, vol. 38, pp. 1428–1432, 2021, doi: 10.1016/j.matpr.2020.08.119.

[104] J. C. Aurich, S. Kieren-Ehses, T. Mayer, M. Bohley, and B. Kirsch, "An investigation of the influence of the coating on the tool lifetime and surface quality for ultra-small micro end mills with different diameters," *CIRP J. Manuf. Sci. Technol.*, vol. 37, pp. 92–102, May 2022, doi: 10.1016/j.cirpj.2022.01.004.

[105] L. Zhang, Z. Zhong, L. Qiu, H. Shi, A. Layyous, and S. Liu, "Coated cemented carbide tool life extension accompanied by comb cracks: The milling case of 316L stainless steel," *Wear*, vol. 418–419, pp. 133–139, Jan. 2019, doi: 10.1016/j.wear.2018.11.019.

[106] B. D. Beake, L. Ning, Ch. Gey, S. C. Veldhuis, A. B. Kornberg, M. Khanna, G.S. Fox-Rabinovichc, "Wear performance of different PVD coatings during hard wet end milling of H13 tool steel," *Surf. Coat. Technol.*, vol. 279, pp. 118–125, Oct. 2015, doi: 10.1016/j.surfcoat.2015.08.038.

[107] A. Thakur and S. Gangopadhyay, "Dry machining of nickel-based super alloy as a sustainable alternative using TiN/TiAlN coated tool," *J. Clean. Prod.*, vol. 129, pp. 256–268, Aug. 2016, doi: 10.1016/j.jclepro.2016.04.074.

[108] K. M. Buddaraju, G. Ravi Kiran Sastry, and S. Kosaraju, "A review on turning of Inconel alloys," *Mater. Today Proc.*, vol. 44, pp. 2645–2652, 2021, doi: 10.1016/j.matpr.2020.12.673.

[109] A. Thakur and S. Gangopadhyay, "State-of-the-art in surface integrity in machining of nickel-based super alloys," *Int. J. Mach. Tools Manuf.*, vol. 100, pp. 25–54, Jan. 2016, doi: 10.1016/j.ijmachtools.2015.10.001.

[110] U. M. R. Paturi, V. D. B., and N. S. Reddy, "Progress of machinability on the machining of Inconel 718: A comprehensive review on the perception of cleaner machining," *Clean. Eng. Technol.*, vol. 5, p. 100323, Dec. 2021, doi: 10.1016/j.clet.2021.100323.

[111] M. Agmell, V. Bushlya, R. M'Saoubi, O. Gutnichenko, O. Zaporozhets, S. V. A. Laakso, J. Stahl, "Investigation of mechanical and thermal loads in pcBN tooling during machining of Inconel 718," *Int. J. Adv. Manuf. Technol.*, vol. 107, no. 3–4, pp. 1451–1462, Mar. 2020, doi: 10.1007/s00170-020-05081-8.

[112] J. Zhou, V. Bushlya, P. Avdovic, and J. E. Ståhl, “Study of surface quality in high speed turning of Inconel 718 with uncoated and coated CBN tools,” *Int. J. Adv. Manuf. Technol.*, vol. 58, no. 1–4, pp. 141–151, Jan. 2012, doi: 10.1007/s00170-011-3374-7.

[113] W. Grzesik, J. Małecka, and W. Kwaśny, “Identification of oxidation process of TiALN coatings versus heat resistant aerospace alloys based on diffusion couples and tool wear tests,” *CIRP Ann.*, vol. 69, no. 1, pp. 41–44, 2020, doi: 10.1016/j.cirp.2020.04.024.

[114] A. P. Kulkarni and V. G. Sargade, “Characterization and Performance of AlTiN, AlTiCrN, TiN/TiAlN PVD Coated Carbide Tools While Turning SS 304,” *Mater. Manuf. Process.*, vol. 30, no. 6, pp. 748–755, Jun. 2015, doi: 10.1080/10426914.2014.984217.

[115] L. Chen, Y. Du, F. Yin, and J. Li, “Mechanical properties of (Ti,Al)N monolayer and TiN/(Ti, Al)N multilayer coatings,” *Int. J. Refract. Met. Hard Mater.*, vol. 25, no. 1, pp. 72–76, Jan. 2007, doi: 10.1016/j.ijrmhm.2006.01.005.

[116] A. Y. Adesina, “Tribological Behavior of TiN/TiAlN, CrN/TiAlN, and CrAlN/TiAlN Coatings at Elevated Temperature,” *J. Mater. Eng. Perform.*, vol. 31, no. 8, pp. 6404–6419, Aug. 2022, doi: 10.1007/s11665-022-06722-7.

[117] J. H. Hsieh, C. Liang, C. H. Yu, and W. Wu, “Deposition and characterization of TiAlN and multi-layered TiN/TiAlN coatings using unbalanced magnetron sputtering,” *Surf. Coat. Technol.*, vol. 108–109, pp. 132–137, Oct. 1998, doi: 10.1016/S0257-8972(98)00684-7.

[118] ISO 4288:1996 – Geometrical Product Specifications (GPS) – Surface texture: Profile method – Rules and procedures for the assessment of surface texture - International Organization for Standardization: Geneva, Switzerland, 1996.

[119] ISO 8688-2:1986 - Tool Life Testing in Milling – Part 2: End Milling; International Organization for Standardization: Geneva, Switzerland, 1986.

[120] M. Wan, W. Yin, and W. H. Zhang, “Study on the Correction of Cutting Force Measurement with Table Dynamometer,” *Procedia CIRP*, vol. 56, pp. 119–123, 2016, doi: 10.1016/j.procir.2016.10.035.

[121] K. Venkatesan, K. Manivannan, S. Devendiran, A. T. Mathew, N. M Ghazaly, Aadhavan, S.M. N. Benny, “Study of Forces, Surface Finish and Chip Morphology on Machining of Inconel 825,” *Procedia Manuf.*, vol. 30, pp. 611–618, 2019, doi: 10.1016/j.promfg.2019.02.086.

[122] K. P. M. Vazquez, C. Giardini, and E. Ceretti, “Cutting force modeling,” *CIRP Encyclopedia of Production Engineering*, pp. 315–329, 2014, doi: 10.1007/978-3-642-20617-7_6399.

[123] M. Vasu and H. S. Nayaka, “Investigation of Cutting Force Tool Tip Temperature and Surface Roughness during Dry Machining of Spring Steel,” *Mater. Today Proc.*, vol. 5, no. 2, pp. 7141–7149, 2018, doi: 10.1016/j.matpr.2017.11.379.

[124] R. P. Martinho, F. J. G. Silva, and A. P. M. Baptista, “Cutting forces and wear analysis of Si_3N_4 diamond coated tools in high speed machining,” *Vacuum*, vol. 82, no. 12, pp. 1415–1420, Aug. 2008, doi: 10.1016/j.vacuum.2008.03.065.

[125] V. Marakini, S. P. Pai, U. K. Bhat, D. S. Thakur, and B. P. Achar, “High-speed face milling of AZ91 Mg alloy: Surface integrity investigations,” *Int. J. Lightweight Mater. Manuf.*, vol. 5, no. 4, pp. 528–542, Dec. 2022, doi: 10.1016/j.ijlmm.2022.06.006.

[126] J. Airao, B. Chaudhary, V. Bajpai, and N. Khanna, “An Experimental Study of Surface Roughness Variation in End Milling of Super Duplex 2507 Stainless Steel,” *Mater. Today Proc.*, vol. 5, no. 2, pp. 3682–3689, 2018, doi: 10.1016/j.matpr.2017.11.619.

[127] A. R. Natasha, J. A. Ghani, C. H. Che Haron, and J. Syarif, “The influence of machining condition and cutting tool wear on surface roughness of AISI 4340 steel,” *IOP Conf. Ser. Mater. Sci. Eng.*, vol. 290, p. 012017, Jan. 2018, doi: 10.1088/1757-899X/290/1/012017.

[128] X. Liang and Z. Liu, “Tool wear behaviors and corresponding machined surface topography during high-speed machining of Ti-6Al-4V with fine grain tools,” *Tribol. Int.*, vol. 121, pp. 321–332, May 2018, doi: 10.1016/j.triboint.2018.01.057.

[129] I. Korkut and M. A. Donertas, “The influence of feed rate and cutting speed on the cutting forces, surface roughness and tool–chip contact length during face milling,” *Mater. Des.*, vol. 28, no. 1, pp. 308–312, Jan. 2007, doi: 10.1016/j.matdes.2005.06.002.

[130] M. Gueli, J. Ma, N. Cococcetta, D. Pearl, and M. P. Jahan, “Experimental investigation into tool wear, cutting forces, and resulting surface finish during dry and flood coolant slot milling of Inconel 718,” *Procedia Manuf.*, vol. 53, pp. 236–245, 2021, doi: 10.1016/j.promfg.2021.06.026.

[131] J. Z. Zhang, J. C. Chen, and E. D. Kirby, “Surface roughness optimization in an end-milling operation using the Taguchi design method,” *J. Mater. Process. Technol.*, vol. 184, no. 1–3, pp. 233–239, Apr. 2007, doi: 10.1016/j.jmatprotec.2006.11.029.

[132] Y. Ning, M. Rahman, and Y. S. Wong, “Investigation of chip formation in high speed end milling,” *J. Mater. Process. Technol.*, vol. 113, no. 1–3, pp. 360–367, Jun. 2001, doi: 10.1016/S0924-0136(01)00628-8.

[133] I. Buj-Corral, J. Vivancos-Calvet, and A. Domínguez-Fernández, “Surface topography in ball-end milling processes as a function of feed per tooth and radial depth of cut,” *Int. J. Mach. Tools Manuf.*, vol. 53, no. 1, pp. 151–159, Feb. 2012, doi: 10.1016/j.ijmachtools.2011.10.006.

[134] R. Čep, A. Janásek, J. Petrů, M. Sadilek, P. Mohyla, J. Valíček, M. Harničárová, A. Czán, “Surface Roughness after Machining and Influence of Feed Rate on Process,” *Key Eng. Mater.*, vol. 581, pp. 341–347, Oct. 2013, doi: 10.4028/www.scientific.net/KEM.581.341.

[135] S. Ramesh, L. Karunamoorthy, and K. Palanikumar, “Surface Roughness Analysis in Machining of Titanium Alloy,” *Mater. Manuf. Process.*, vol. 23, no. 2, pp. 174–181, Jan. 2008, doi: 10.1080/10426910701774700.

[136] R. Zimmermann, D. Welling, T. Venek, P. Ganser, and T. Bergs, “Tool wear progression of SiAlON ceramic end mills in five-axis high-feed rough machining of an Inconel 718 BLISK,” *Procedia CIRP*, vol. 101, pp. 13–16, 2021, doi: 10.1016/j.procir.2021.02.003.

[137] B. Breidenstein and B. Denkena, “Significance of residual stress in PVD-coated carbide cutting tools,” *CIRP Ann.*, vol. 62, no. 1, pp. 67–70, 2013, doi: 10.1016/j.cirp.2013.03.101.

[138] Field M, Kahles JF (1964) The Surface Integrity of Machined and Ground High Strength Steels. DMIC Report 210:54–77.

[139] M. Dhananchezian and K. Rajkumar, “Comparative Study of Cutting Insert Wear and Roughness Parameter (Ra) while turning Nimonic 90 and Hastelloy C-276 by Coated Carbide Inserts,” *Mater. Today Proc.*, vol. 22, pp. 1409–1416, 2020, doi: 10.1016/j.matpr.2020.01.484.

[140] M. Rahman, Md S. Bhuiyan, S. Sharma, M. S. Kamal, M. M. M. Imtiaz, A. Alfaify, T. T. Nguyen, N. Khanna, S. Sharma, M. K. Gupta, S. Anwar, M. Mia, “Influence of Feed Rate Response (FRR) on Chip Formation in Micro and Macro Machining of Al Alloy,” *Metals*, vol. 11, no. 1, p. 159, Jan. 2021, doi: 10.3390/met11010159.

[141] W. Grzesik, “Tool Wear and Damage,” in *Advanced Machining Processes of Metallic Materials*, Elsevier, 2017, pp. 215–239. doi: 10.1016/B978-0-444-63711-6.00012-0.

[142] N. Narutaki, Y. Yamane, K. Hayashi, T. Kitagawa, and K. Uehara, “High-speed Machining of Inconel 718 with Ceramic Tools,” *CIRP Ann.*, vol. 42, no. 1, pp. 103–106, 1993, doi: 10.1016/S0007-8506(07)62402-0.

[143] V. F. C. Sousa, F. J. G. Silva, R. Alexandre, J. S. Fecheira, and F. P. N. Silva, “Study of the wear behaviour of TiAlSiN and TiAlN PVD coated tools on milling operations of pre-hardened tool steel,” *Wear*, vol. 476, p. 203695, Jul. 2021, doi: 10.1016/j.wear.2021.203695.

[144] A. Çelik, M. Sert Alağaç, S. Turan, A. Kara, and F. Kara, “Wear behavior of solid SiAlON milling tools during high speed milling of Inconel 718,” *Wear*, vol. 378–379, pp. 58–67, May 2017, doi: 10.1016/j.wear.2017.02.025.

[145] A. De Bartolomeis, S. T. Newman, I. S. Jawahir, D. Biermann, and A. Shokrani, “Future research directions in the machining of Inconel 718,” *J. Mater. Process. Technol.*, vol. 297, p. 117260, Nov. 2021, doi: 10.1016/j.jmatprotec.2021.117260.

[146] V. Ferreira, F. J. G. Silva, R. P. Martinho, C. Pimentel, R. Godina, and B. Pinto, “A comprehensive supplier classification model for SME outsourcing,” *Procedia Manuf.*, vol. 38, pp. 1461–1472, 2019, doi: 10.1016/j.promfg.2020.01.141.

[147] A. Rodrigues, F. J. G. Silva, V. F. C. Sousa, A. G. Pinto, L. P. Ferreira, and T. Pereira, “Using an Artificial Neural Network Approach to Predict Machining Time,” *Metals*, vol. 12, no. 10, p. 1709, Oct. 2022, doi: 10.3390/met12101709.

[148] F. J. G. Silva, V. F. C. Sousa, A. G. Pinto, L. P. Ferreira, and T. Pereira, “Build-Up an Economical Tool for Machining Operations Cost Estimation,” *Metals*, vol. 12, no. 7, p. 1205, Jul. 2022, doi: 10.3390/met12071205.

[149] M. S. Damião, “The incremental innovation in the machining process in relation to cutting tool materials,” *Sinergia, São Paulo*, v. 21, n. 1, p. 48-52, 2020.

[150] K. Kamdani, S. Hasan, and M. A. Lajis, “The Effects of TiAlN and TiN Coating during End Milling of INCONEL 718,” *Appl. Mech. Mater.*, vol. 564, pp. 566–571, Jun. 2014, doi: 10.4028/www.scientific.net/AMM.564.566.

[151] A. R. Motorcu, A. Kuş, R. Arslan, Y. Tekin, and R. Ezentaş, “Evaluation of tool life - tool wear in milling of inconel 718 superalloy and the investigation of effects of cutting parameters on surface roughness with taguchi method,” 2013.

[152] Y. W. Wang, J. F. Li, Z. M. Li, T. C. Ding, and S. Zhang, “Experimental Investigation on Tool Wear when End-Milling Inconel 718 with Coated Carbide Inserts,” *Adv. Mater. Res.*, vol. 188, pp. 410–415, Mar. 2011, doi: 10.4028/www.scientific.net/AMR.188.410.

[153] L. Bouzid, S. Berkani, M. A. Yallese, F. Girardin, and T. Mabrouki, “Estimation and optimization of flank wear and tool lifespan in finish turning of AISI 304 stainless steel using desirability function approach,” *Int. J. Ind. Eng. Comput.*, pp. 349–368, 2018, doi: 10.5267/j.ijiec.2017.8.002.

[154] D. G. Thakur, B. Ramamoorthy, and L. Vijayaraghavan, “Some Investigations on High Speed Dry Machining of Aerospace Material Inconel 718 Using Multicoated Carbide Inserts,” *Mater. Manuf. Process.*, vol. 27, no. 10, pp. 1066–1072, Oct. 2012, doi: 10.1080/10426914.2011.654158.

[155] J. Zhao and Z. Liu, “Influences of coating thickness on cutting temperature for dry hard turning Inconel 718 with PVD TiAlN coated carbide tools in initial tool wear stage,” *J. Manuf. Process.*, vol. 56, pp. 1155–1165, Aug. 2020, doi: 10.1016/j.jmapro.2020.06.010.

[156] N. A. Krishnan and J. Mathew, “Studies on wear behavior of AlTiN-coated WC tool and machined surface quality in micro endmilling of Inconel 718,” *Int. J. Adv. Manuf. Technol.*, vol. 110, no. 1–2, pp. 291–307, Sep. 2020, doi: 10.1007/s00170-020-05875-w.

[157] S. Gürgen, D. Tali, and M. C. Kushan, “An Investigation on Surface Roughness and Tool Wear in Turning Operation of Inconel 718,” *J. Aerosp. Technol. Manag.*, 2019, doi: 10.5028/jatm.v11.1030.

[158] E. O. Ezugwu, Z. M. Wang, and C. I. Okeke, “Tool Life and Surface Integrity When Machining Inconel 718 With PVD- and CVD-Coated Tools,” *Tribol. Trans.*, vol. 42, no. 2, pp. 353–360, Jan. 1999, doi: 10.1080/10402009908982228.

[159] R. K. Yadav, S. Chatterjee, K. Abhishek, and S. S. Mahapatra, “Assessment of machinability of inconel 718: A comparative study of CVD & PVD coated tools,” *INDIAN J ENG MATER SCI*, 2019.

[160] R. P. Martinho, F. J. G. Silva, C. Martins, and H. Lopes, “Comparative study of PVD and CVD cutting tools performance in milling of duplex stainless steel,” *Int. J. Adv. Manuf. Technol.*, vol. 102, no. 5–8, pp. 2423–2439, Jun. 2019, doi: 10.1007/s00170-019-03351-8.

[161] A. I. Fernández-Abia, J. Barreiro, J. Fernández-Larrinoa, L. N. L. de Lacalle, A. Fernández-Valdivielso, and O. M. Pereira, “Behaviour of PVD Coatings in the Turning of Austenitic Stainless Steels,” *Procedia Eng.*, vol. 63, pp. 133–141, 2013, doi: 10.1016/j.proeng.2013.08.241.